

Hybrid Detector for Microdosimetry (HDM) readout and experimental results

E. Pierobon, M. Missiaggia, V. Monaco, C. Schuy, C. La Tessa

TWEPP 2023



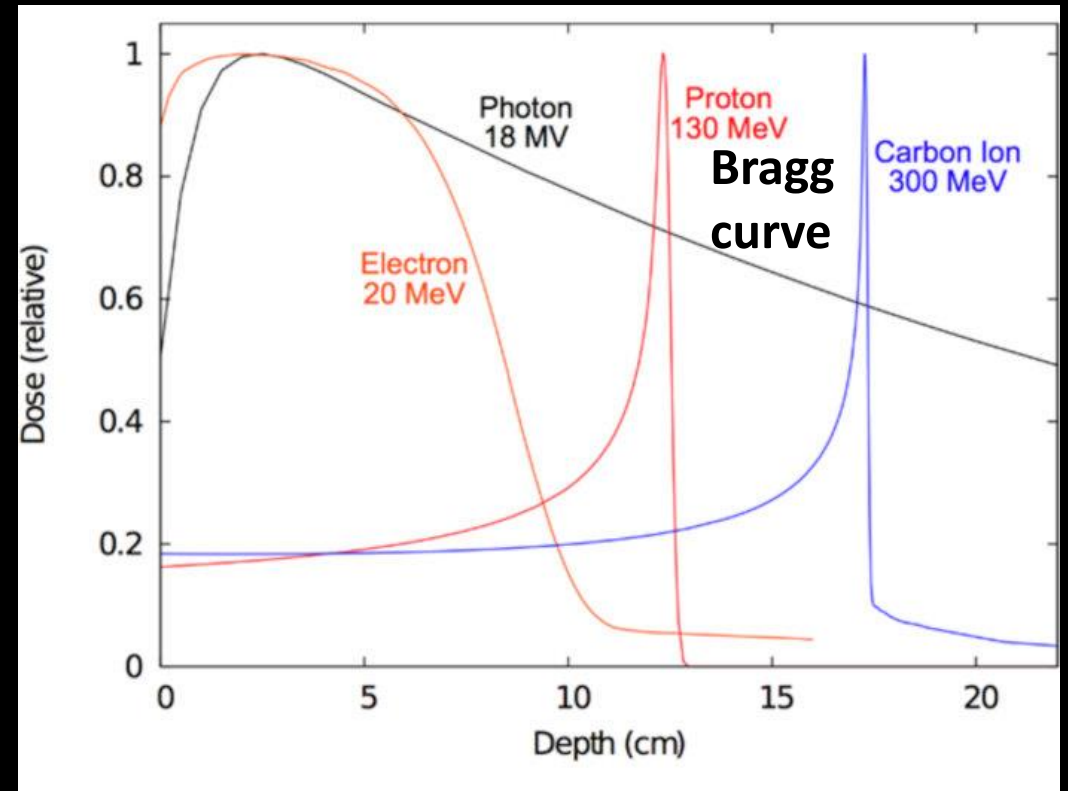
**UNIVERSITY
OF TRENTO**



Trento Institute for
Fundamental Physics
and Applications

Why proton therapy?

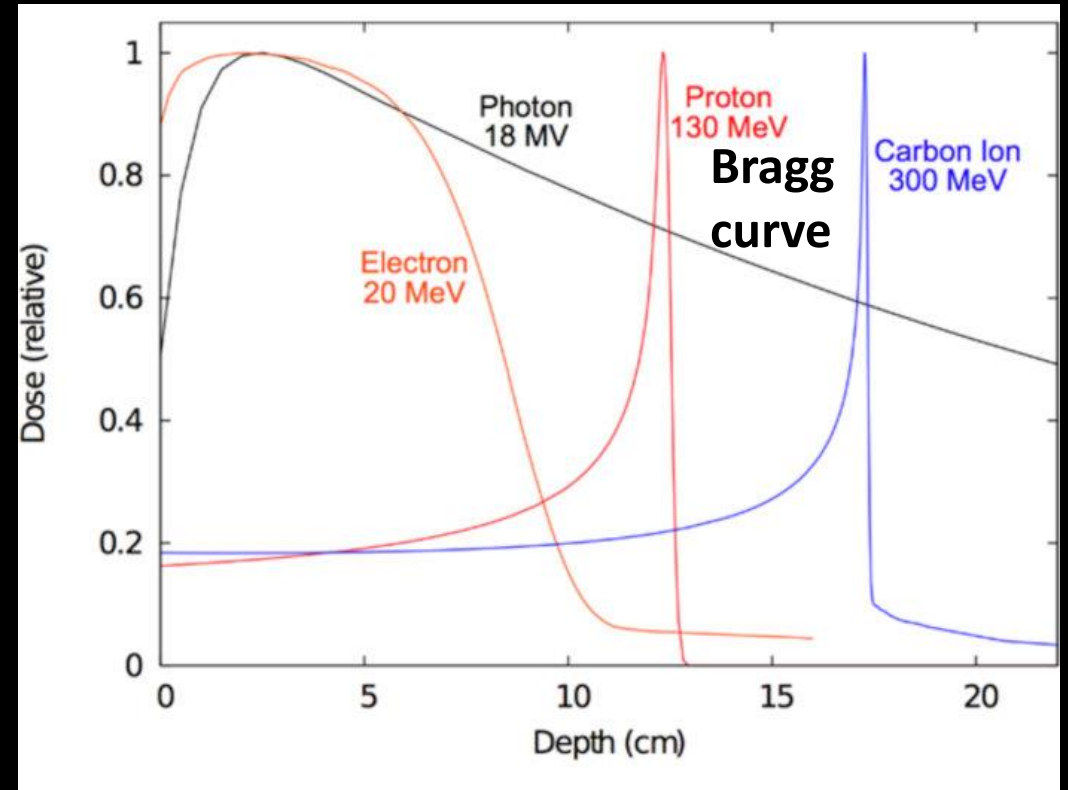
Why proton therapy?



Kaiser, Adeel et al. 10.3791/58372.

Why proton therapy?

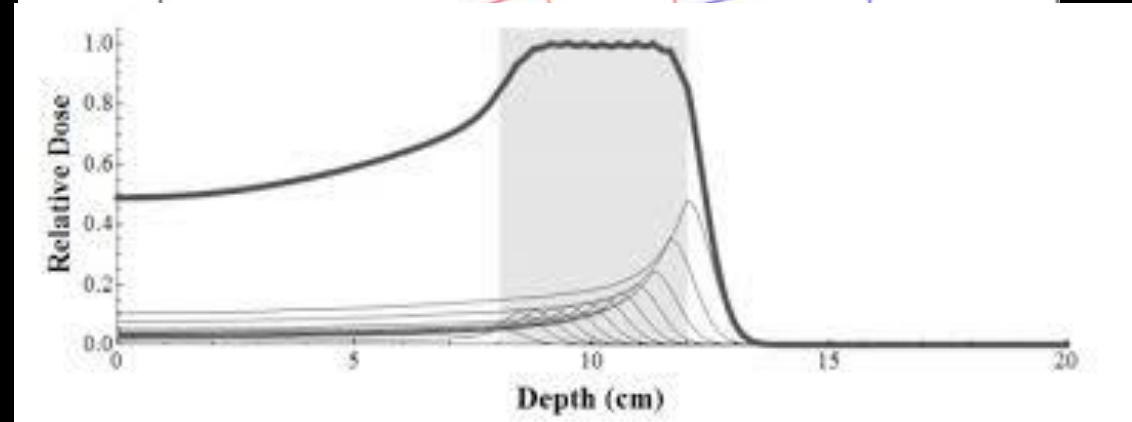
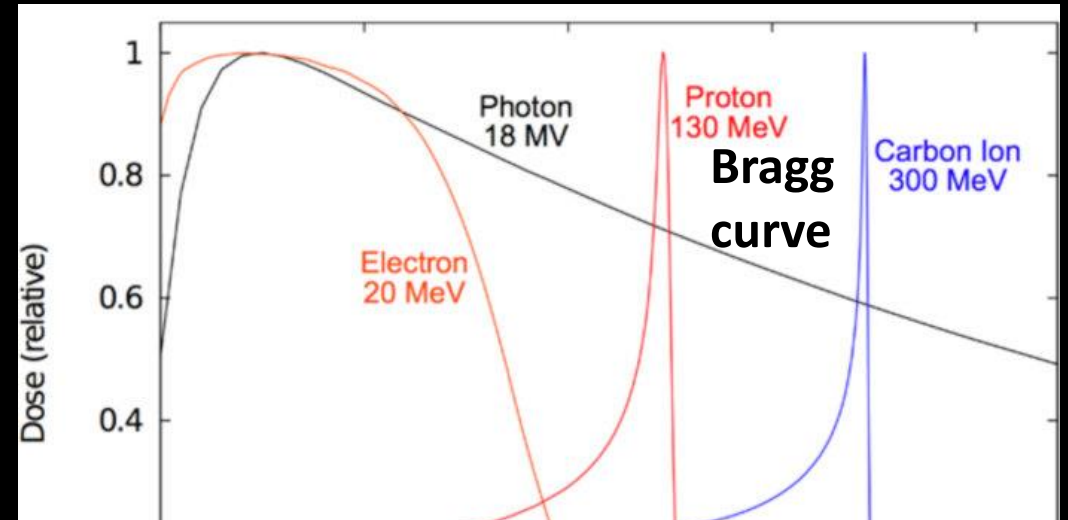
- Very localized dose deposition



Kaiser, Adeel et al. 10.3791/58372.

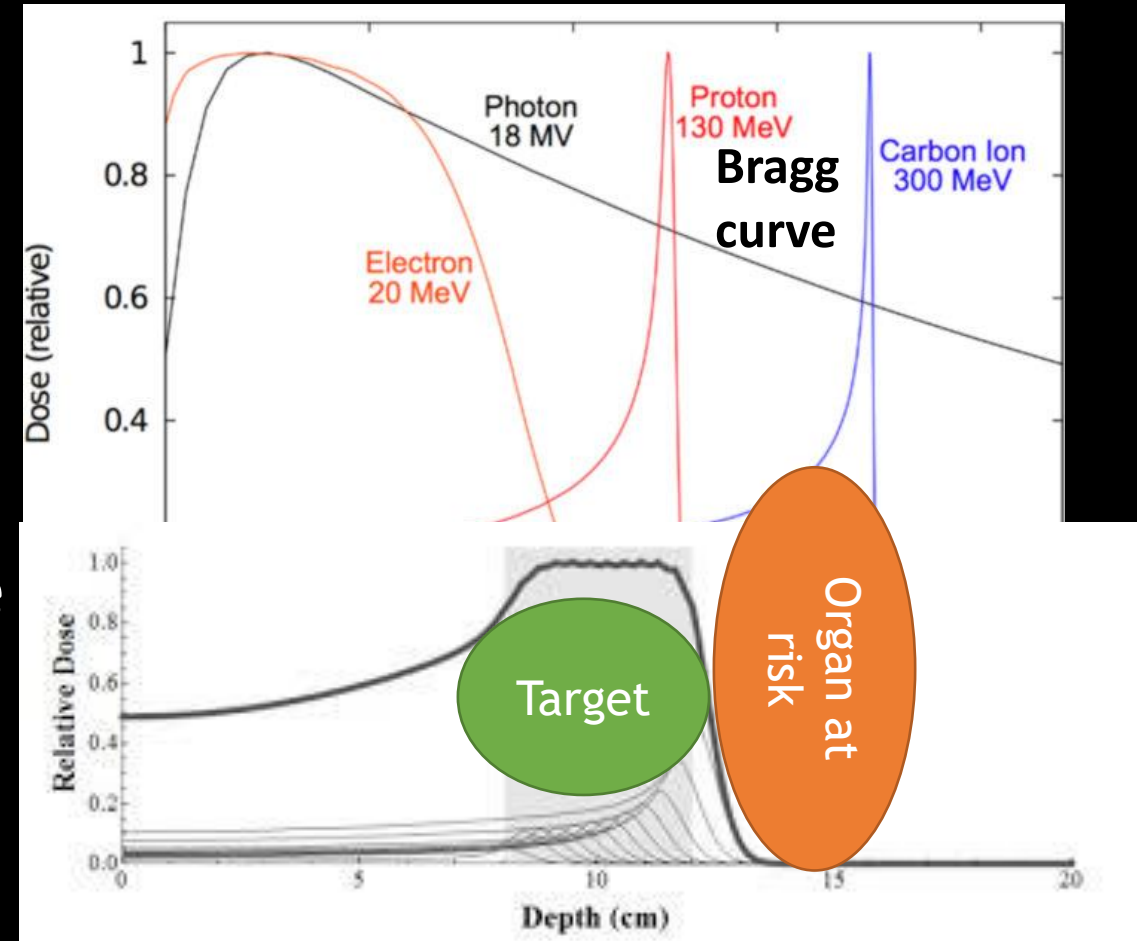
Why proton therapy?

- Very localized dose deposition
- It is possible to create a uniform dose as sum of Bragg peaks



Why proton therapy?

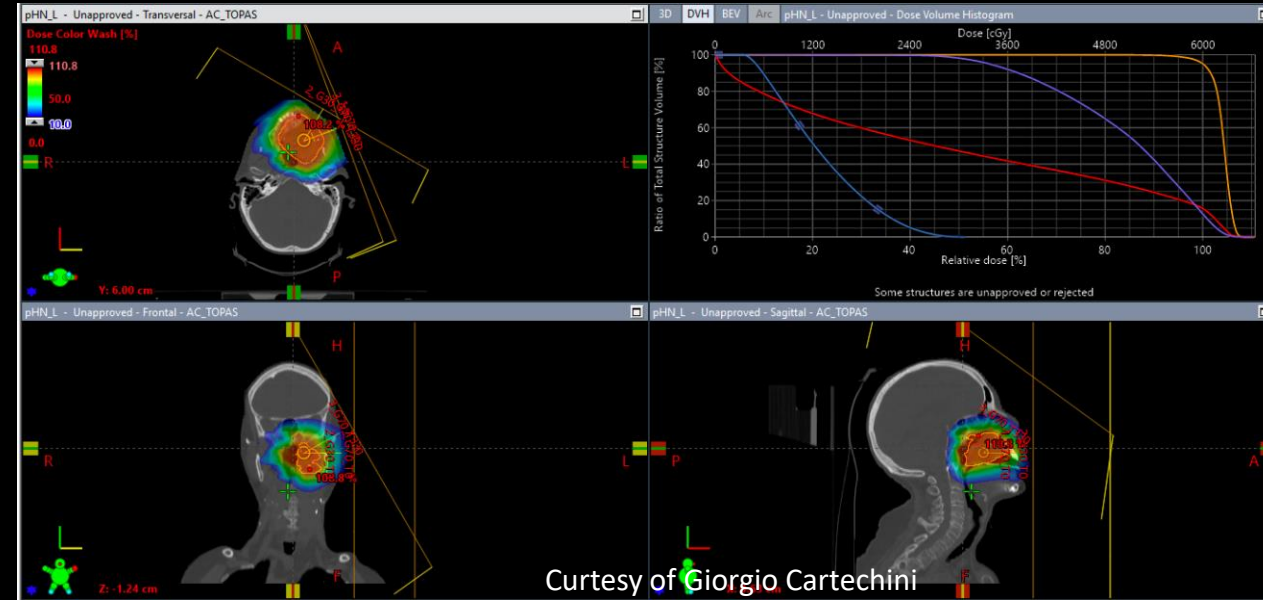
- Very localized dose deposition
- It is possible to create a uniform dose as sum of Bragg peaks
- Ideal when a sensitive target is on the edge



Proton therapy - goals

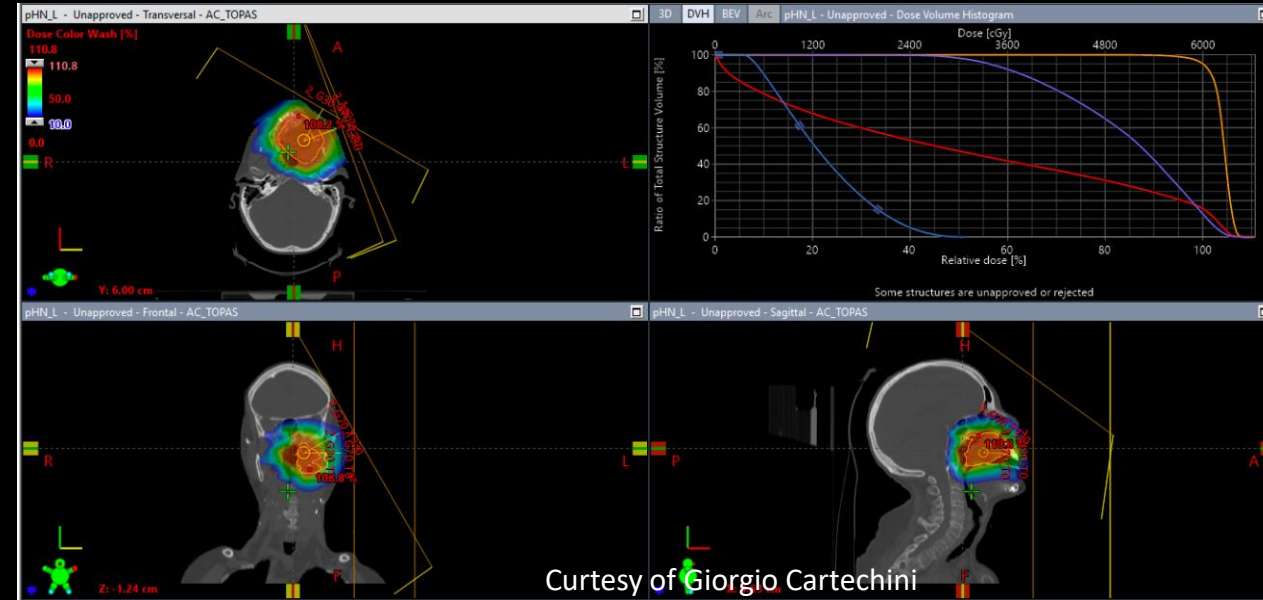
Proton therapy - goals

- The dose delivery is planned with the help of a software: the Treatment Planning System (TPS)



Proton therapy - goals

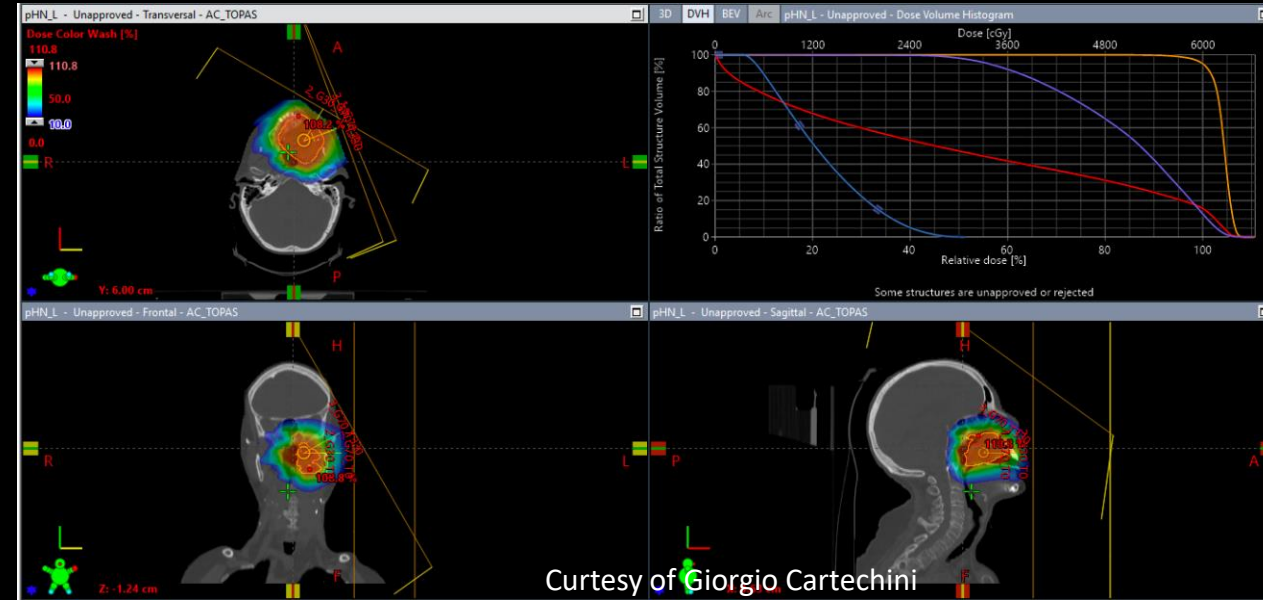
- The dose delivery is planned with the help of a software: the Treatment Planning System (TPS)



- TPS requires information particle specie and energy - **radiation quality**

Proton therapy - goals

- The dose delivery is planned with the help of a software: the Treatment Planning System (TPS)

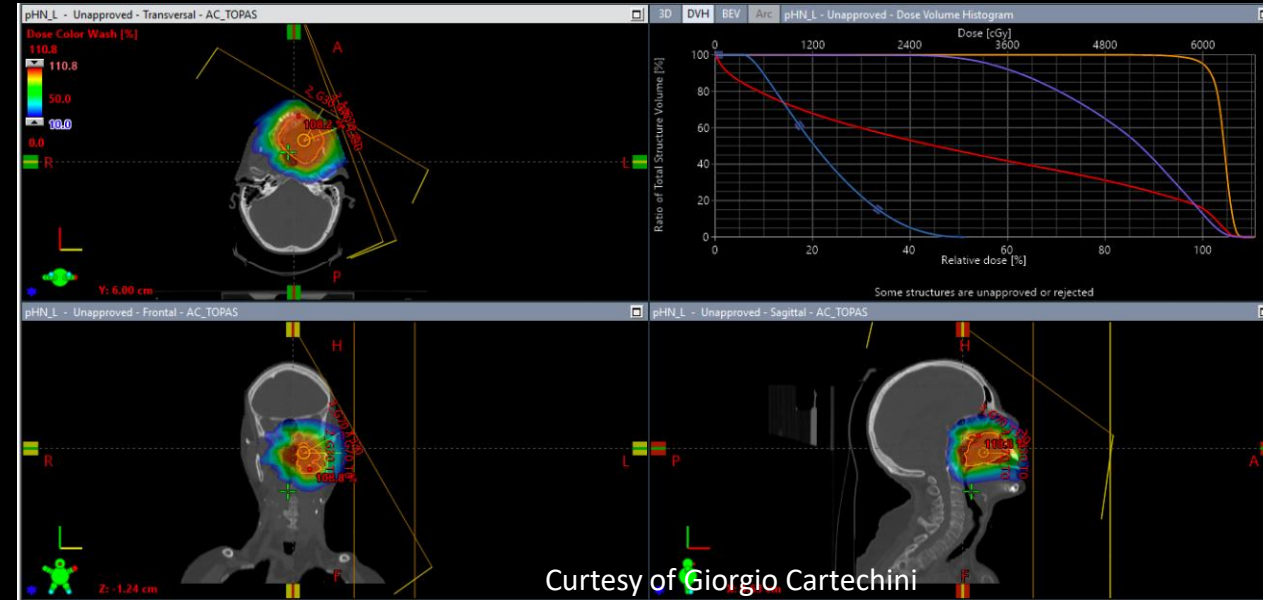


- TPS requires information particle specie and energy - **radiation quality**

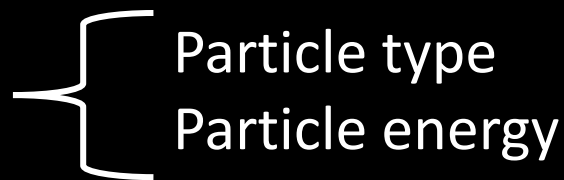
Particle type
Particle energy

Proton therapy - goals

- The dose delivery is planned with the help of a software: the Treatment Planning System (TPS)



- TPS requires information particle specie and energy - **radiation quality**

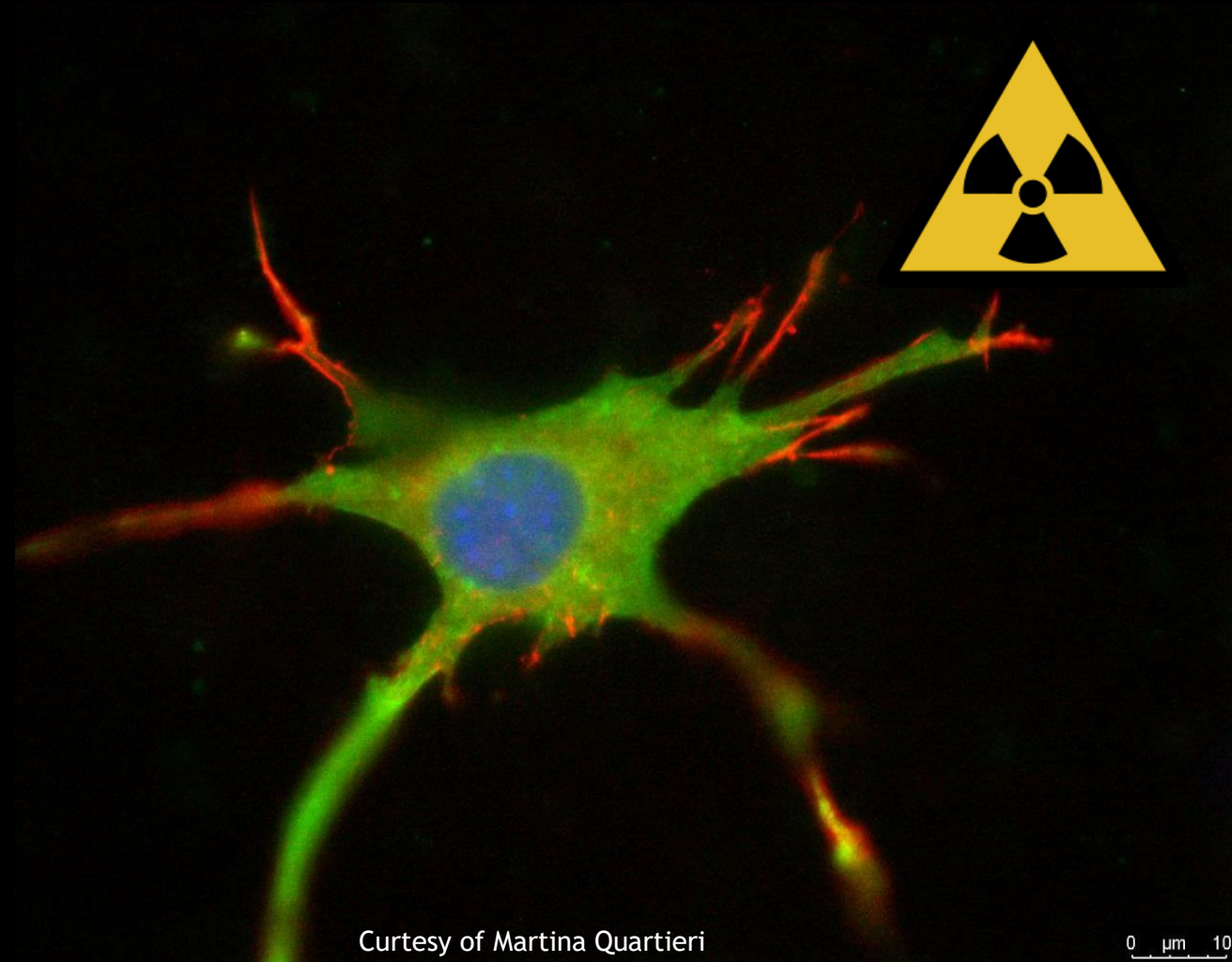


- **Good description** of the radiation quality will result in a **better TPS plan**

How radiation damage occurs

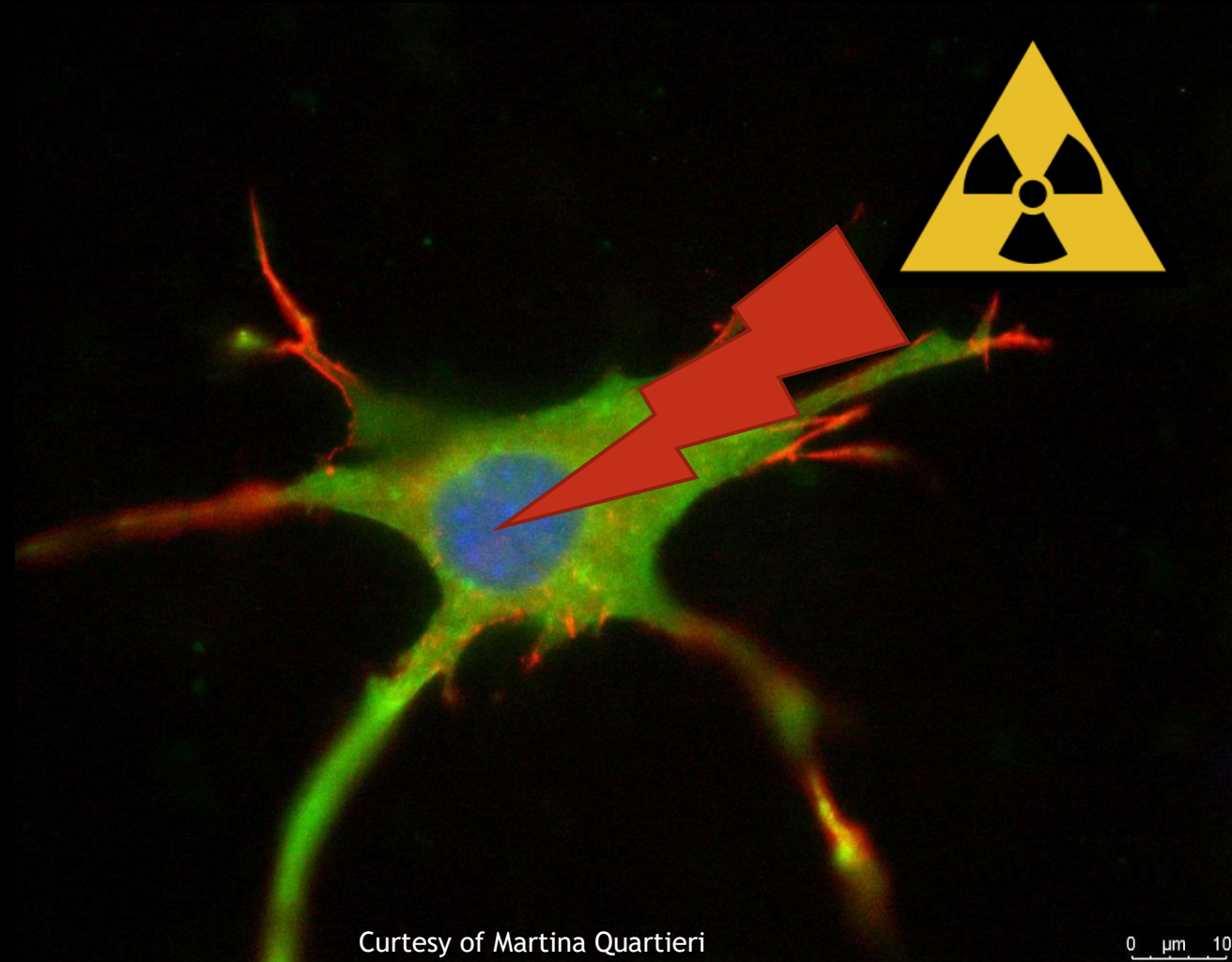
How radiation damage occurs

- Radiation damages occurs at cellular level



How radiation damage occurs

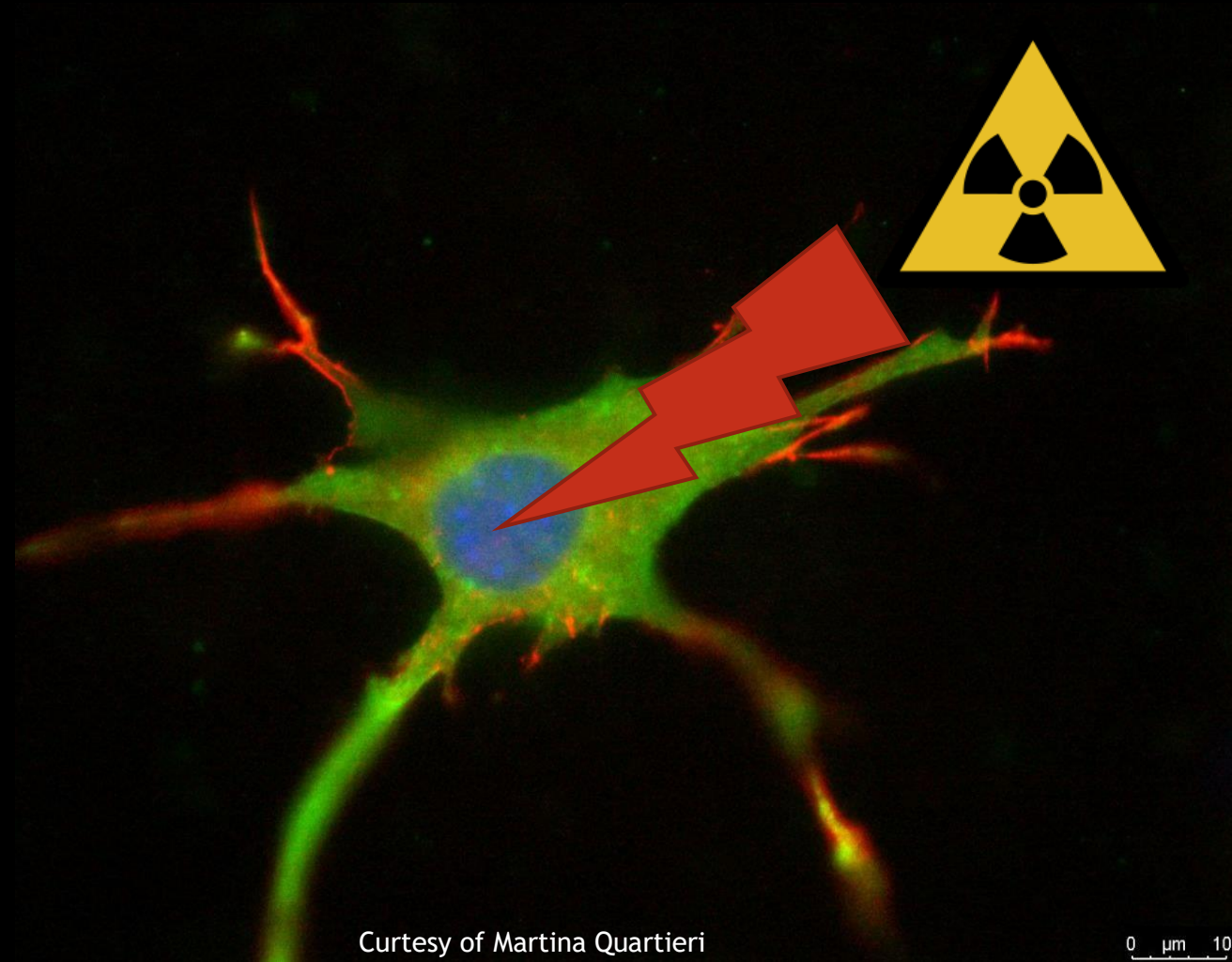
- Radiation damages occurs at cellular level
- The most sensitive region is the DNA inside the cell nucleus



Courtesy of Martina Quartieri

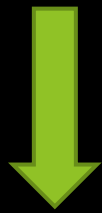
How radiation damage occurs

- Radiation damages occurs at cellular level
- The most sensitive region is the DNA inside the cell nucleus
- Energy deposition has to be described at a micrometric scale (cell nucleus size)

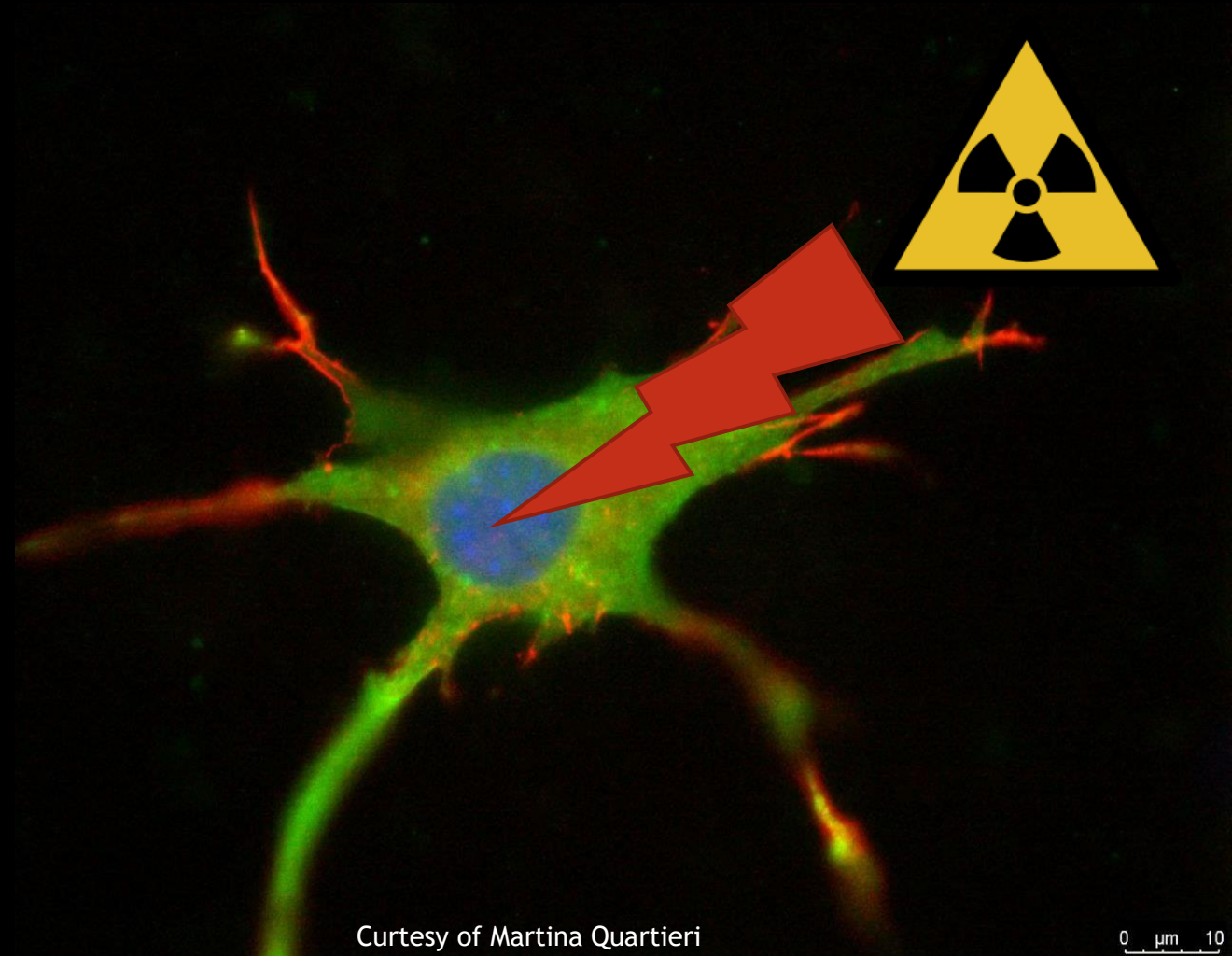


How radiation damage occurs

- Radiation damages occurs at cellular level
- The most sensitive region is the DNA inside the cell nucleus
- Energy deposition has to be described at a micrometric scale (cell nucleus size)



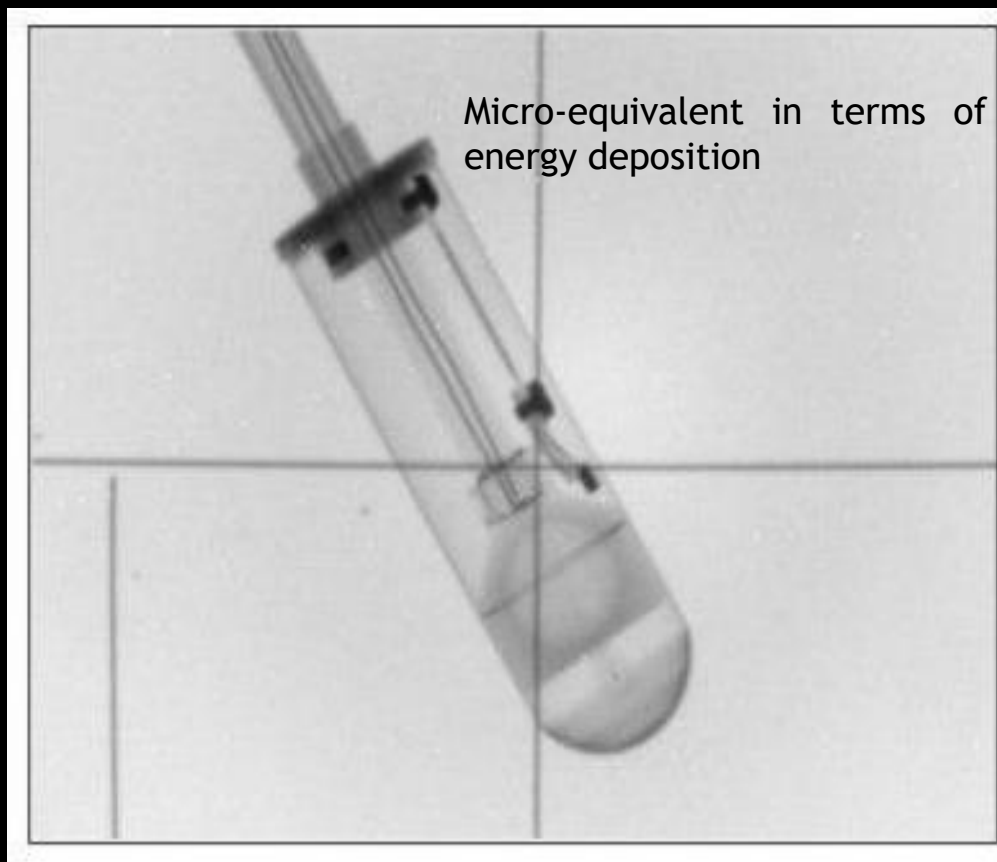
MICRODOSIMETRY



Tissue equivalent proportional counter (TEPC)

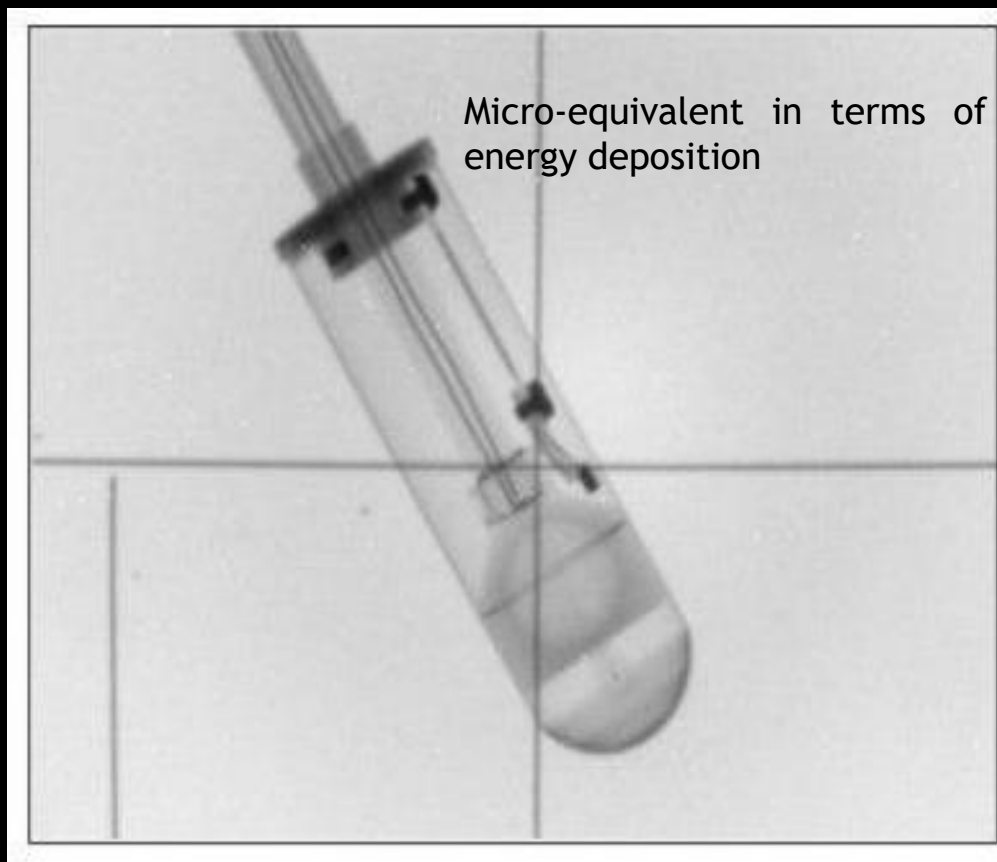
Tissue equivalent proportional counter (TEPC)

Reference microdosimeter according to ICRU36



Tissue equivalent proportional counter (TEPC)

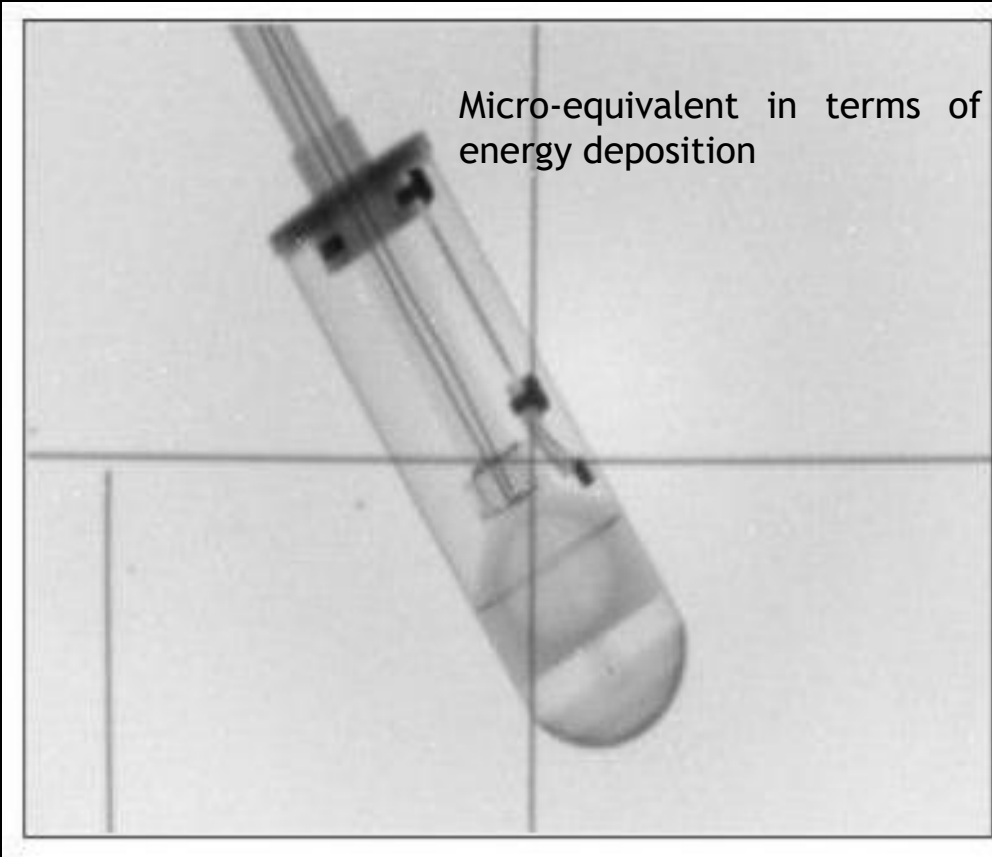
Reference microdosimeter according to ICRU36



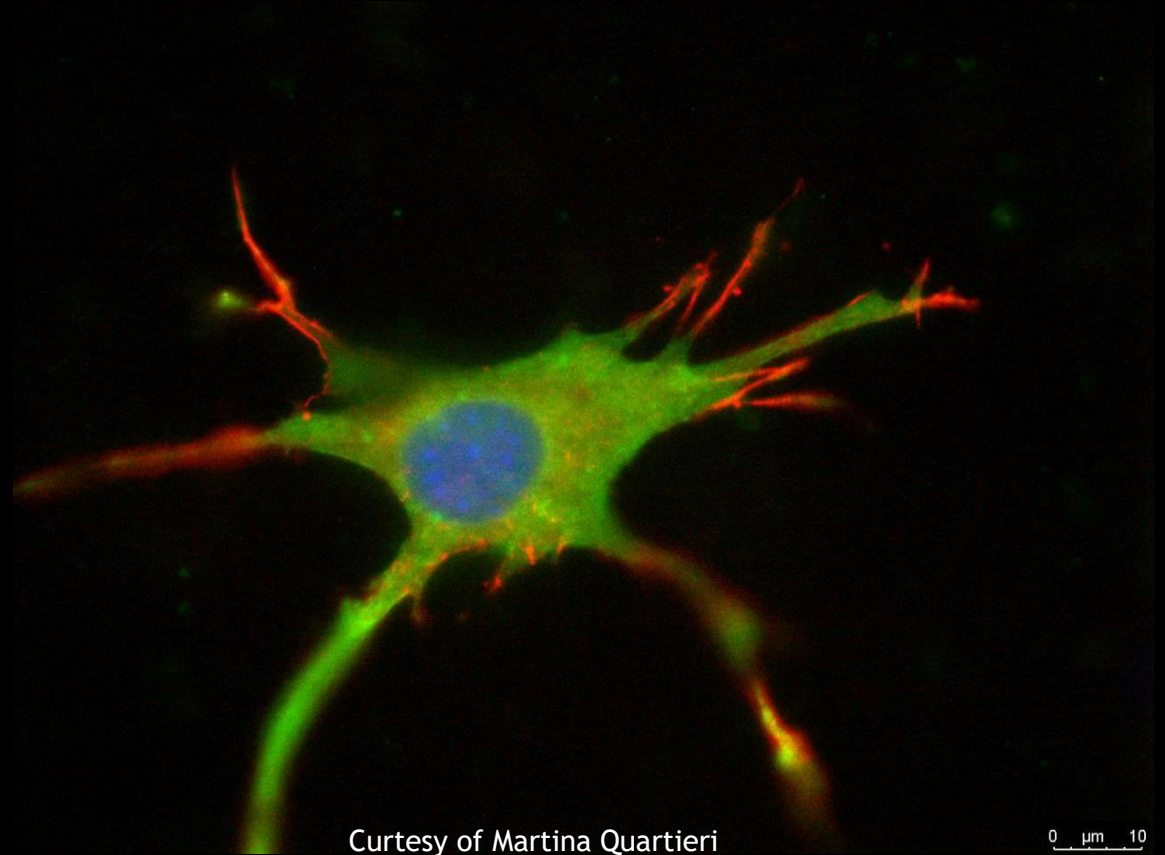
≈

Tissue equivalent proportional counter (TEPC)

Reference microdosimeter according to ICRU36

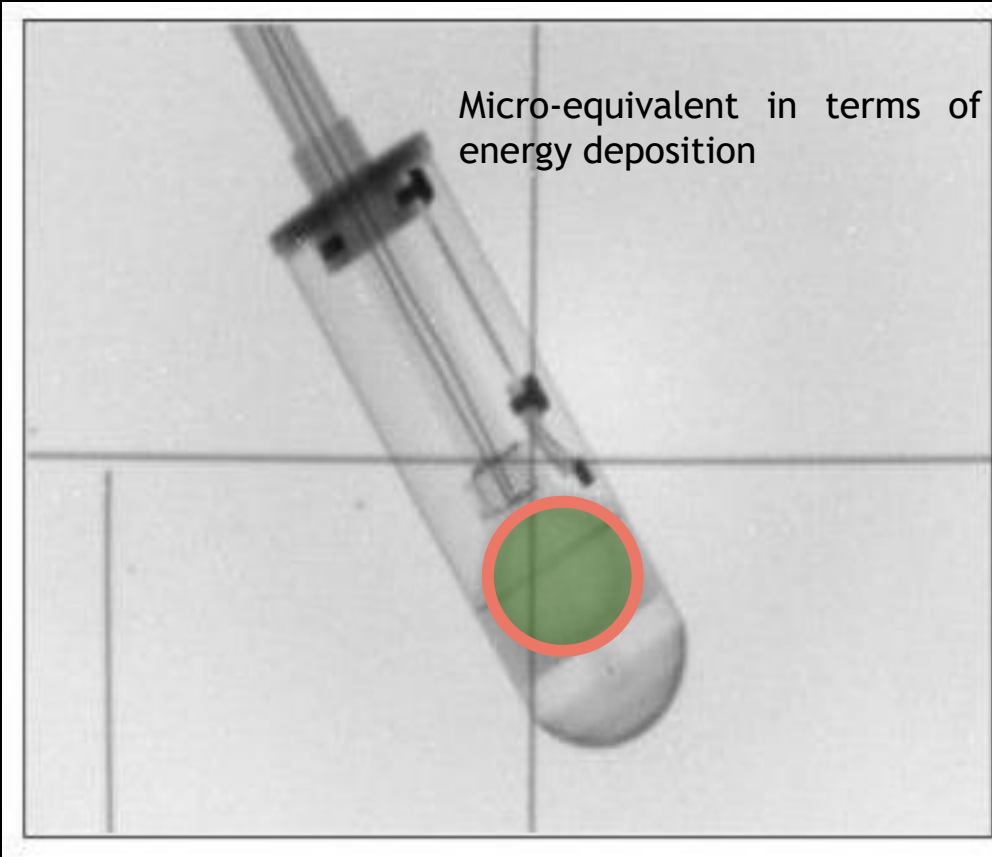


≈

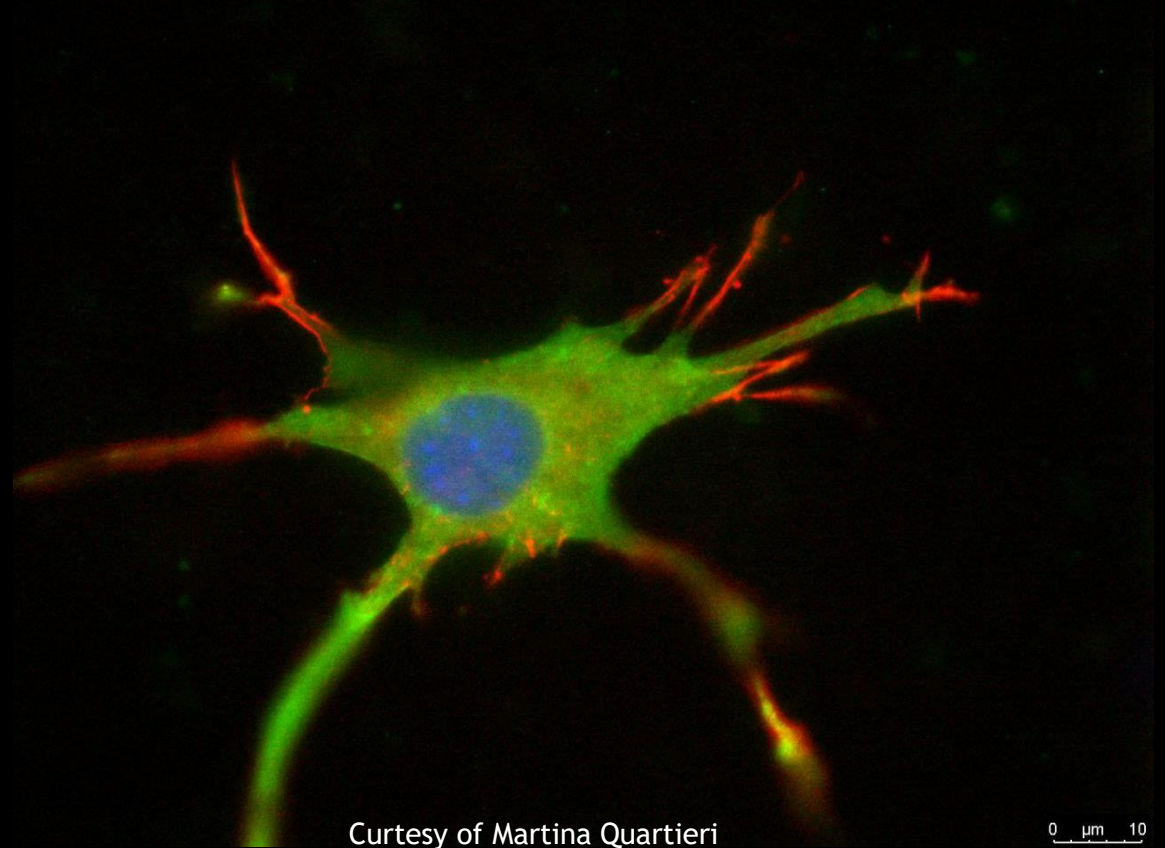


Tissue equivalent proportional counter (TEPC)

Reference microdosimeter according to ICRU36

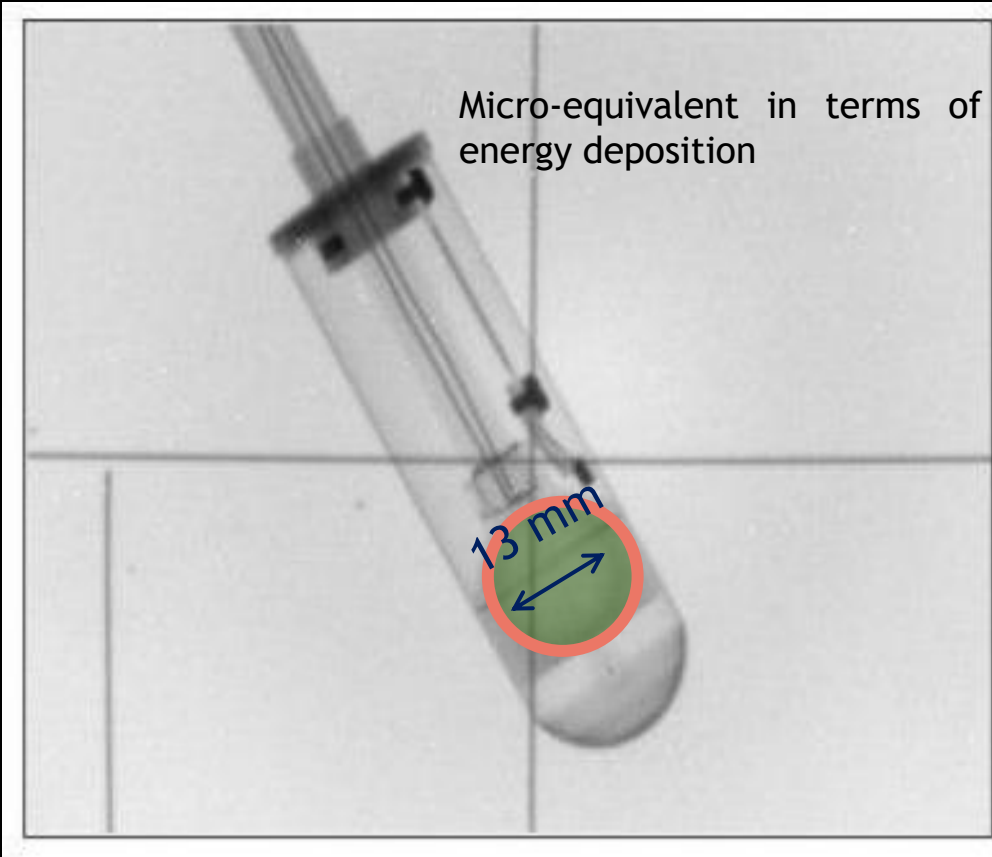


≈

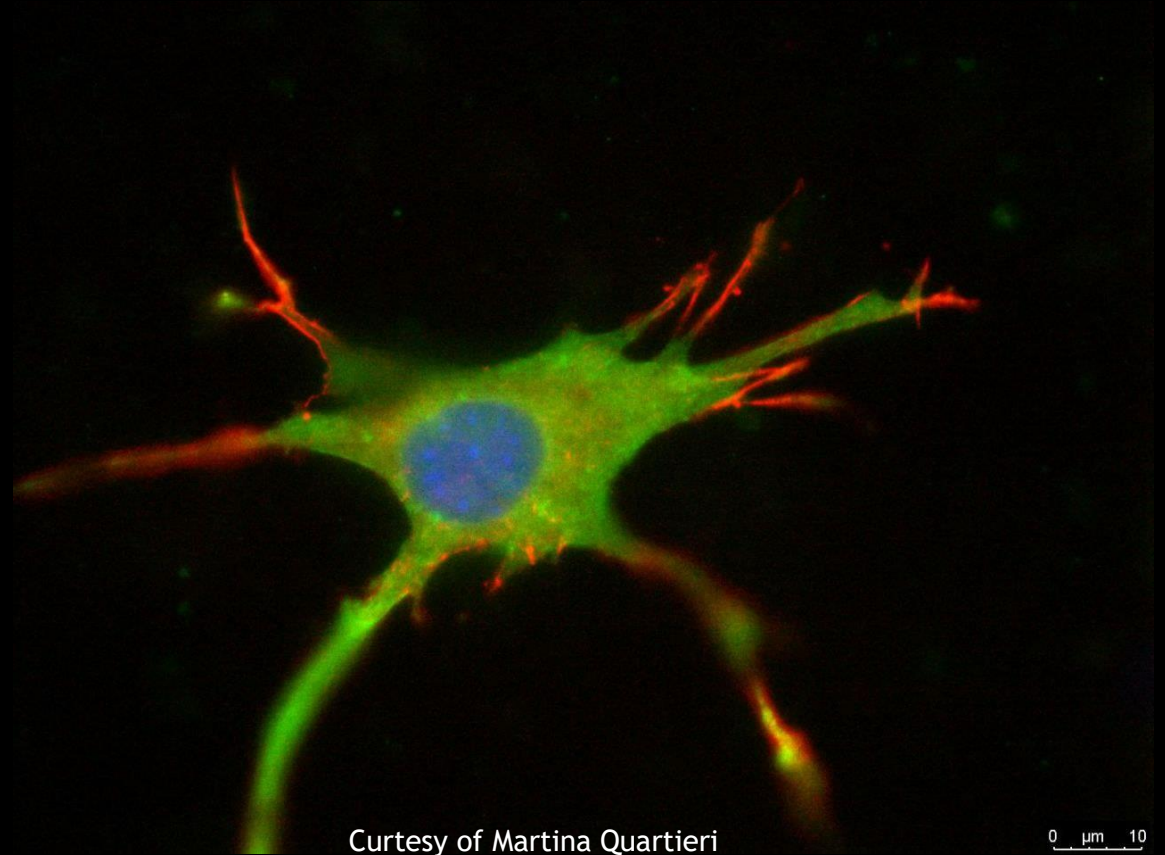


Tissue equivalent proportional counter (TEPC)

Reference microdosimeter according to ICRU36



~



Microdosimetry main quantity

$$y = \frac{\textit{Energy deposited}}{\textit{MCL}}$$

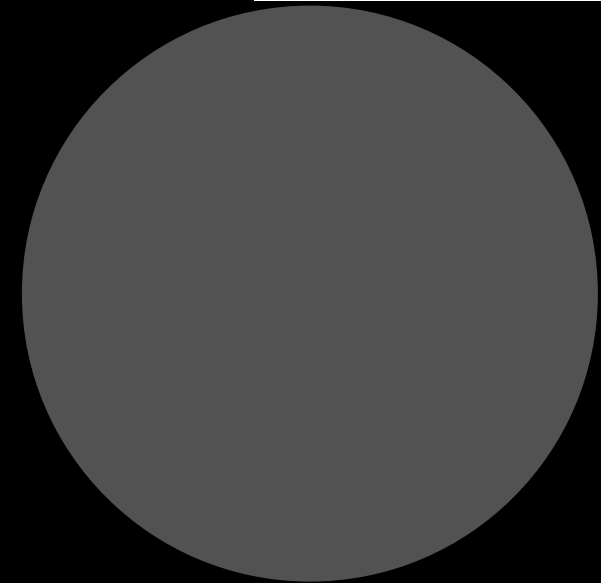
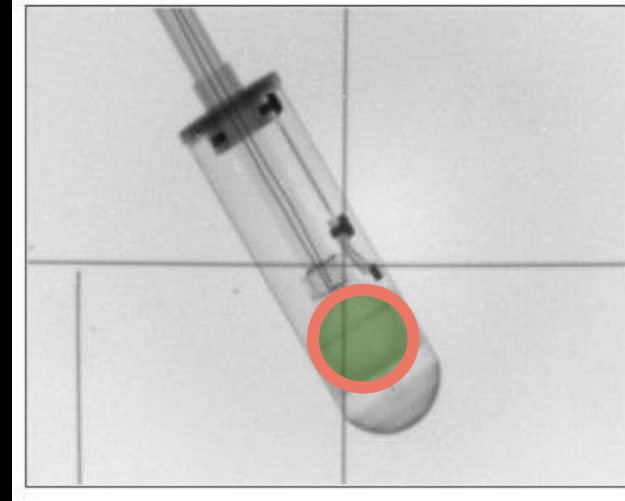
Microdosimetry main quantity

$$y = \frac{\text{Energy deposited}}{MCL}$$


Microdosimetry main quantity

$$y = \frac{\text{Energy deposited}}{MCL}$$

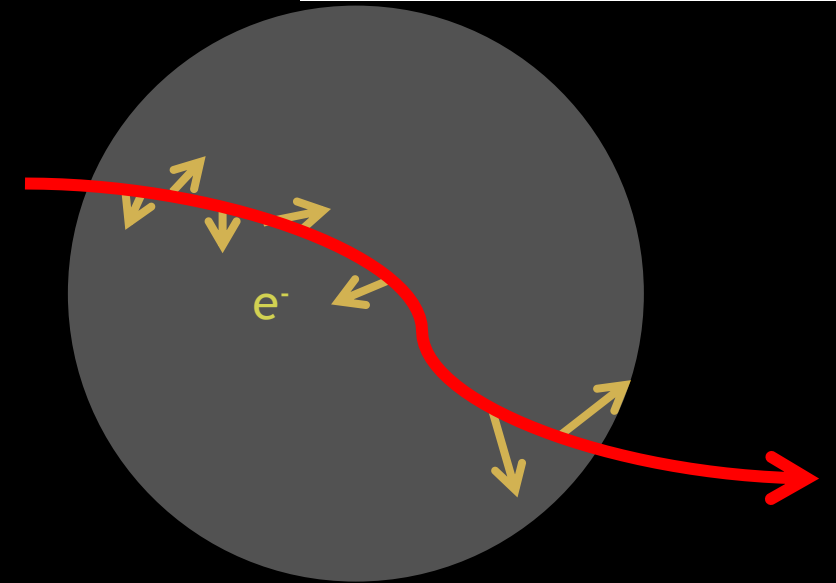
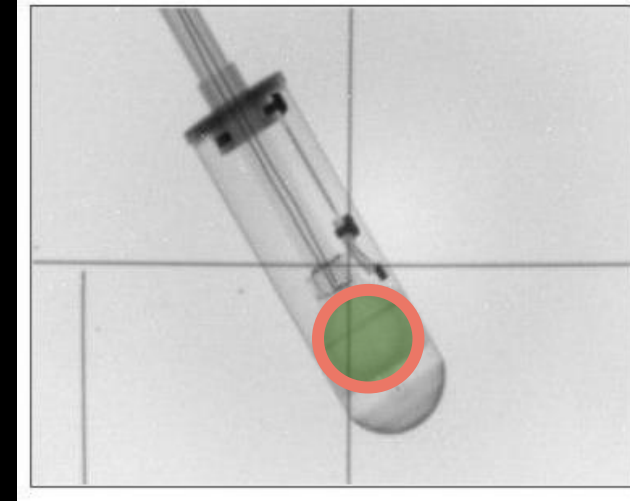
Energy recorded in the detector



Microdosimetry main quantity

$$y = \frac{\text{Energy deposited}}{MCL}$$

Energy recorded in the detector

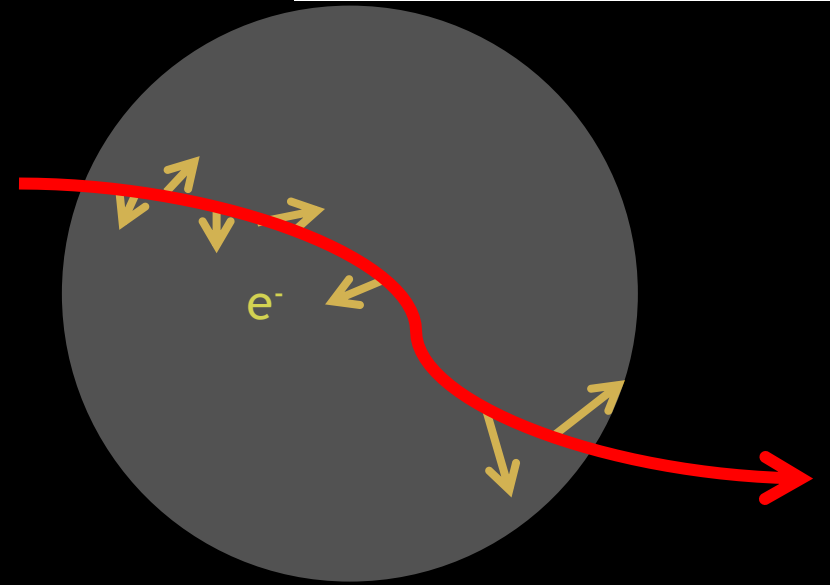
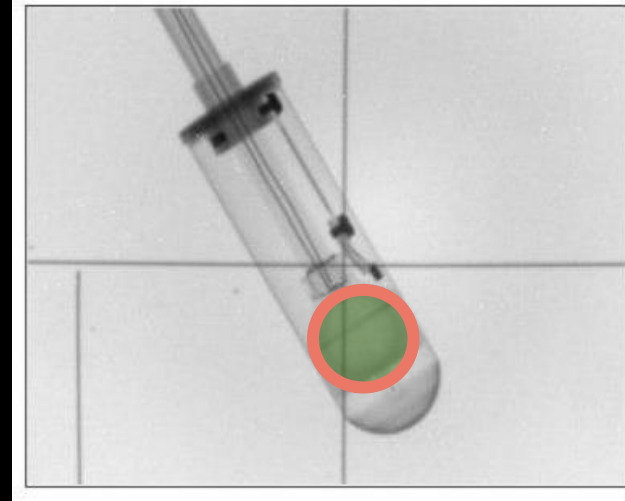


Microdosimetry main quantity

$$y = \frac{\text{Energy deposited}}{\text{MCL}}$$

Energy recorded in the detector

Mean Chord Length: average particle track length in isotropic and uniform radiation field

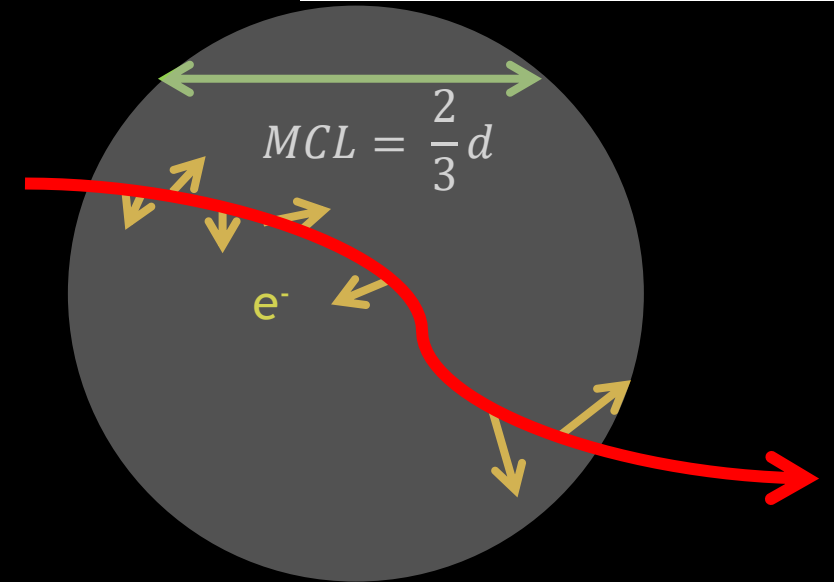
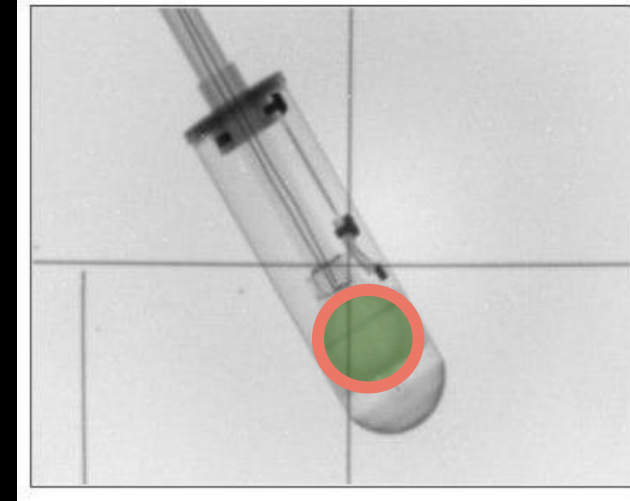


Microdosimetry main quantity

$$y = \frac{\text{Energy deposited}}{\text{MCL}}$$

Energy recorded in the detector

Mean Chord Length: average particle track length in isotropic and uniform radiation field



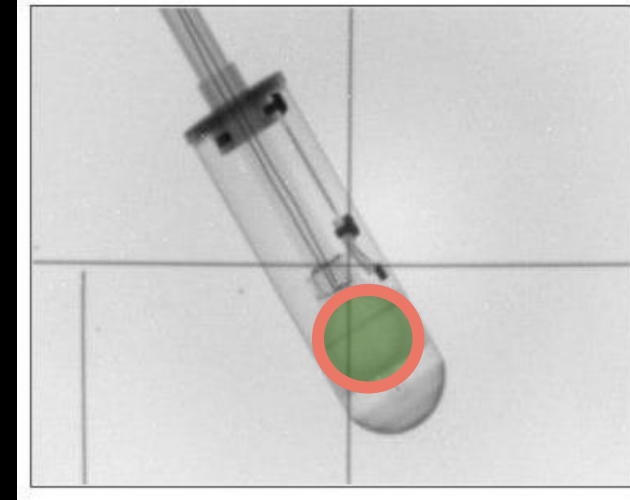
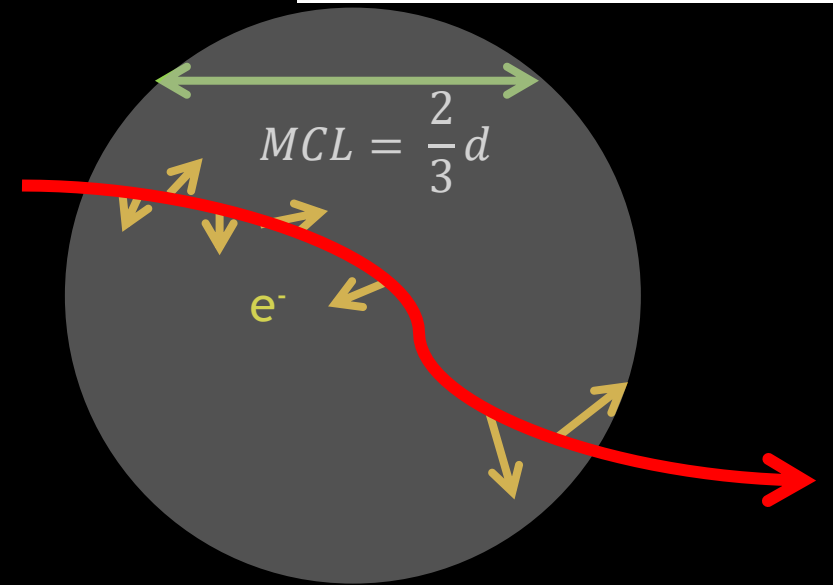
Microdosimetry main quantity

$$y = \frac{\text{Energy deposited}}{\text{MCL}}$$

Energy recorded in the detector

Mean Chord Length: average particle track length in isotropic and uniform radiation field

All particles are assumed to travel the same distance

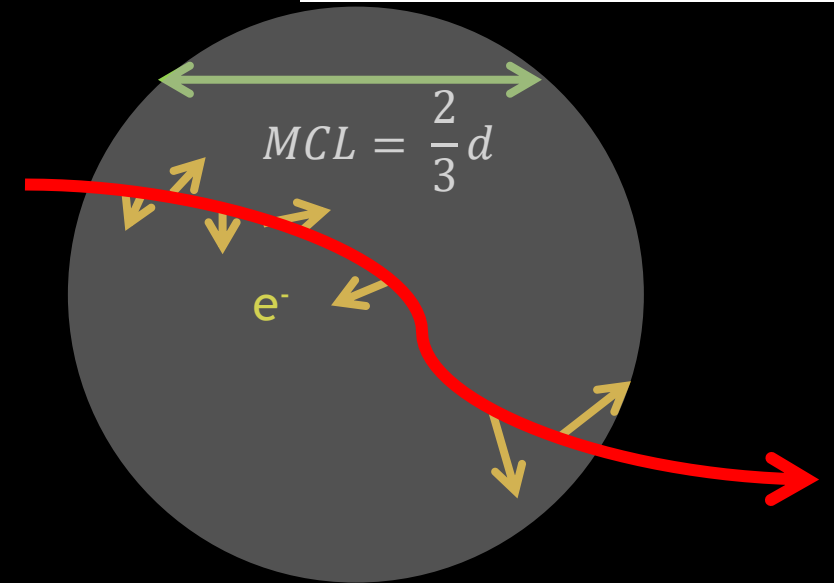
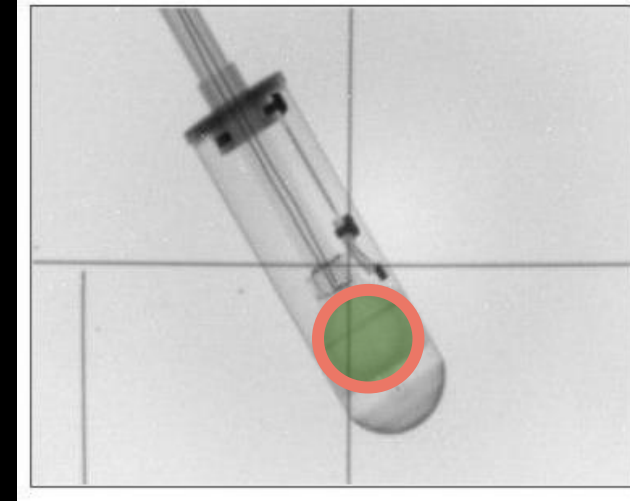


Microdosimetry main quantity

$$y = \frac{\text{Energy deposited}}{\text{MCL}}$$

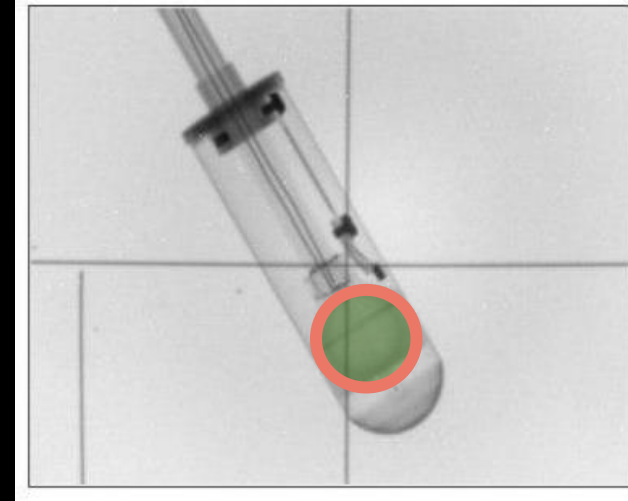
Energy recorded in the detector

Mean Chord Length: average particle track length in isotropic and uniform radiation field



All particles are assumed to travel the same distance
What if we use the **real track length**?
To provide a better radiation quality description

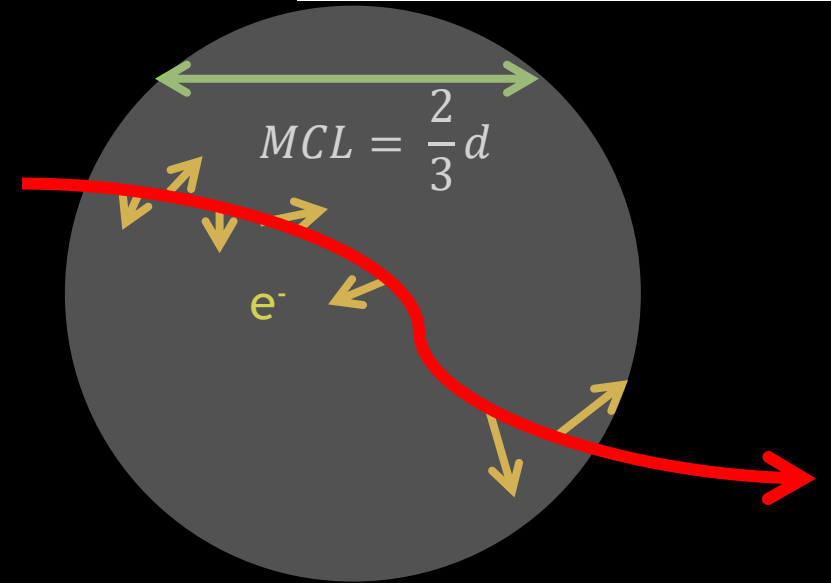
Microdosimetry main quantity



$$y = \frac{\text{Energy deposited}}{\text{MCL}}$$

Energy recorded in the detector

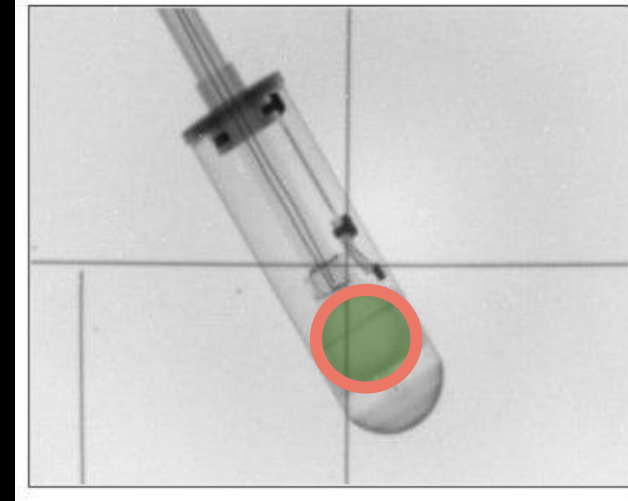
Mean Chord Length: average particle track length in isotropic and uniform radiation field



All particles are assumed to travel the same distance
What if we use the **real track length**?
To provide a better radiation quality description

$$y_t = \frac{\text{Energy deposited}}{\text{Real track length}}$$

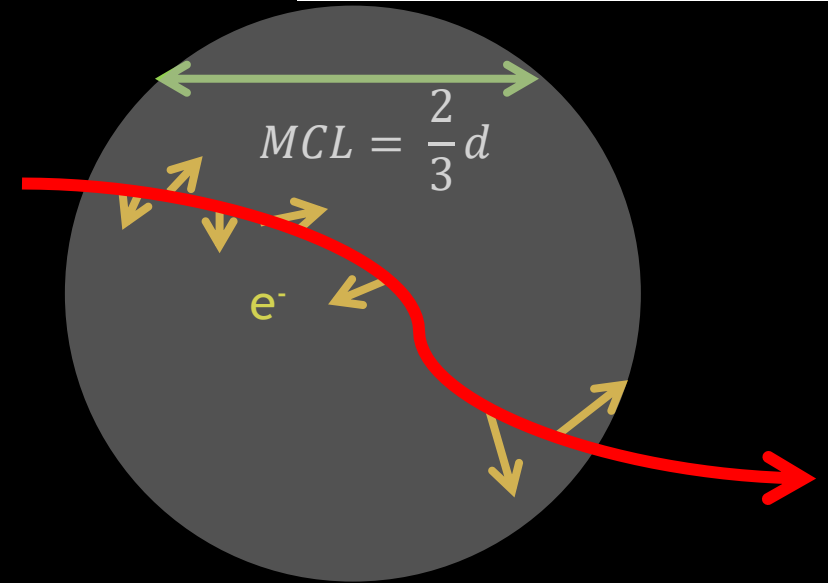
Microdosimetry main quantity



$$y = \frac{\text{Energy deposited}}{\text{MCL}}$$

Energy recorded in the detector

Mean Chord Length: average particle track length in isotropic and uniform radiation field



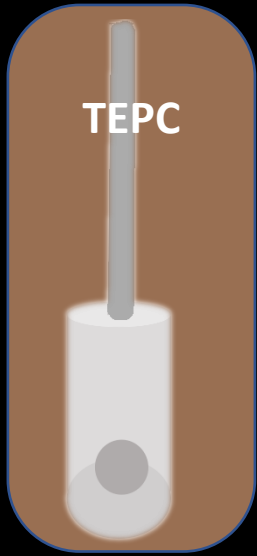
All particles are assumed to travel the same distance
What if we use the **real track length**?
To provide a better radiation quality description

$$y_t = \frac{\text{Energy deposited}}{\text{Real track length}}$$

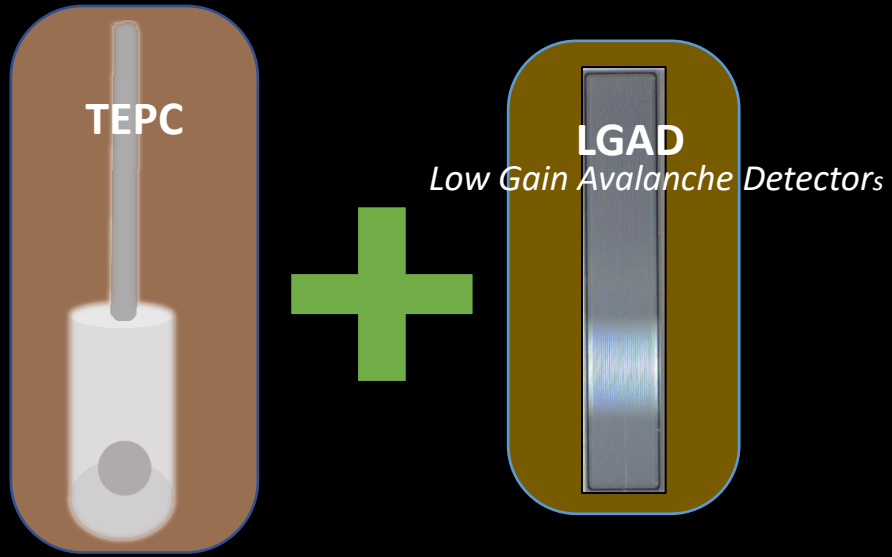
A tracker is needed

Hybrid Detector for Microdosimetry (HDM) design

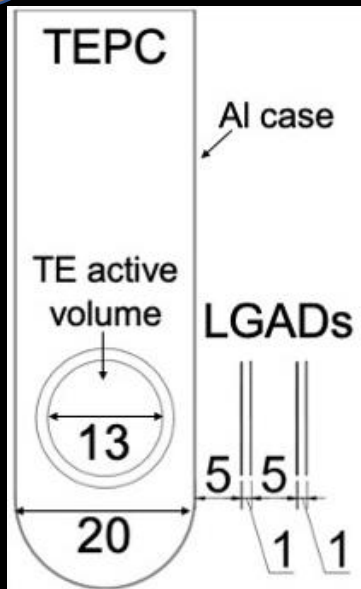
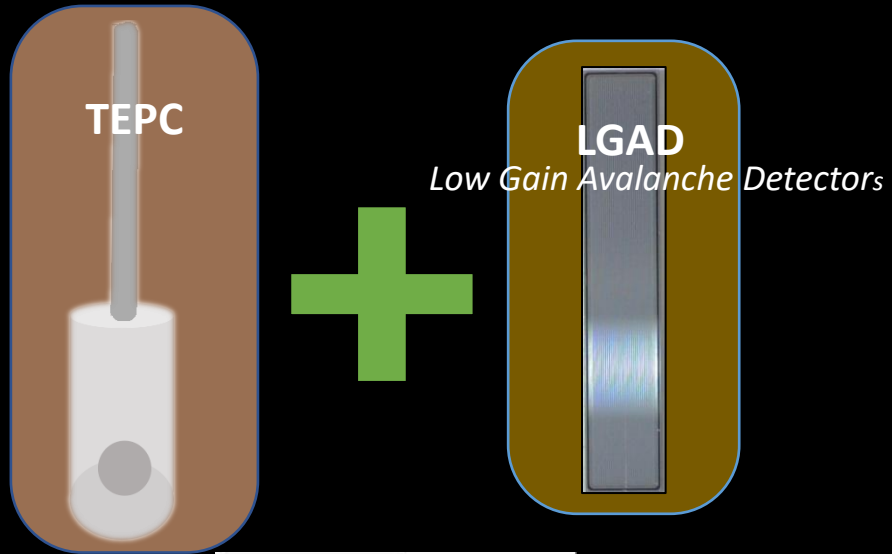
Hybrid Detector for Microdosimetry (HDM) design



Hybrid Detector for Microdosimetry (HDM) design

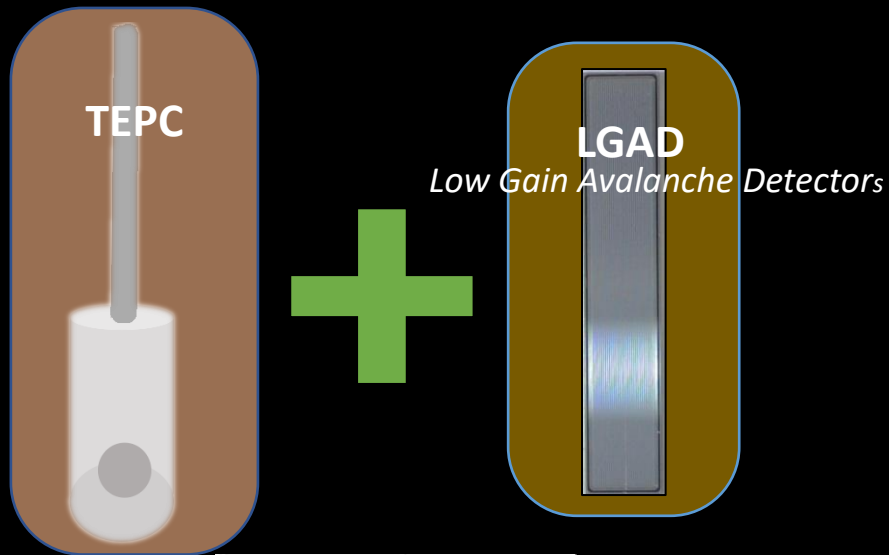


Hybrid Detector for Microdosimetry (HDM) design

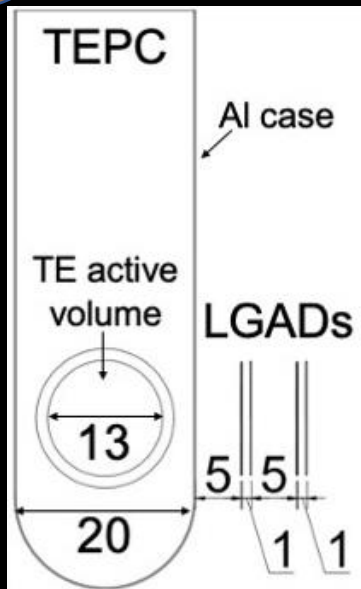
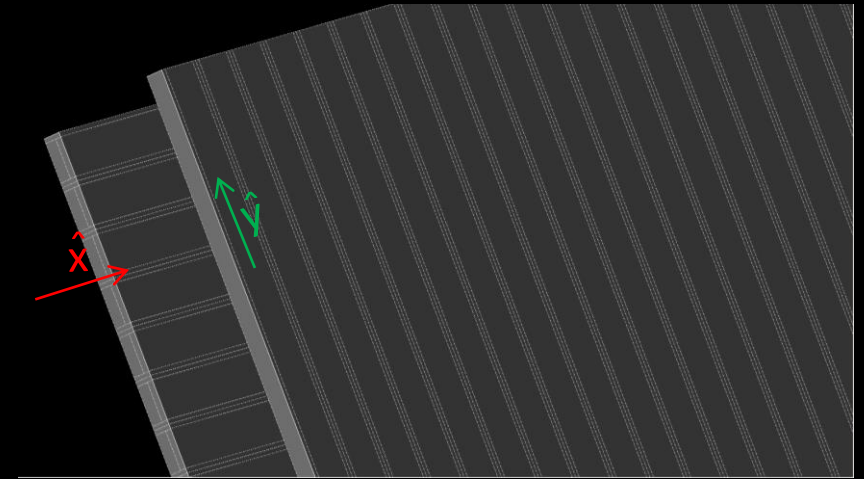


Units in mm

Hybrid Detector for Microdosimetry (HDM) design

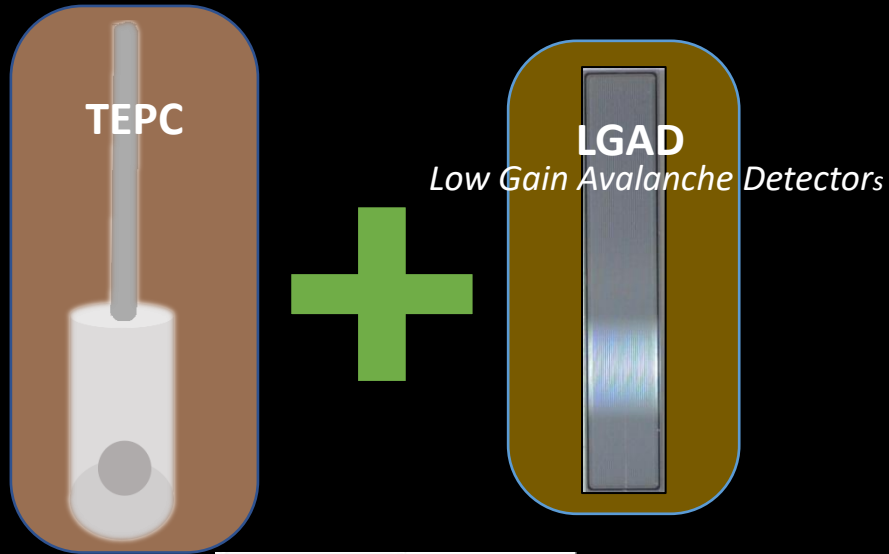


Strip is activated

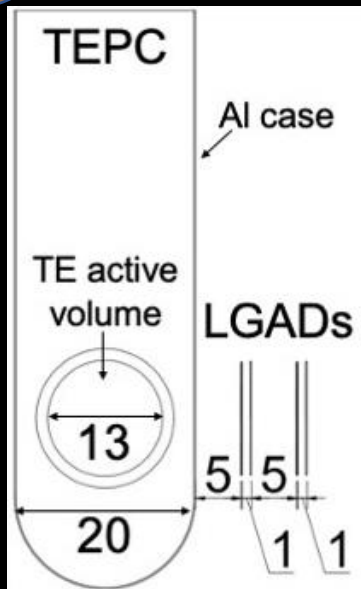
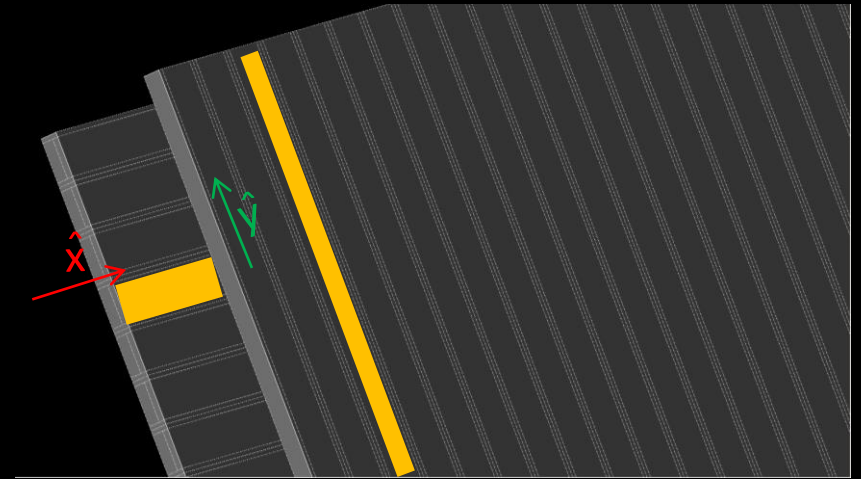


Units in mm

Hybrid Detector for Microdosimetry (HDM) design

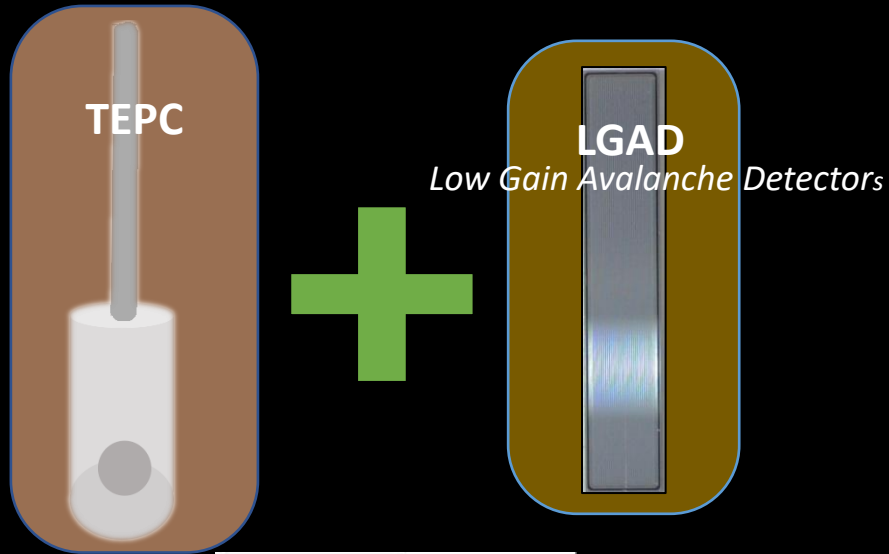


Strip is activated

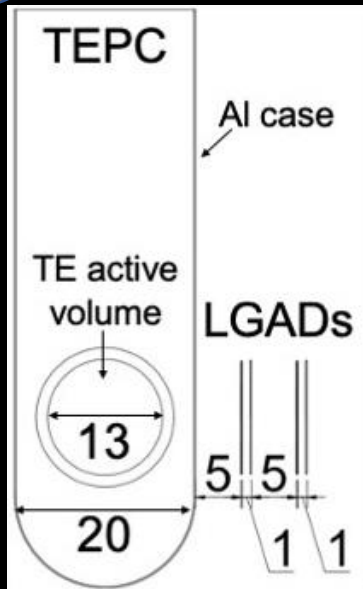
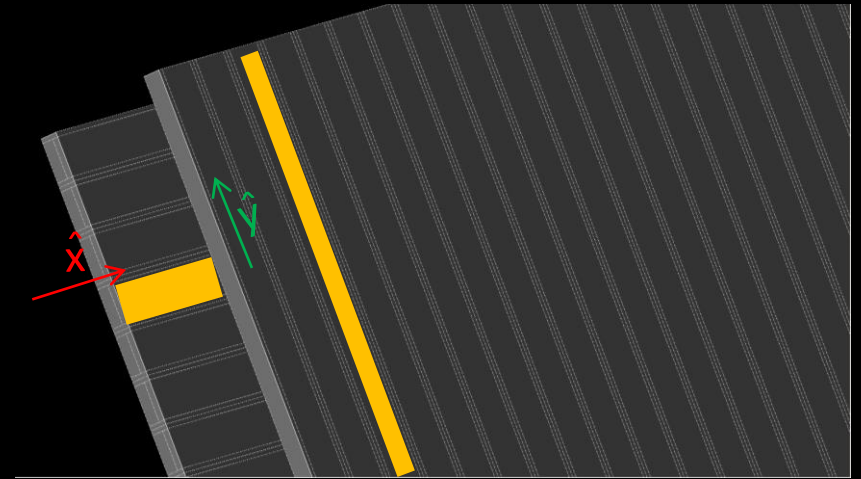


Units in mm

Hybrid Detector for Microdosimetry (HDM) design



Strip is activated



Units in mm

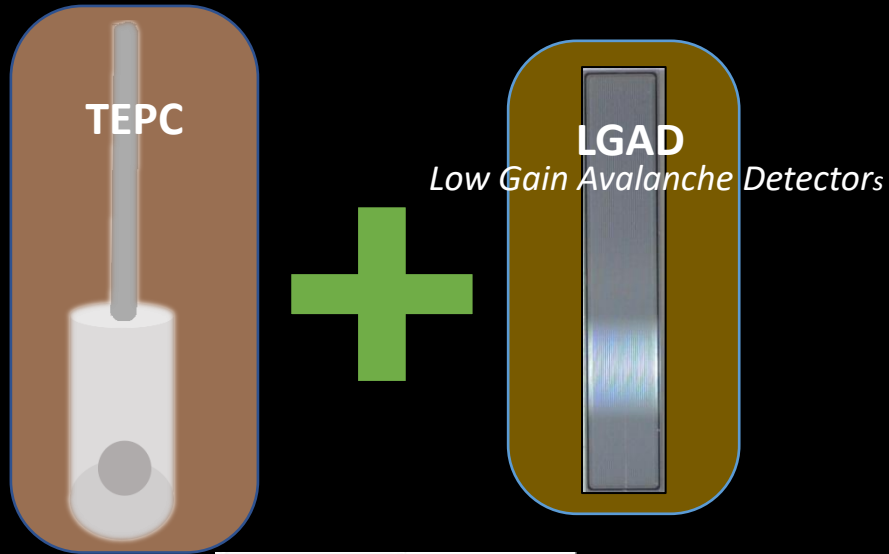


Tissue equivalent proportional counter

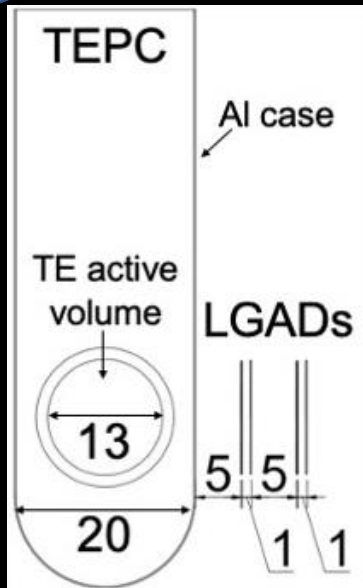
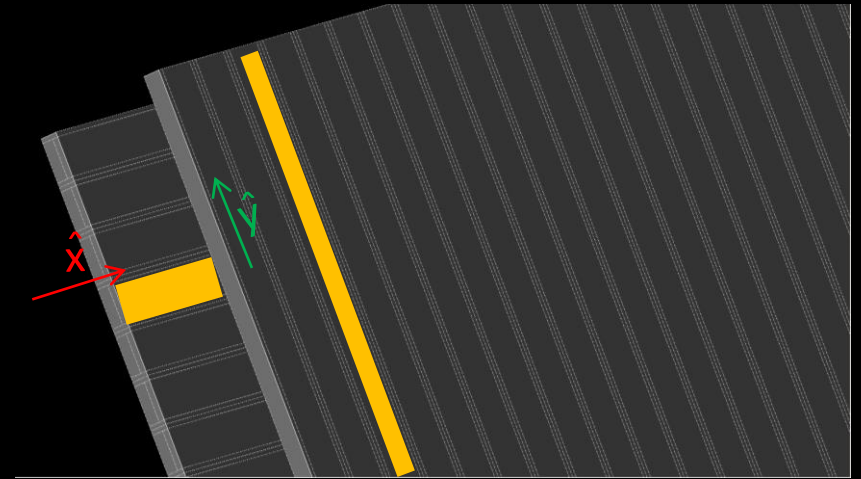


Low Gain Avalanche Detector

Hybrid Detector for Microdosimetry (HDM) design

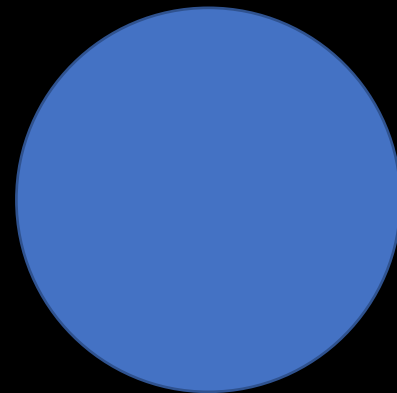


Strip is activated



Units in mm

4 Planes (\hat{x} , \hat{y}) to reconstruct the track

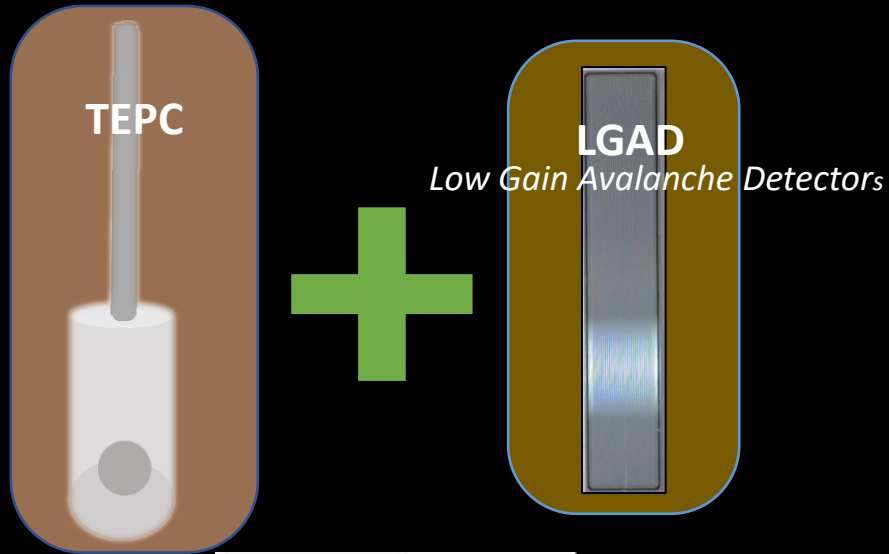


Tissue equivalent proportional counter

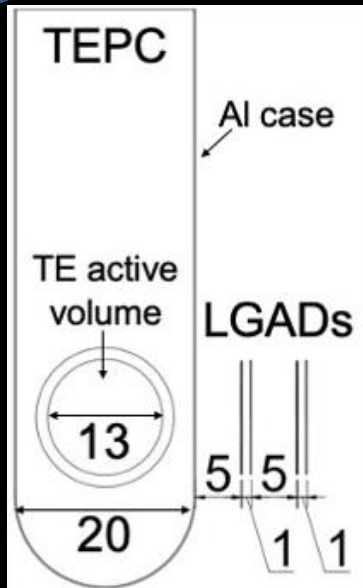
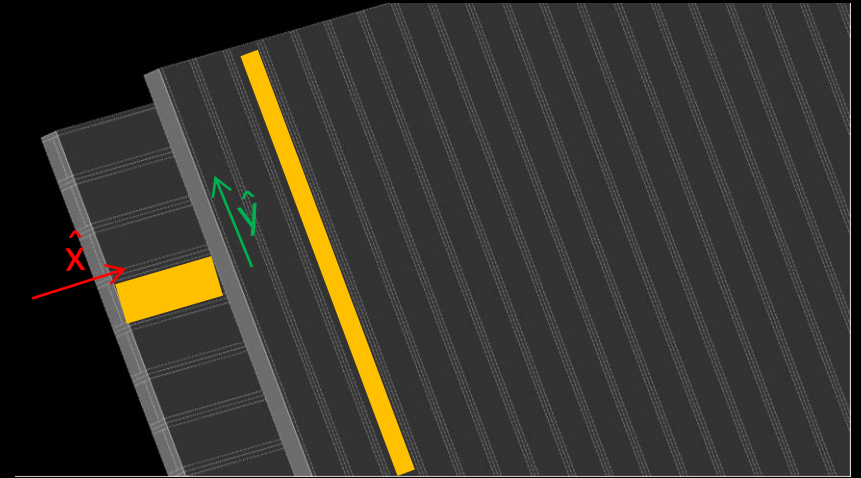


Low Gain Avalanche Detector

Hybrid Detector for Microdosimetry (HDM) design

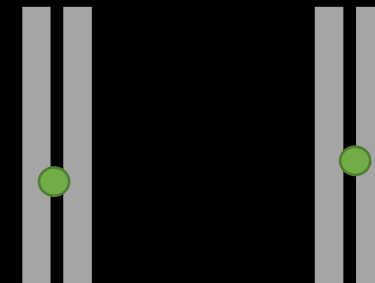
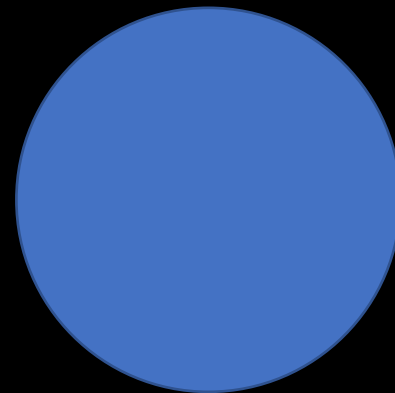


Strip is activated

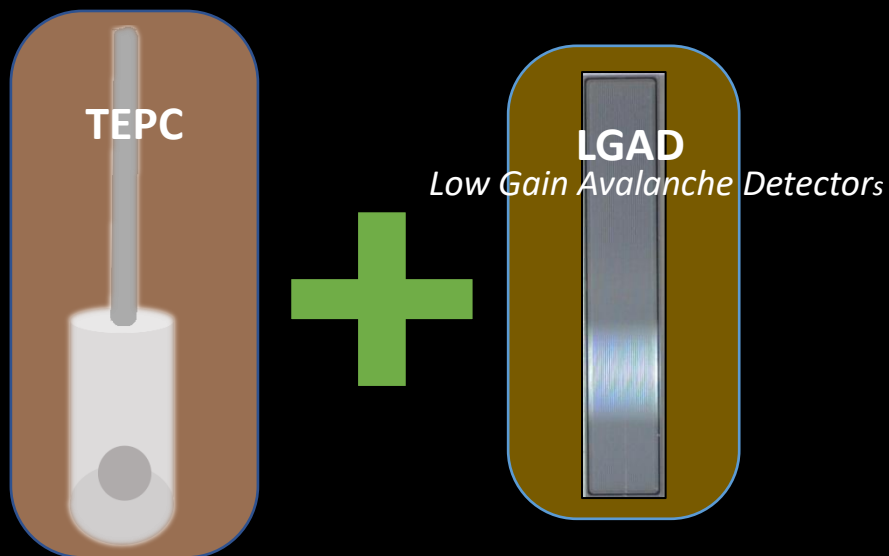


Units in mm

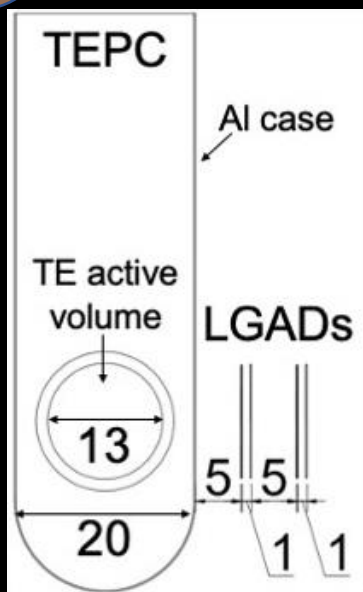
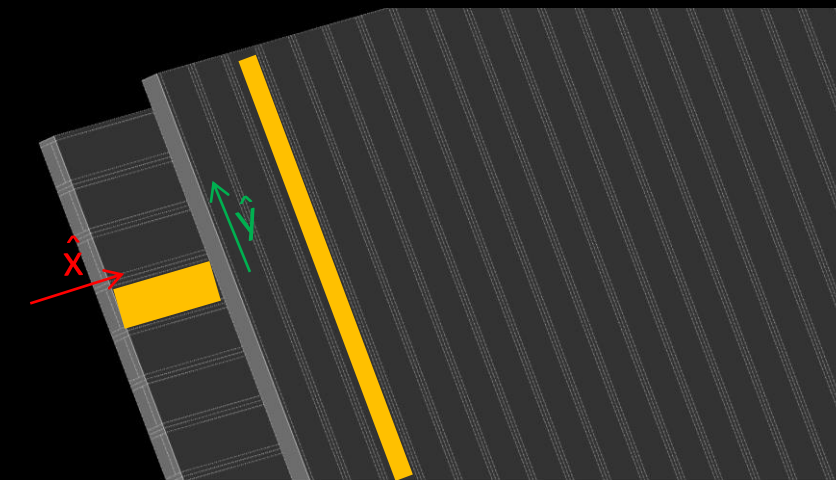
4 Planes (\hat{x} , \hat{y}) to reconstruct the track



Hybrid Detector for Microdosimetry (HDM) design

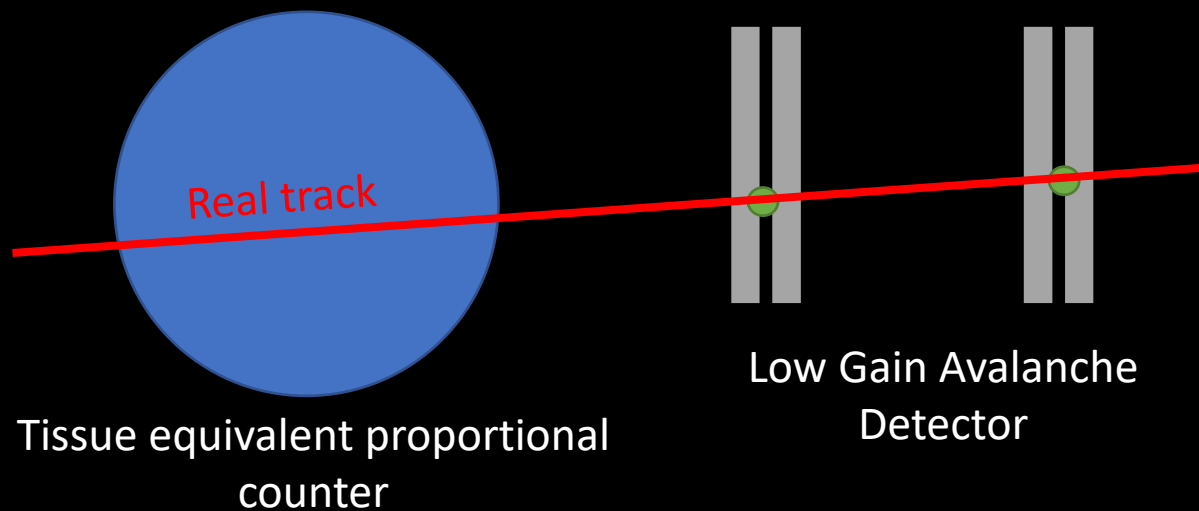


Strip is activated

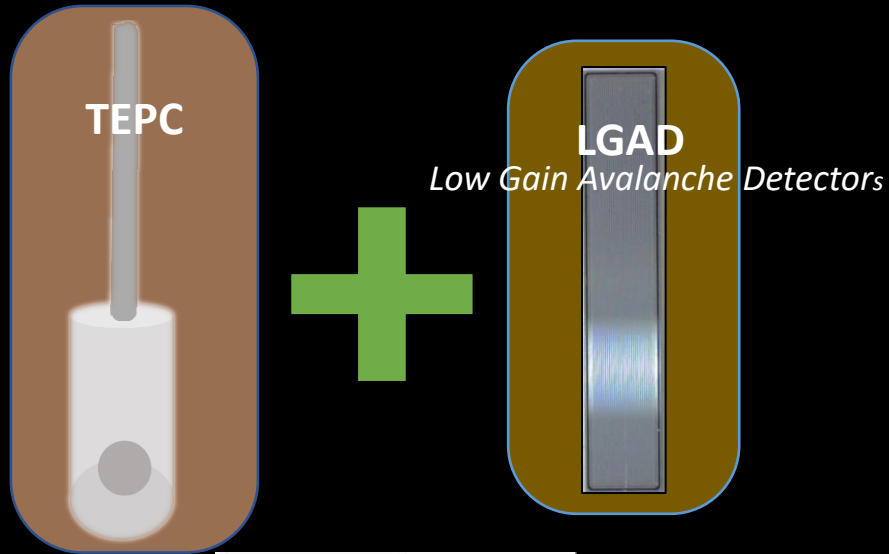


Units in mm

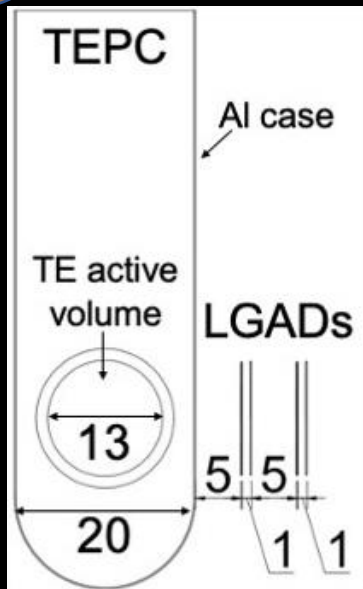
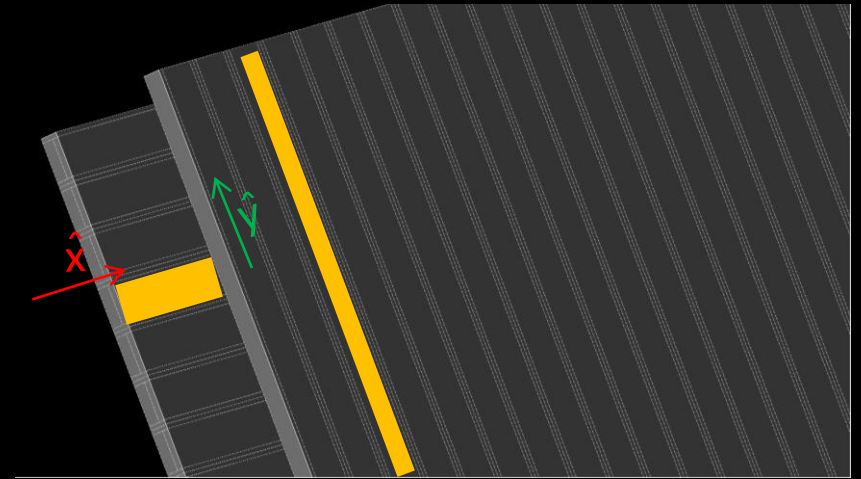
4 Planes ($2-x$, $2-y$) to reconstruct the track



Hybrid Detector for Microdosimetry (HDM) design

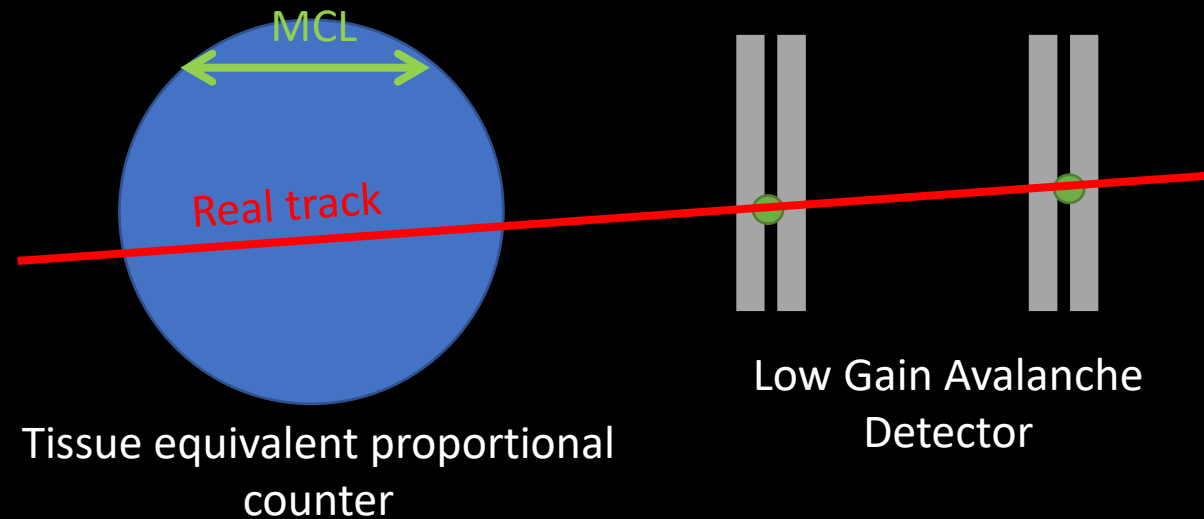


Strip is activated



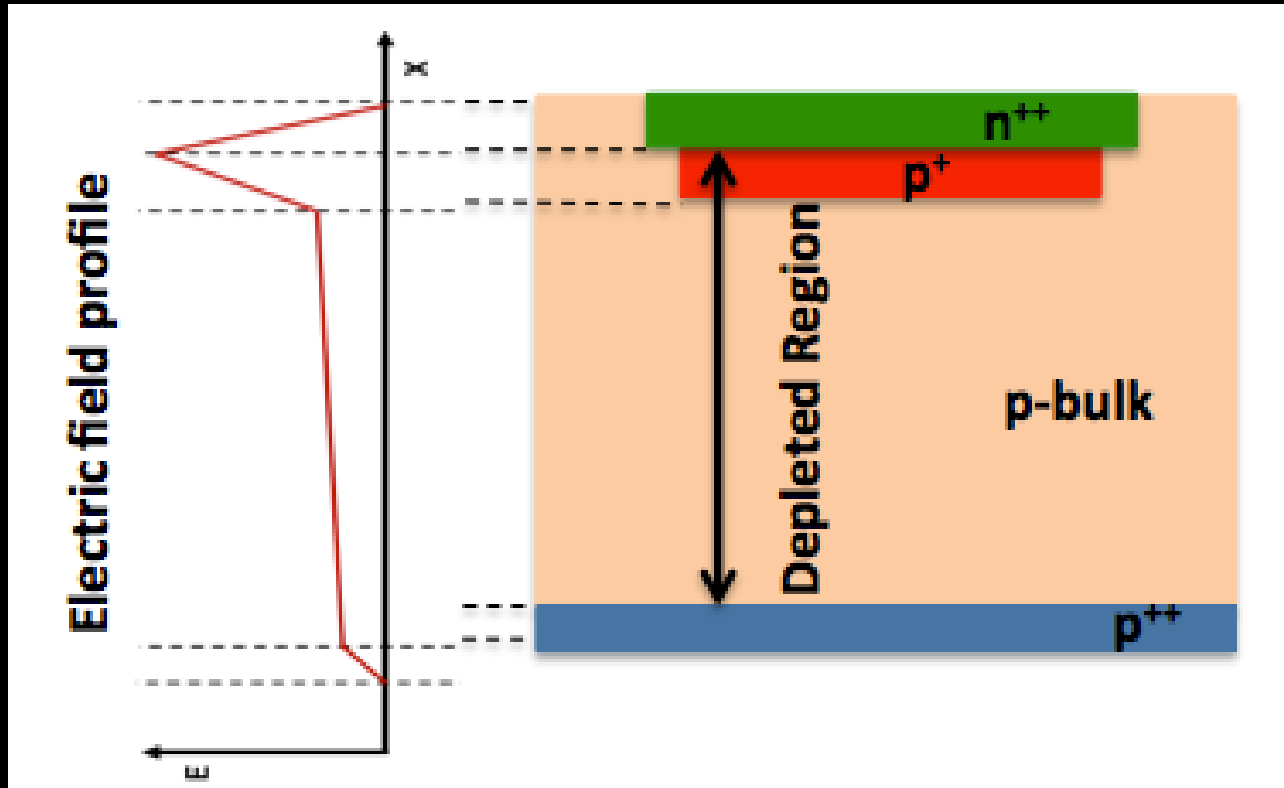
Units in mm

4 Planes ($\hat{2-x}$, $\hat{2-y}$) to reconstruct the track

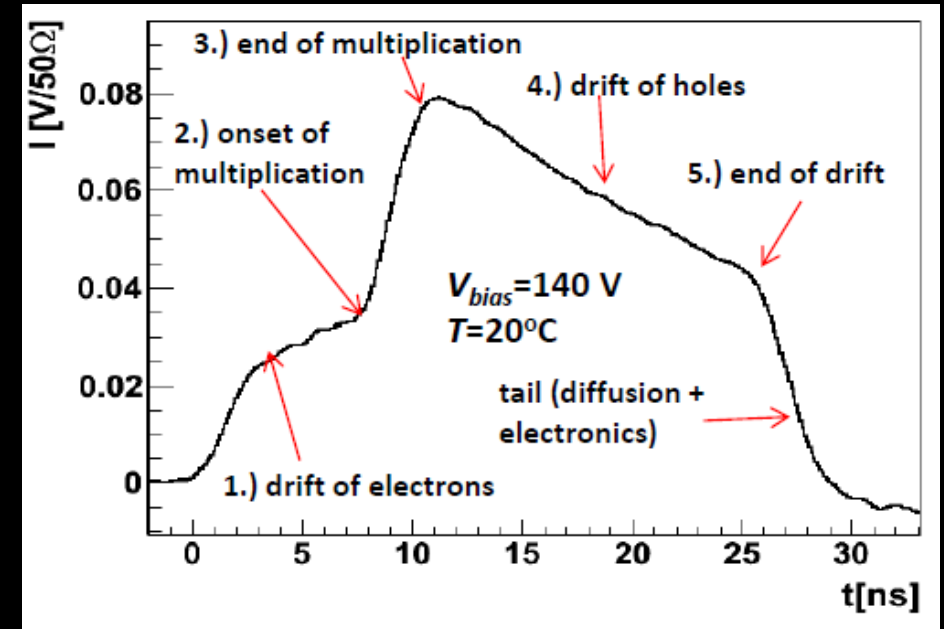
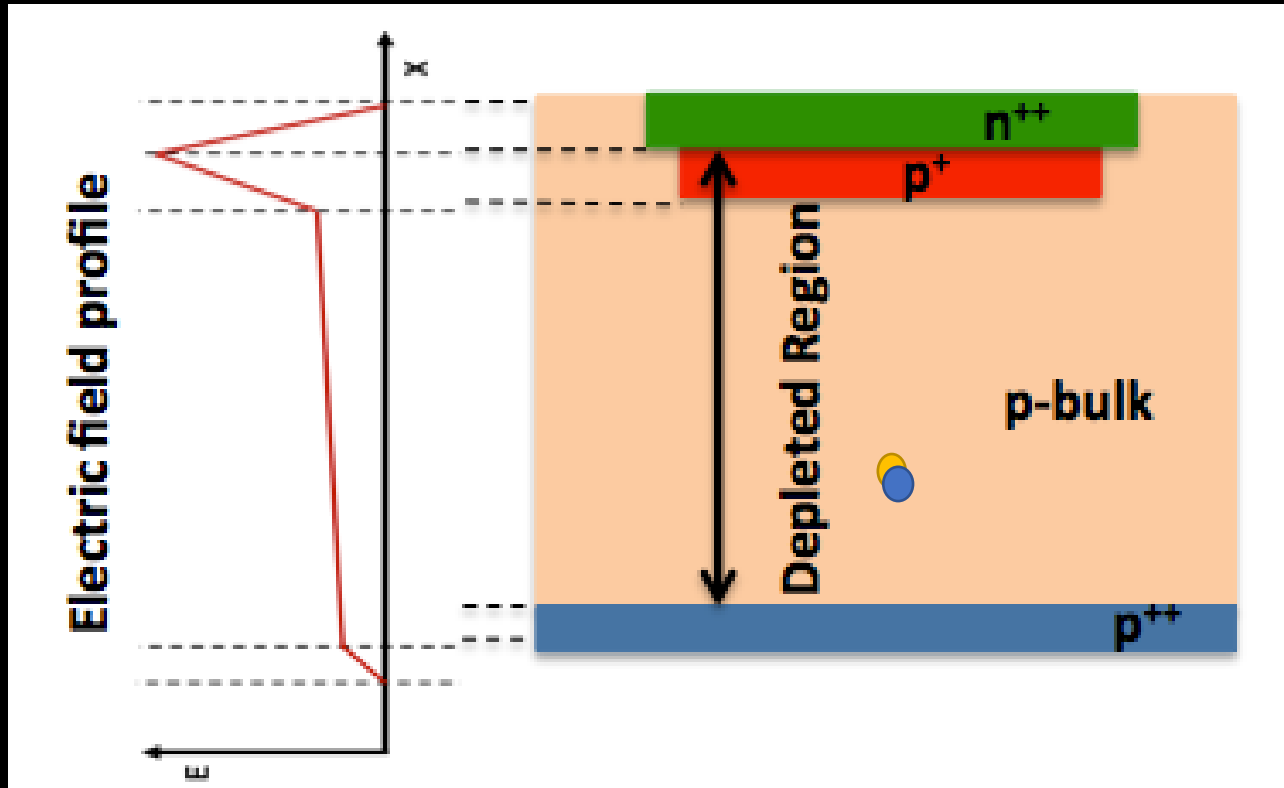


Low Gain Avalanche Diode (LGAD) detectors

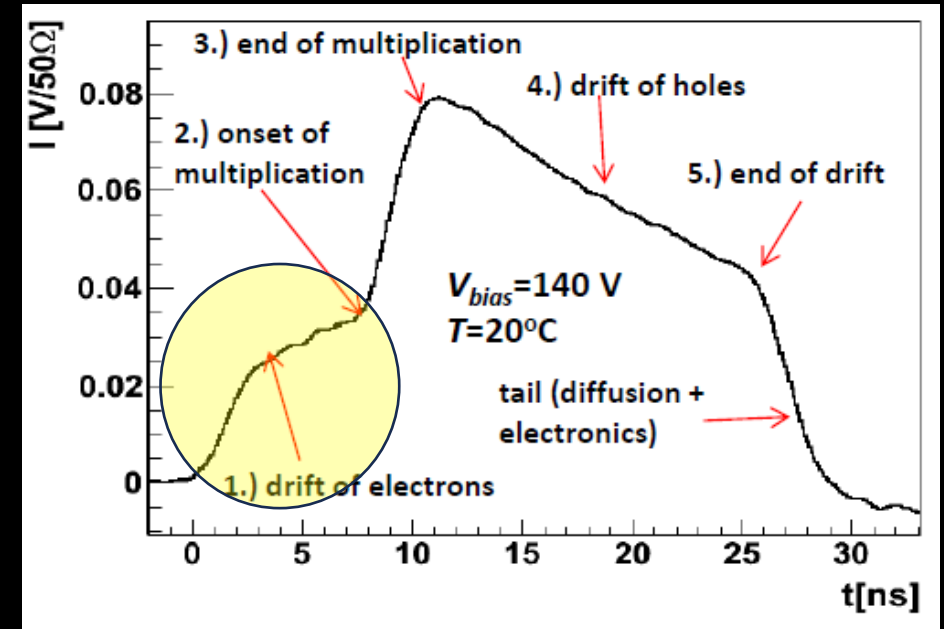
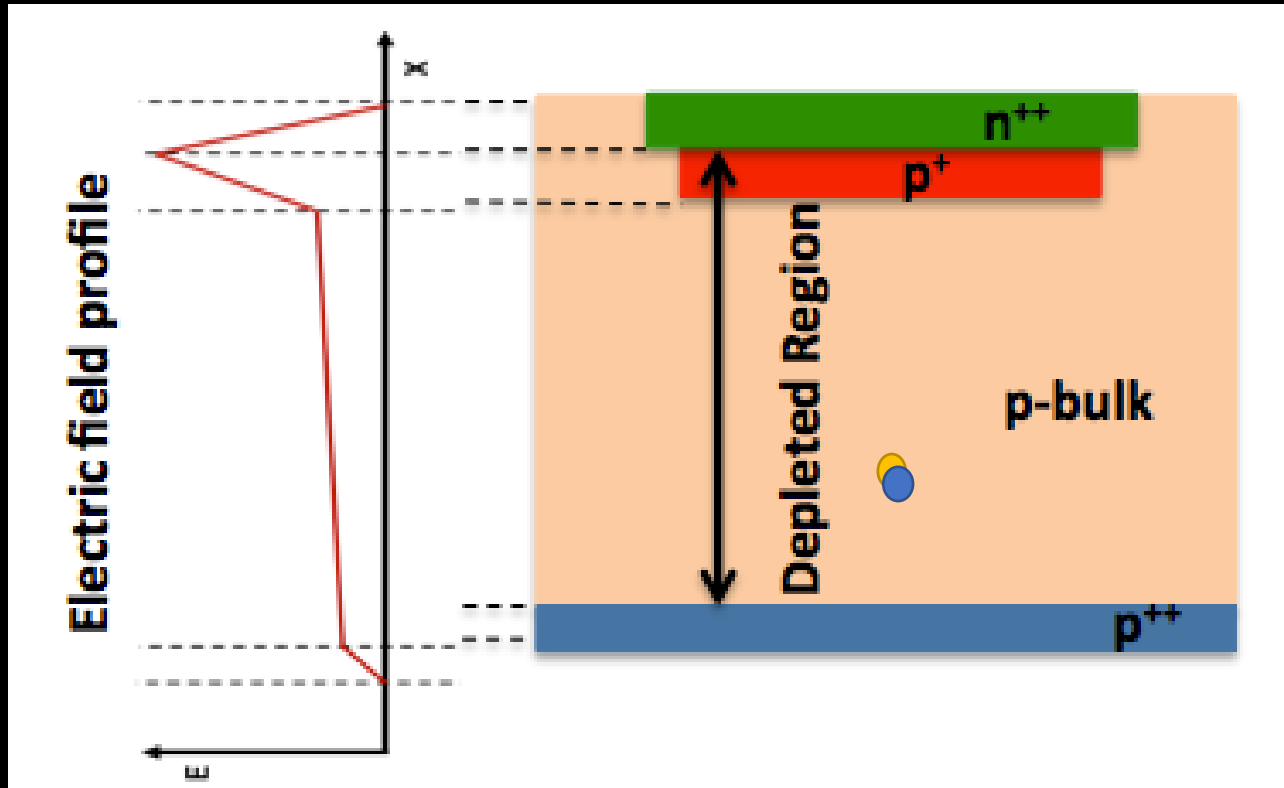
Low Gain Avalanche Diode (LGAD) detectors



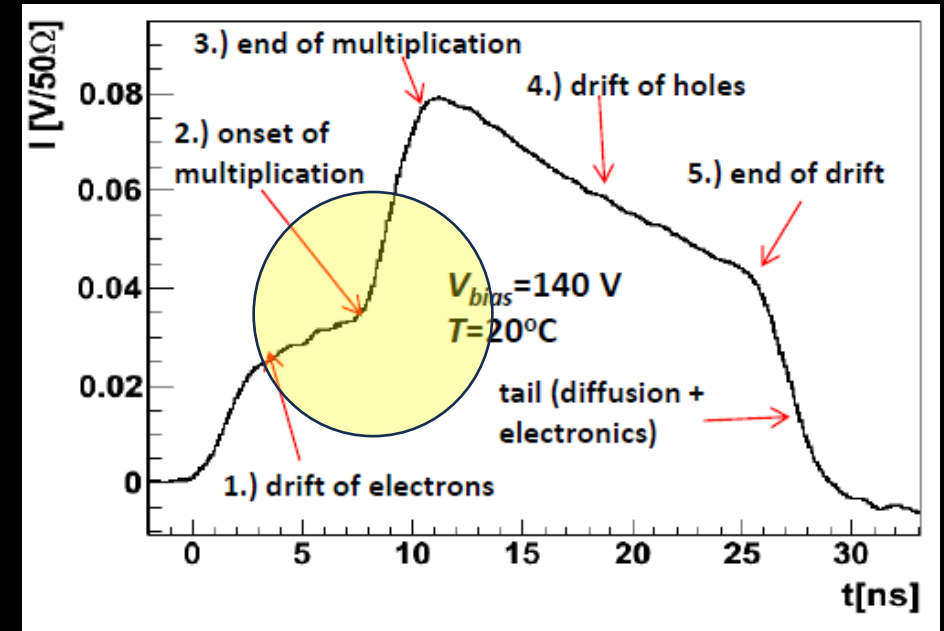
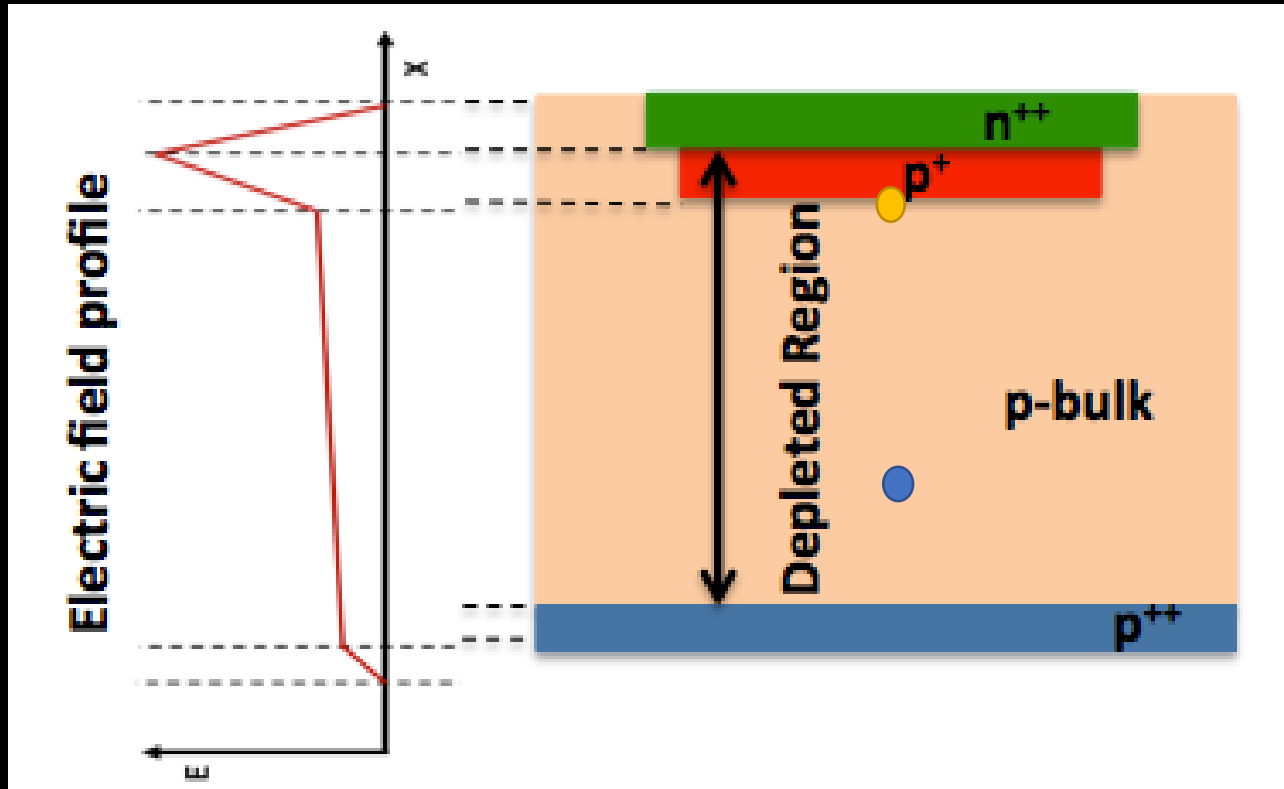
Low Gain Avalanche Diode (LGAD) detectors



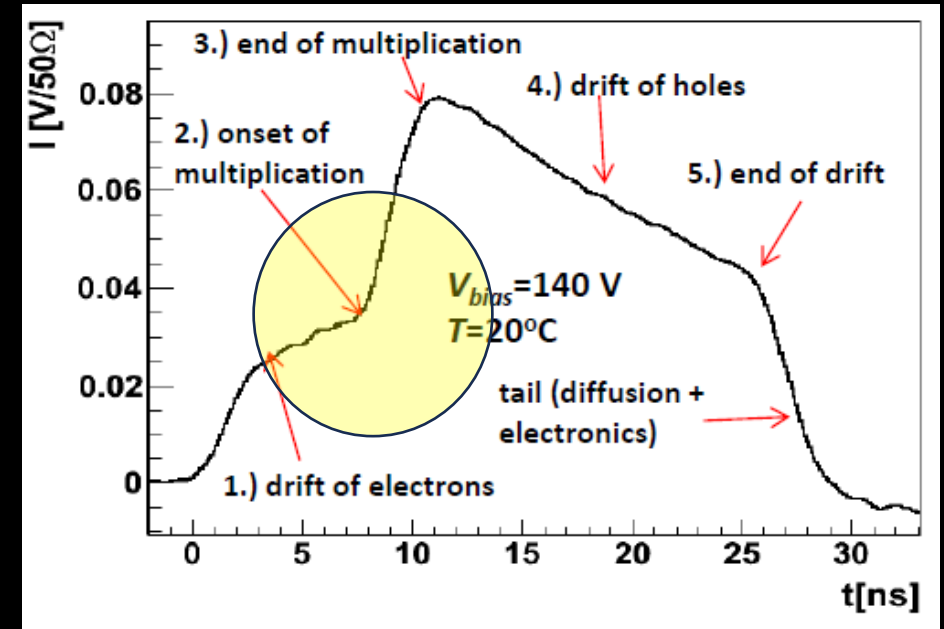
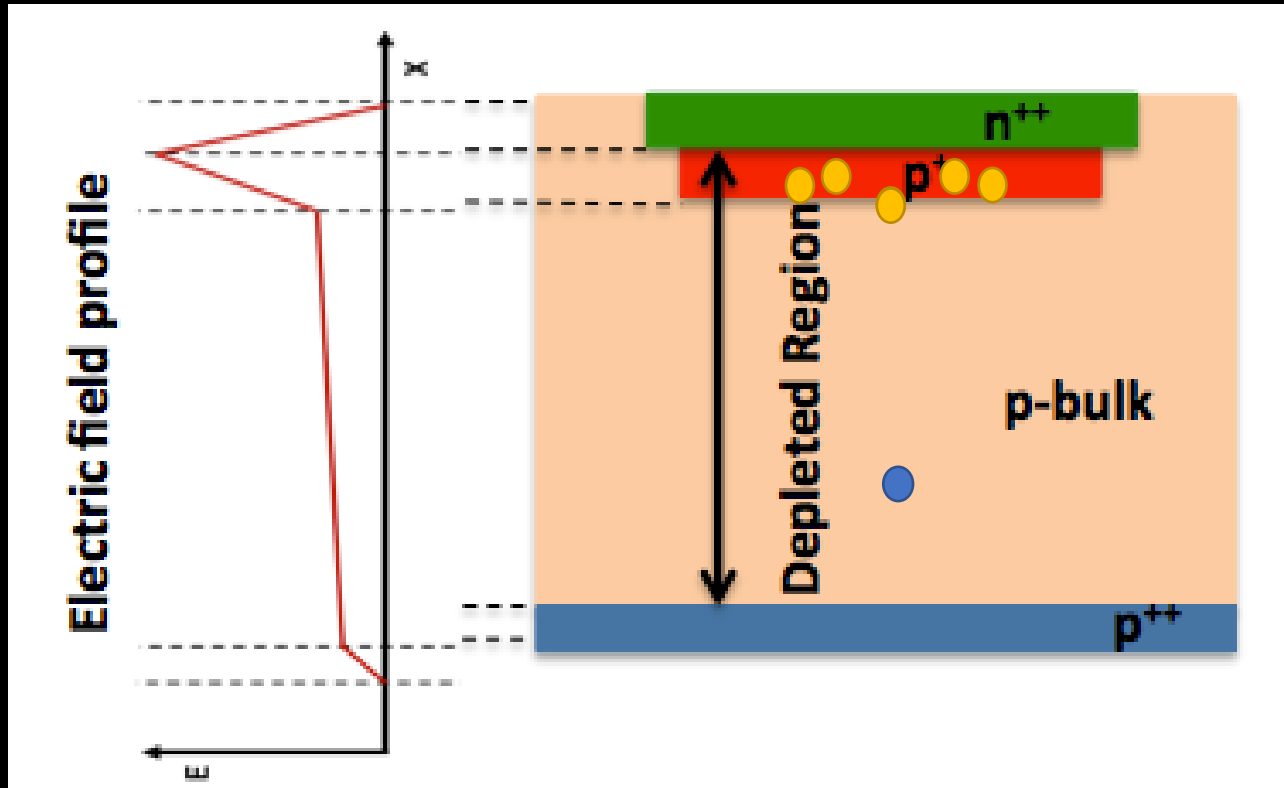
Low Gain Avalanche Diode (LGAD) detectors



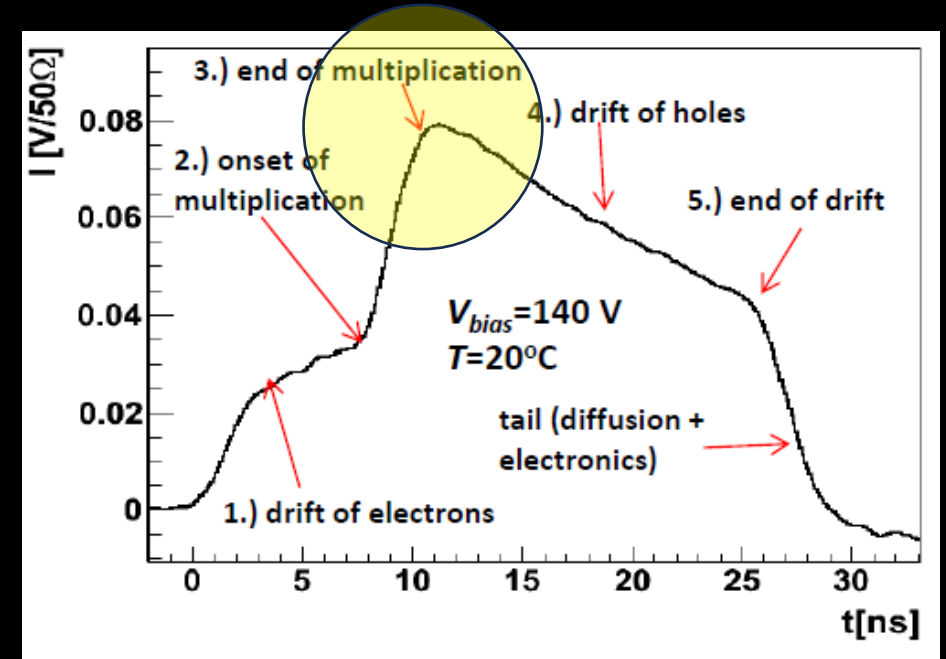
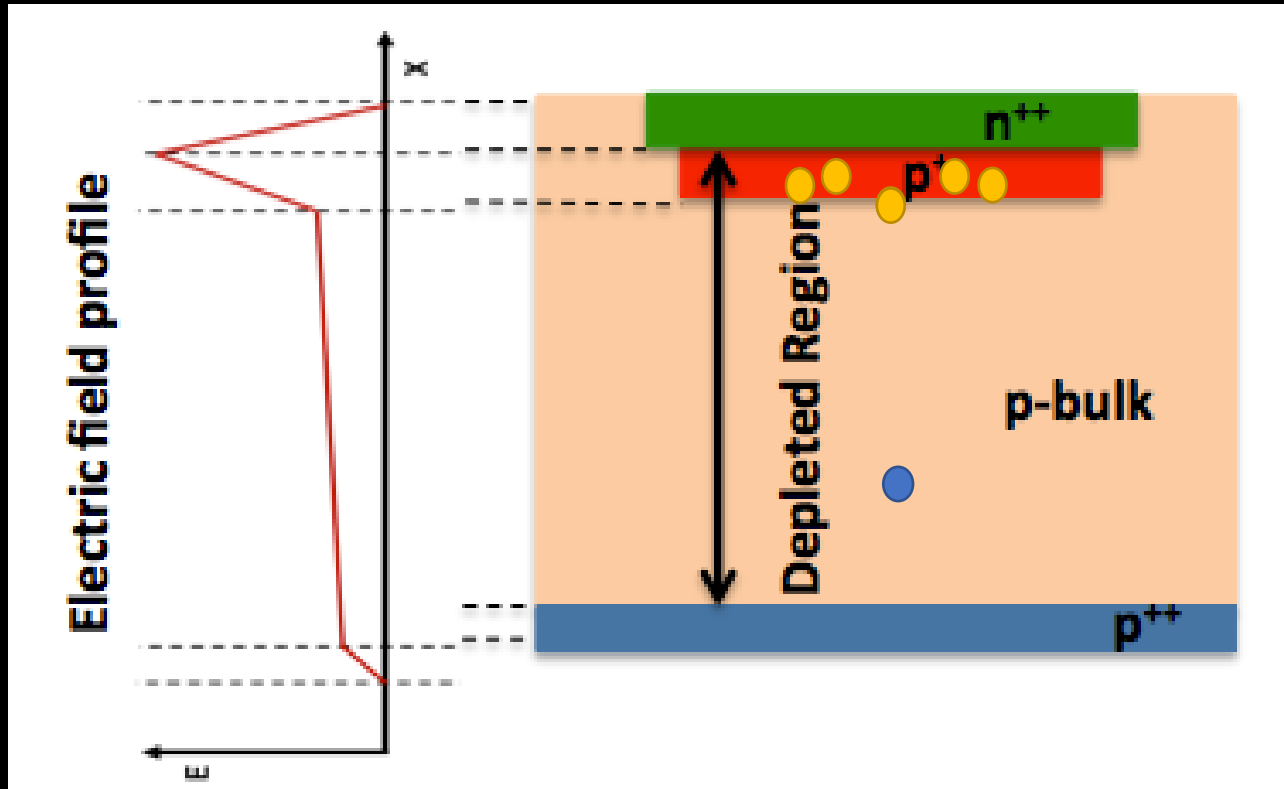
Low Gain Avalanche Diode (LGAD) detectors



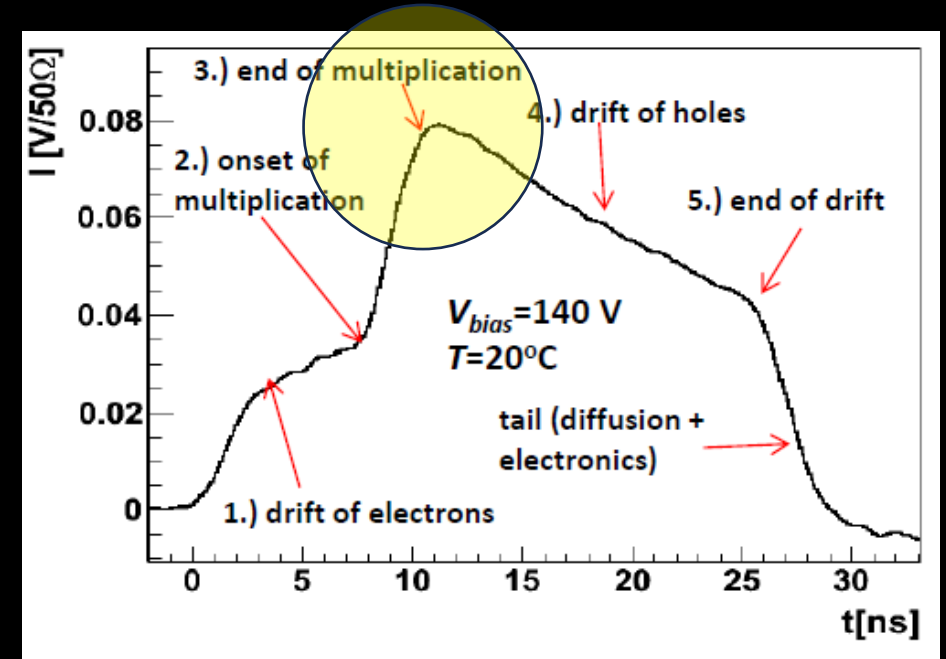
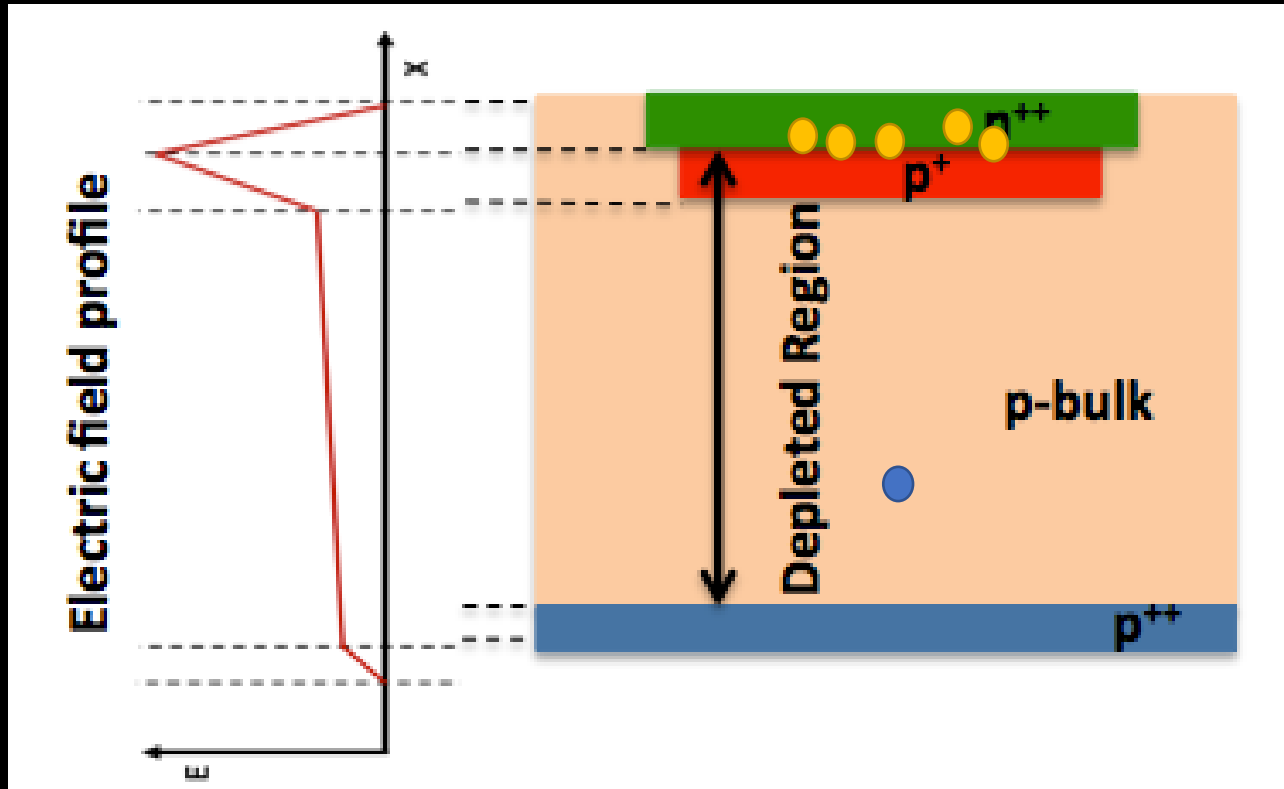
Low Gain Avalanche Diode (LGAD) detectors



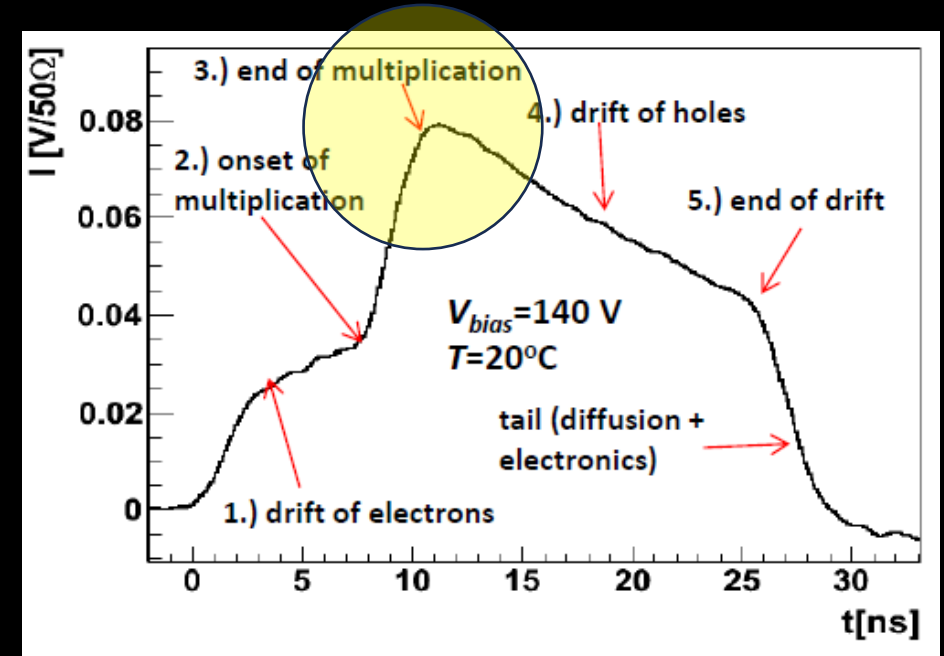
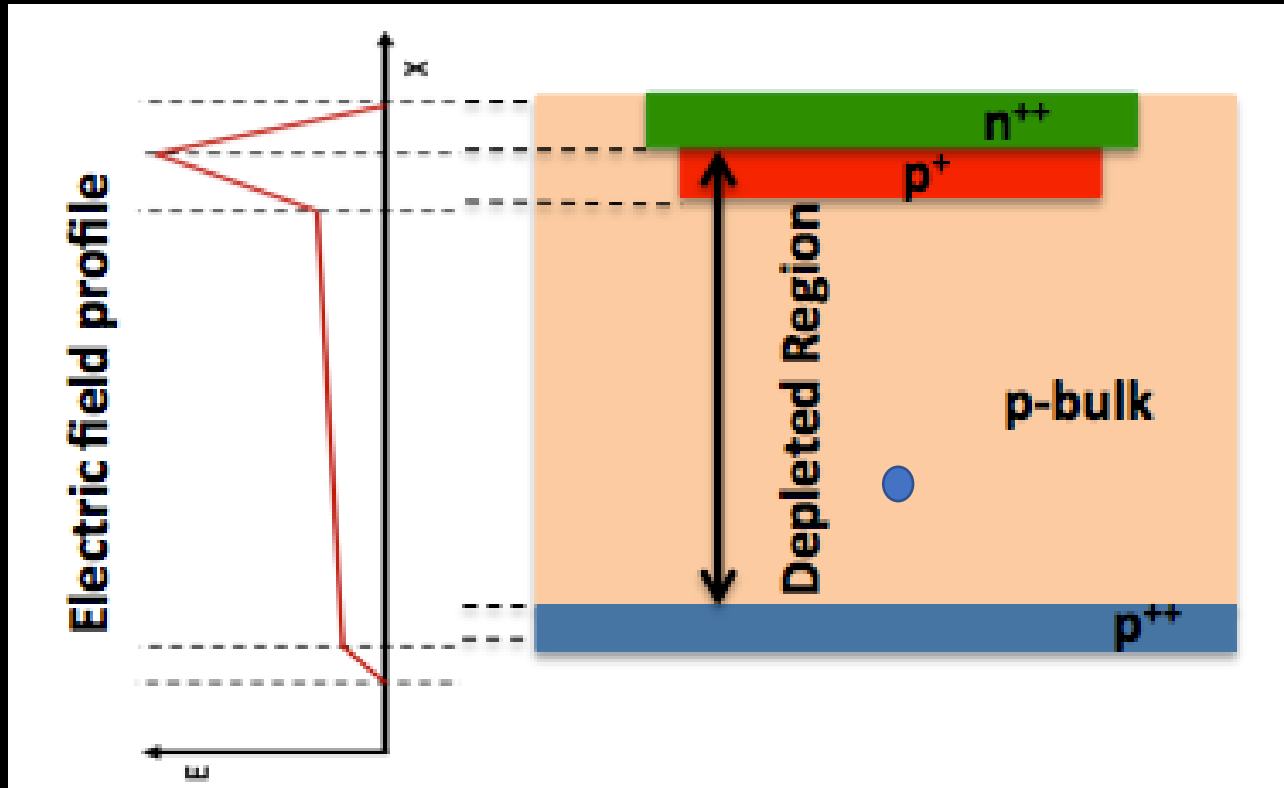
Low Gain Avalanche Diode (LGAD) detectors



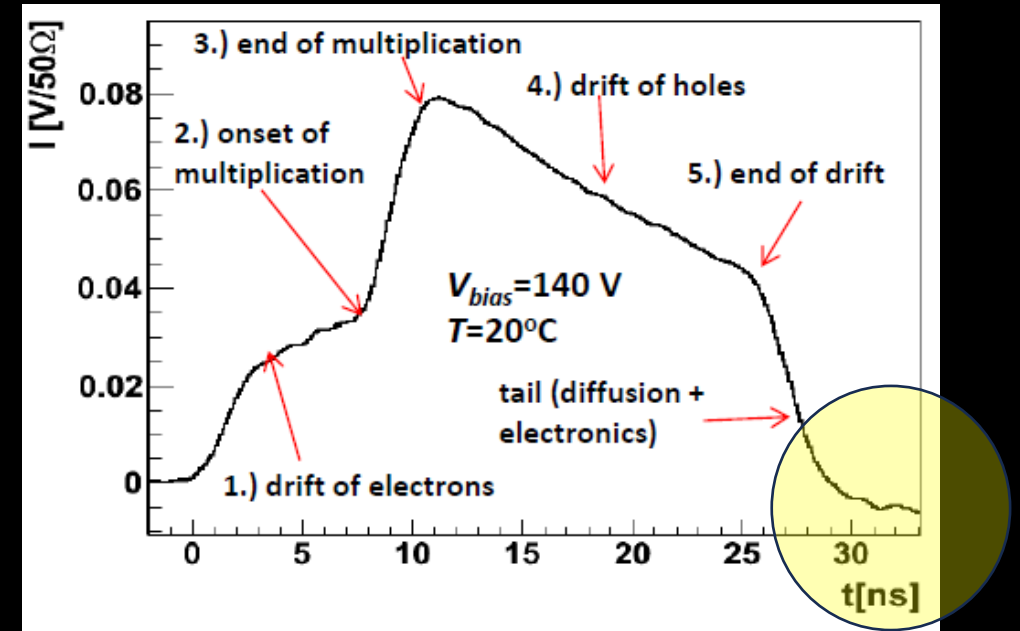
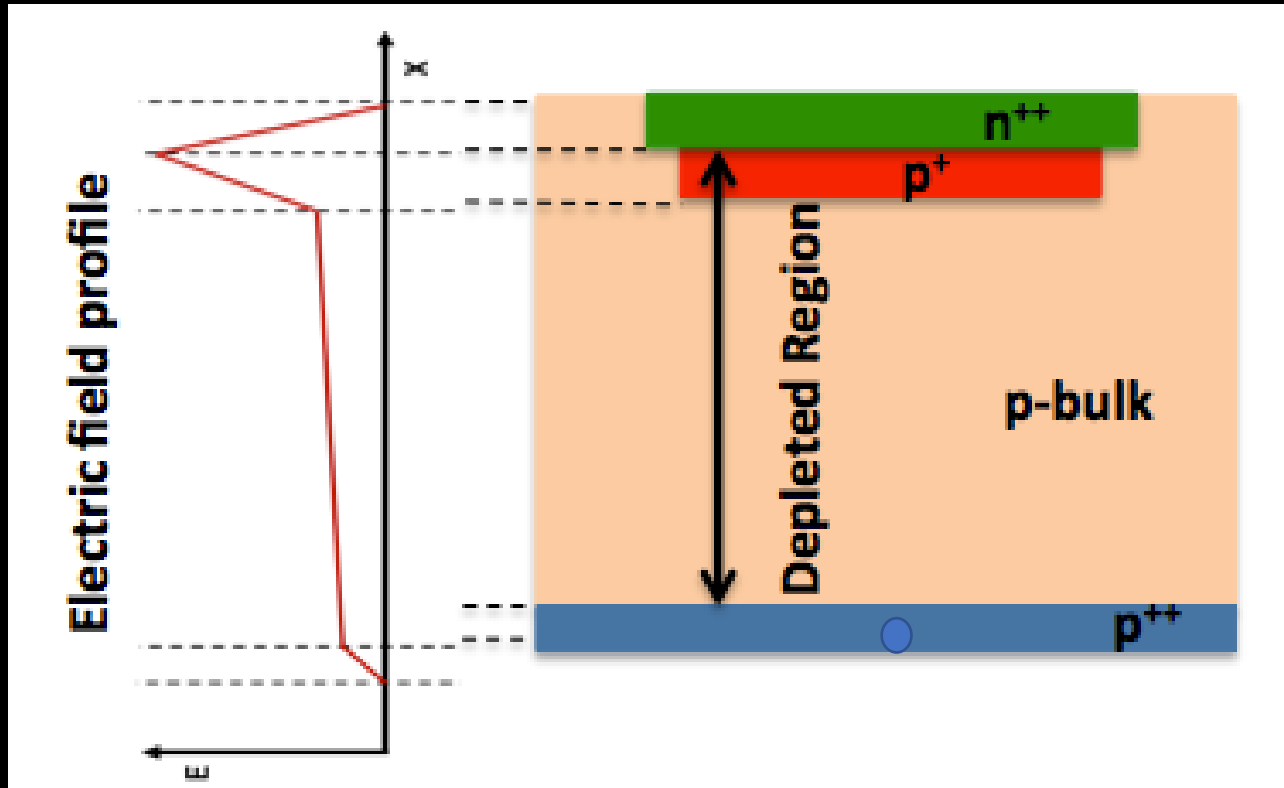
Low Gain Avalanche Diode (LGAD) detectors



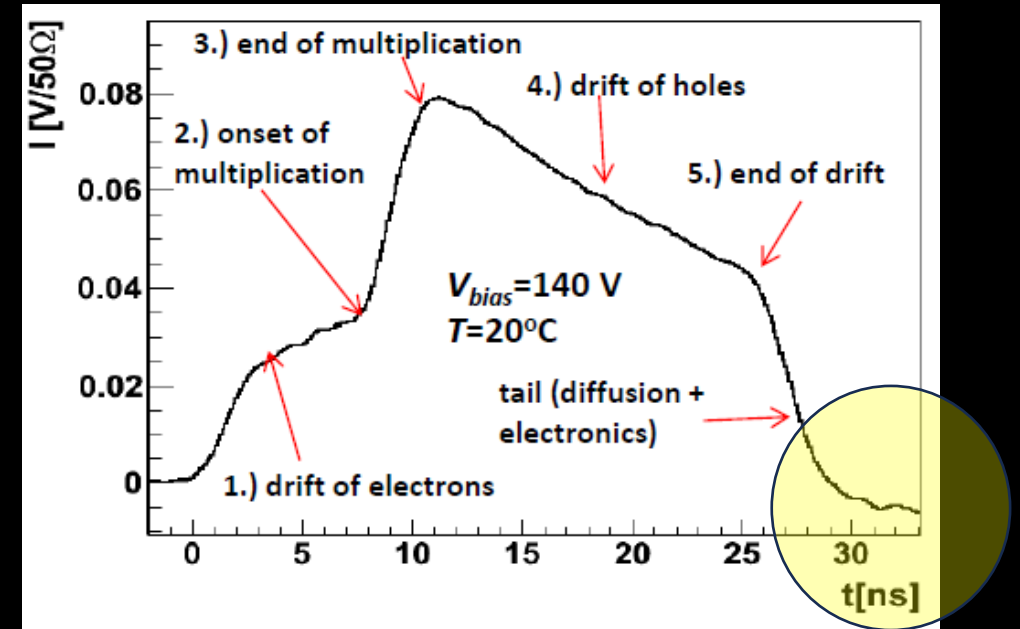
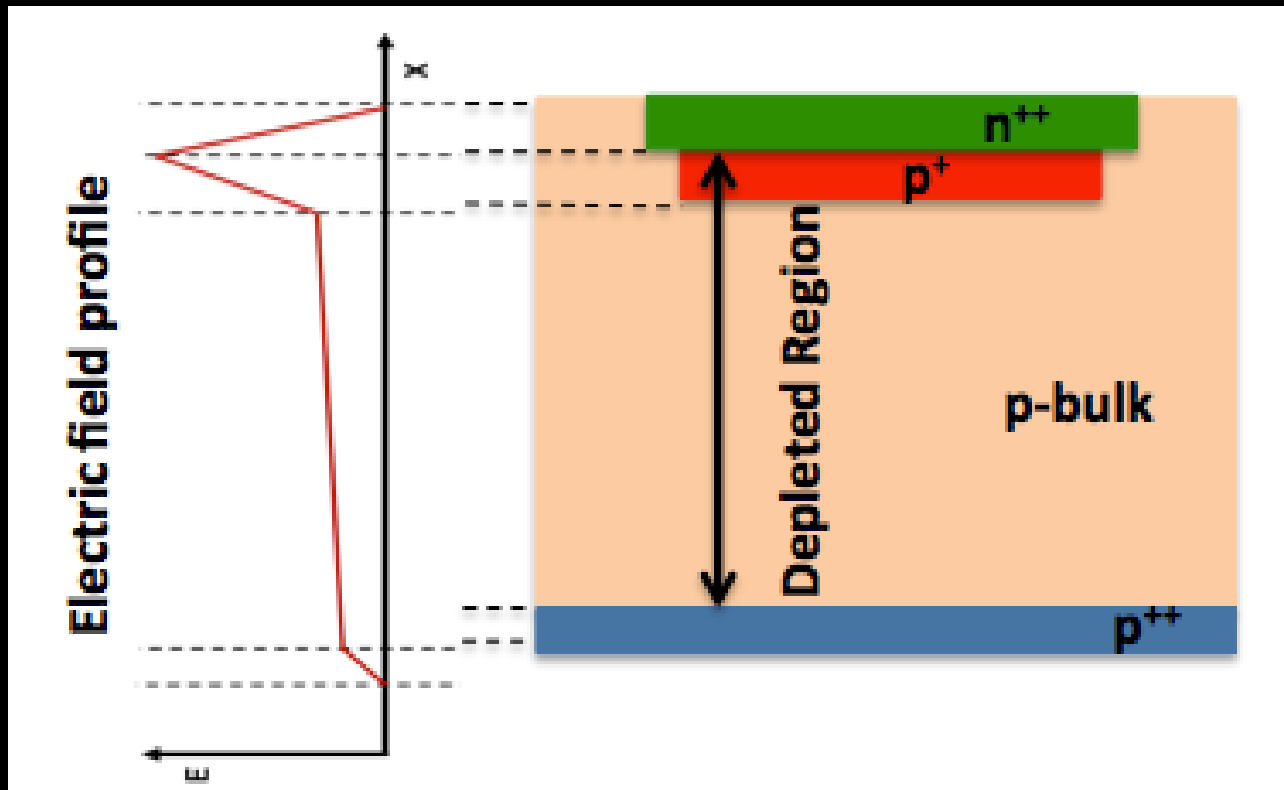
Low Gain Avalanche Diode (LGAD) detectors



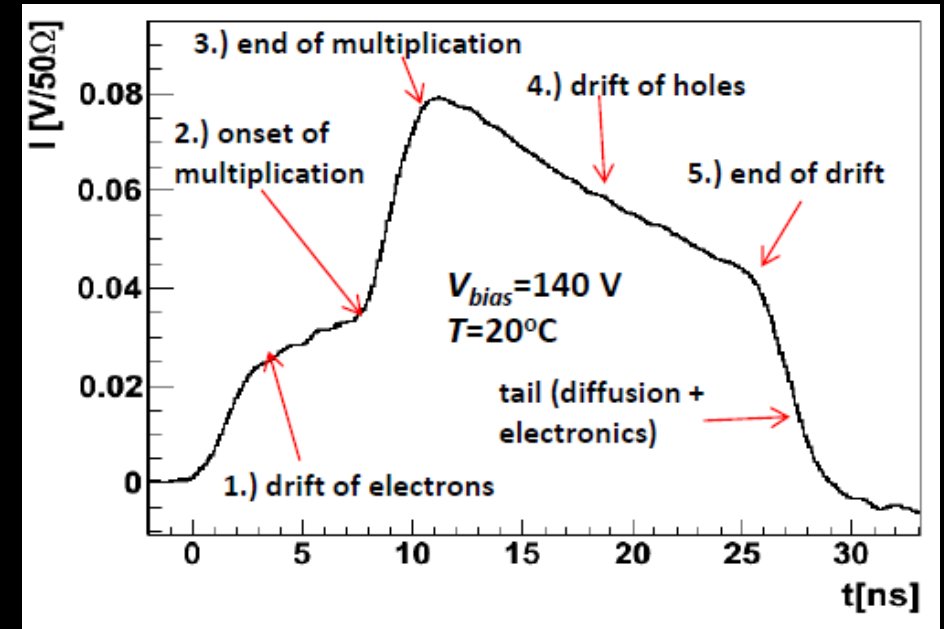
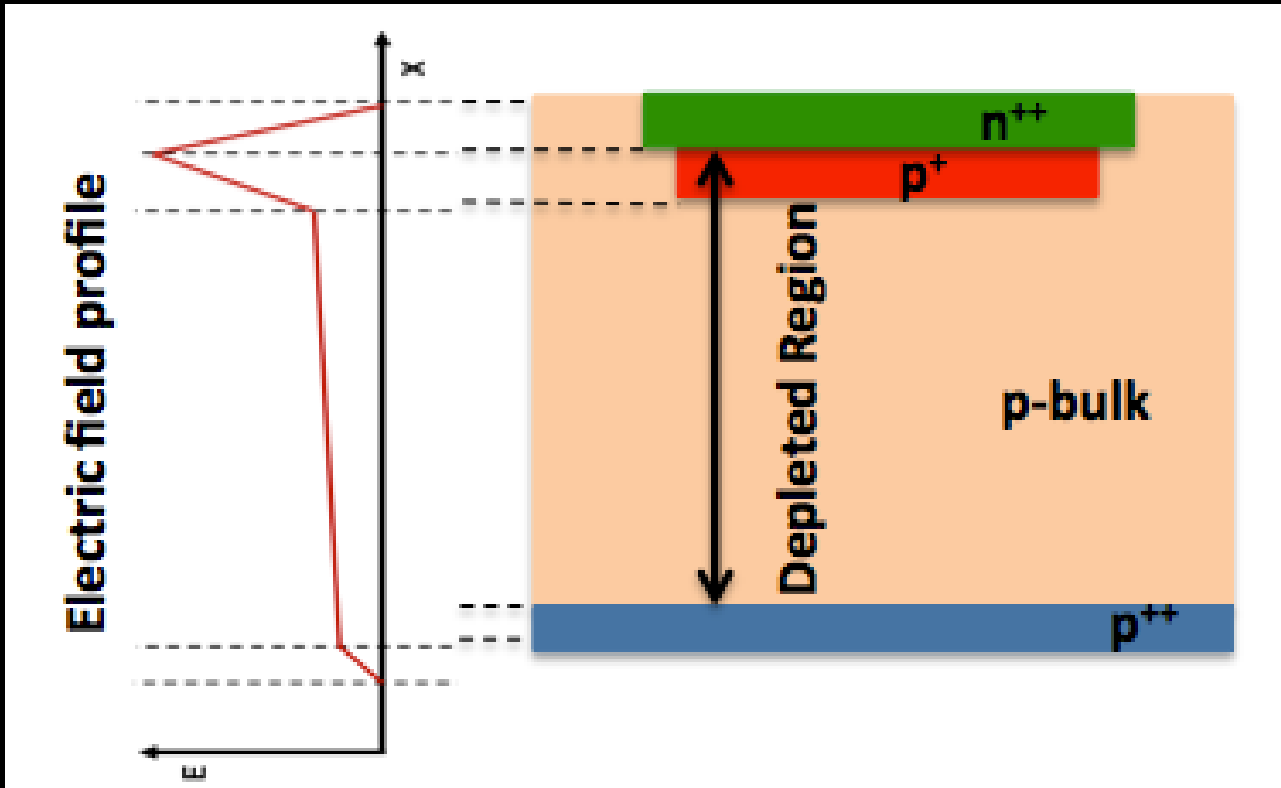
Low Gain Avalanche Diode (LGAD) detectors



Low Gain Avalanche Diode (LGAD) detectors

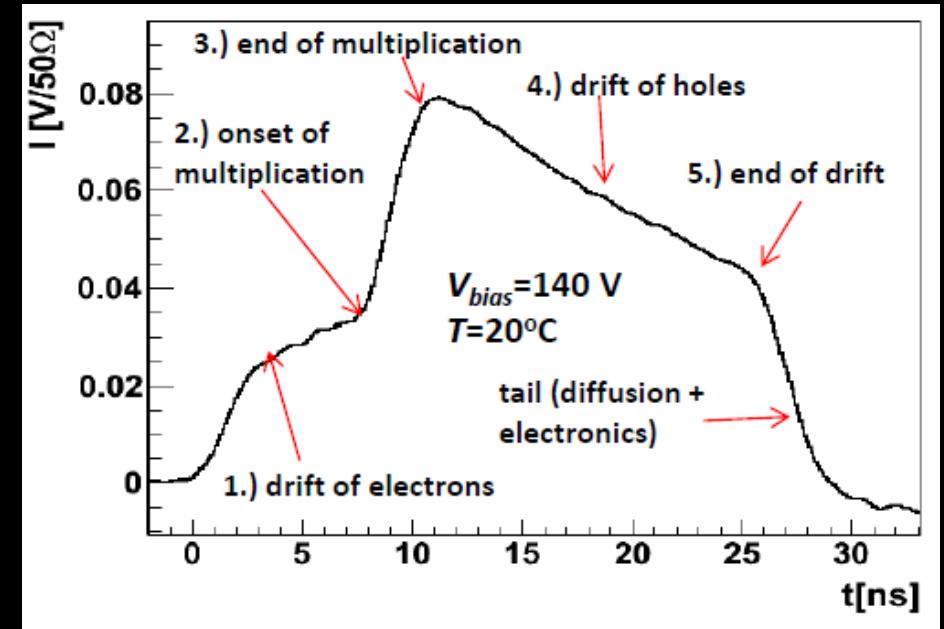
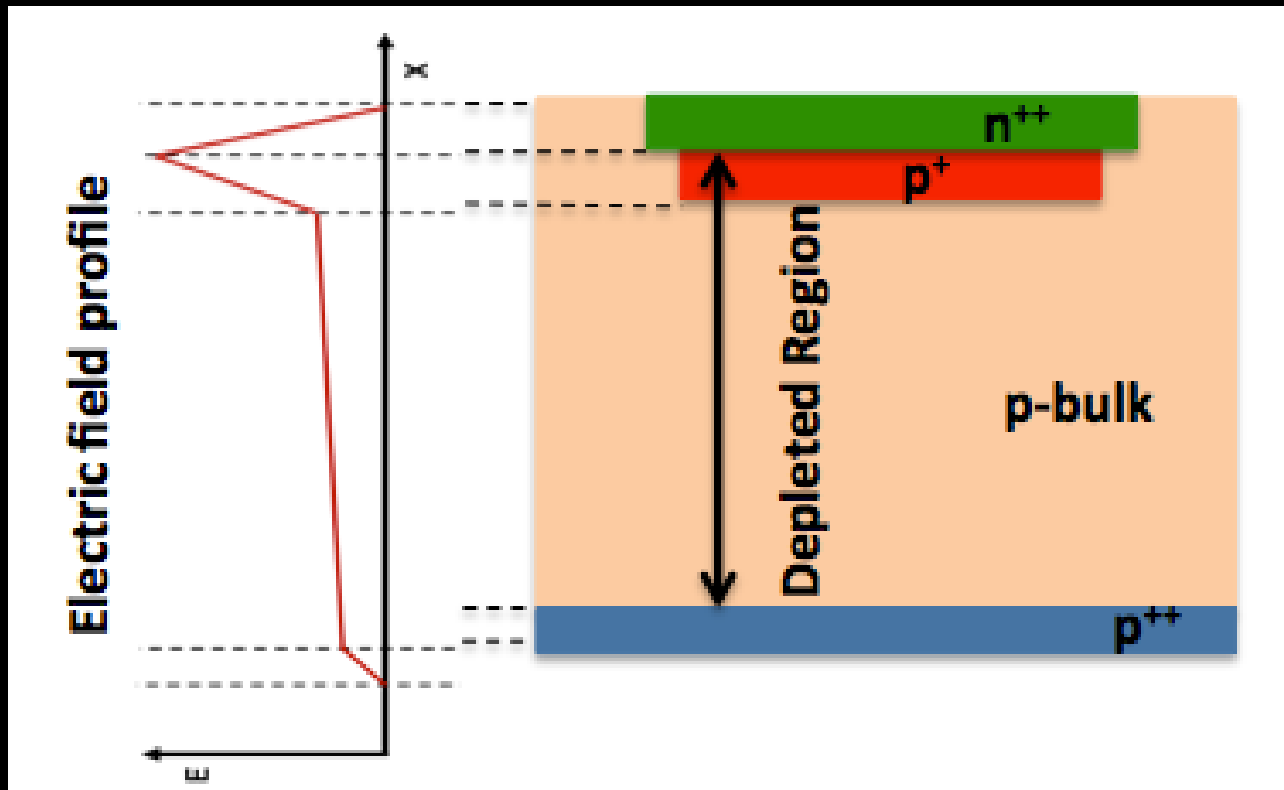


Low Gain Avalanche Diode (LGAD) detectors



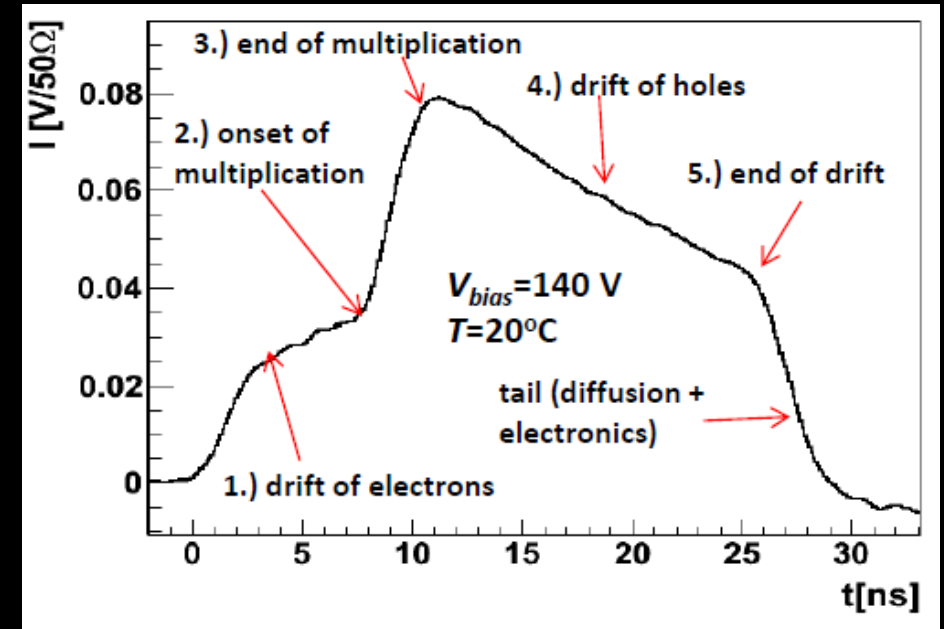
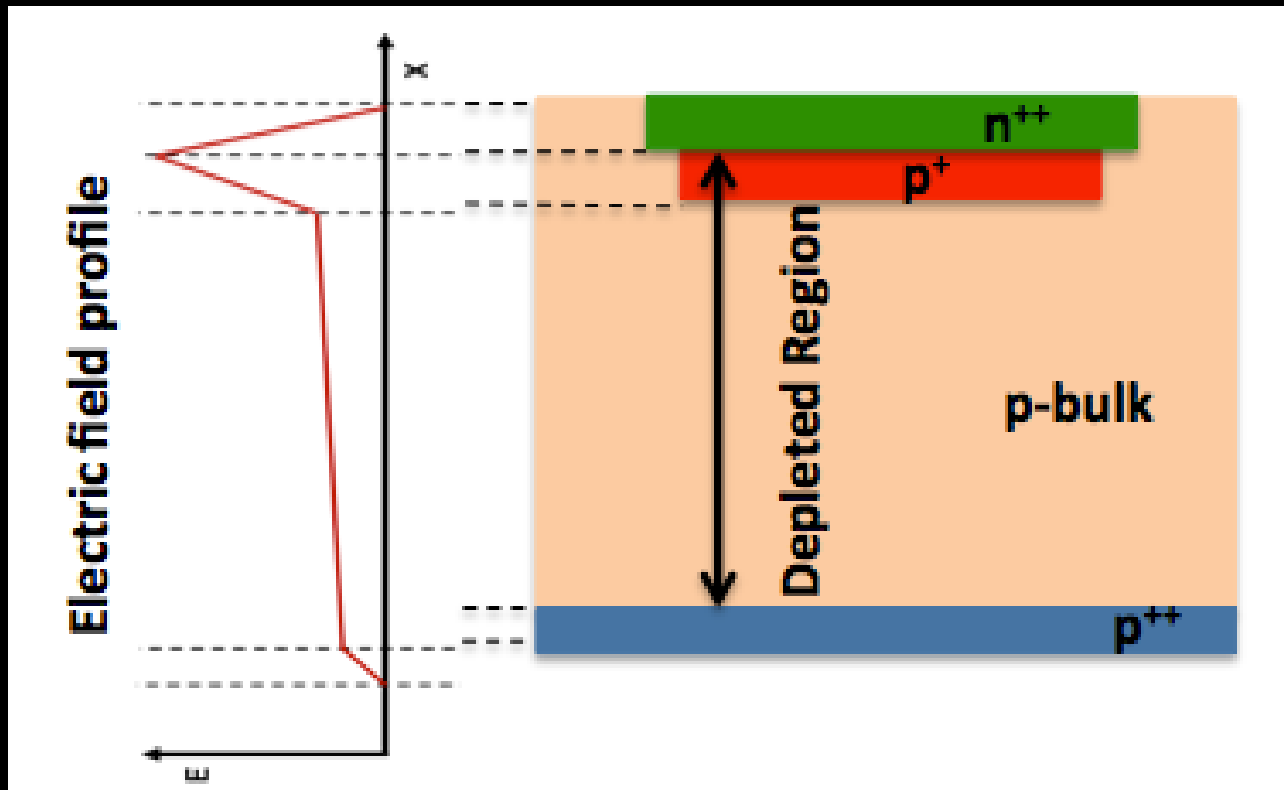
- Strip detector

Low Gain Avalanche Diode (LGAD) detectors



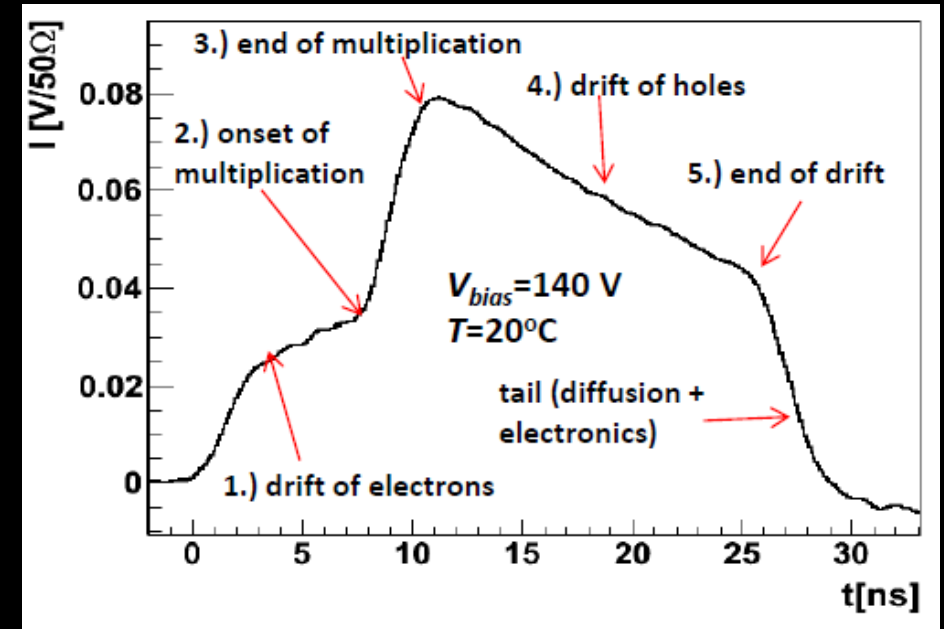
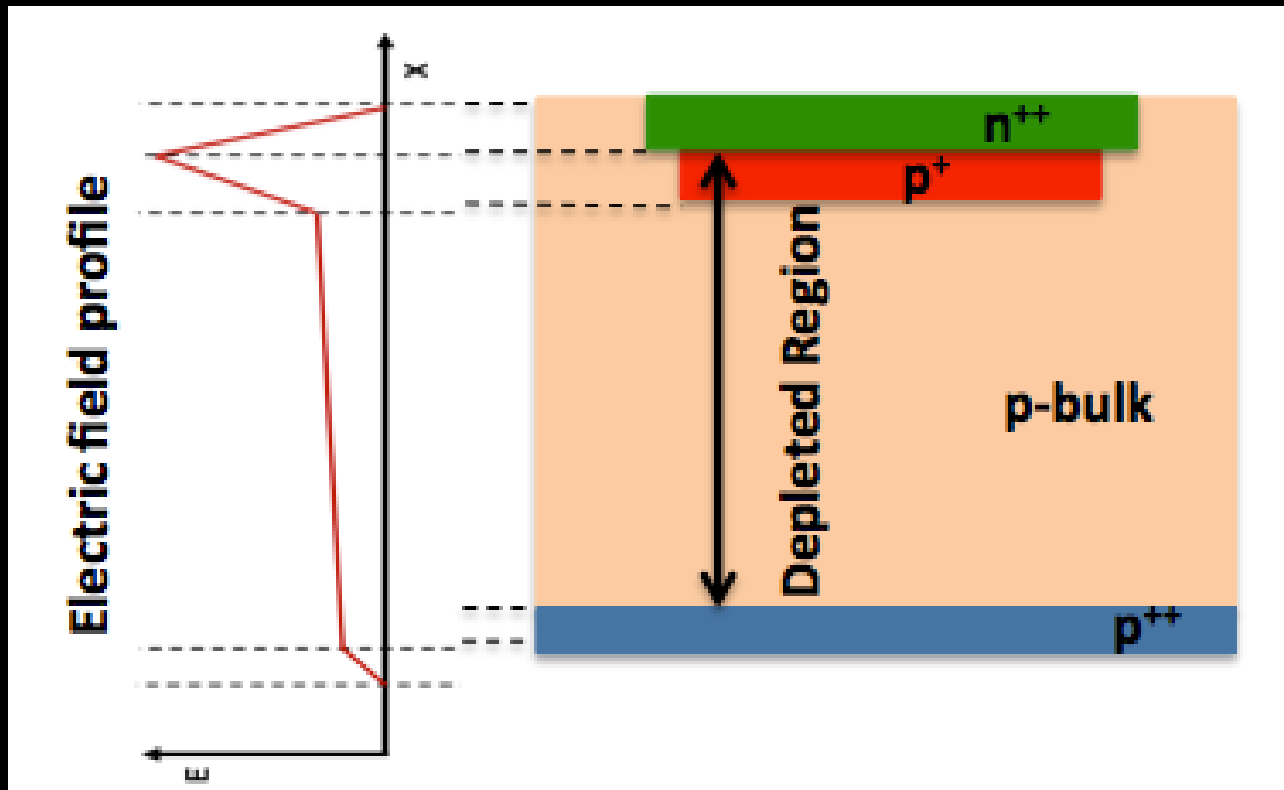
- Strip detector
- Low (1-100) gain is customizable depending on the doping

Low Gain Avalanche Diode (LGAD) detectors



- Strip detector
- Low (1-100) gain is customizable depending on the doping
- Thin sensor down to 70 μm . High radioresistance

Low Gain Avalanche Diode (LGAD) detectors

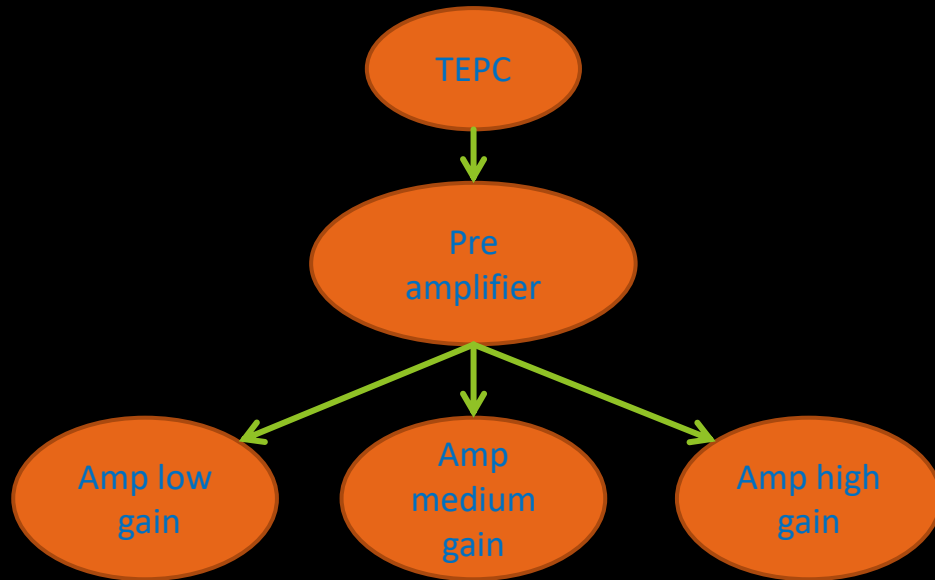


- Strip detector
- Low (1-100) gain is customizable depending on the doping
- Thin sensor down to 70 μm . High radioresistance
- Fast sensor: signal pulse ≈ 1 ns

Readout

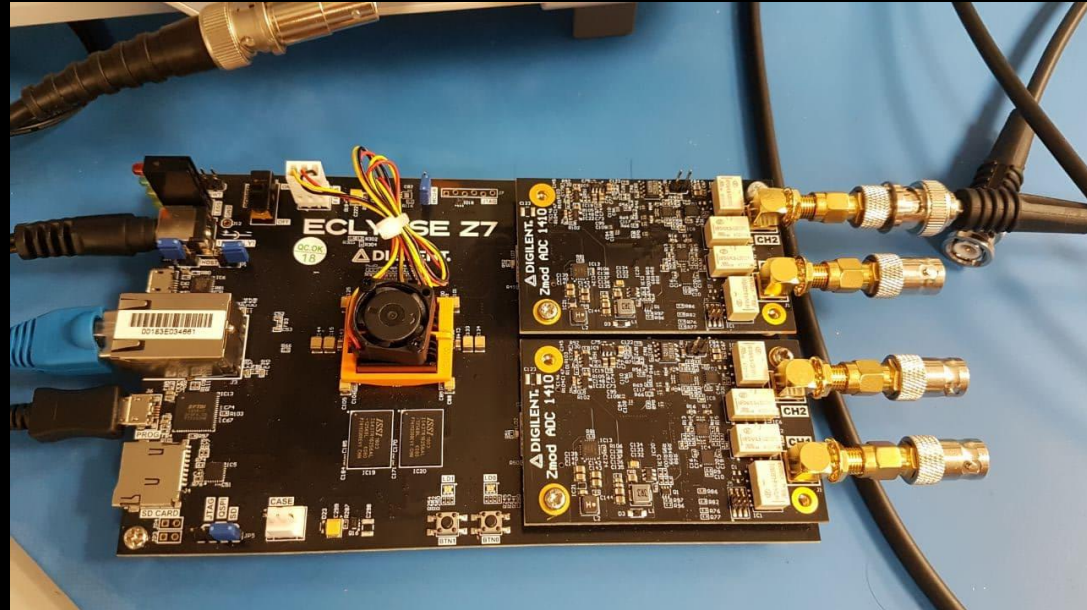
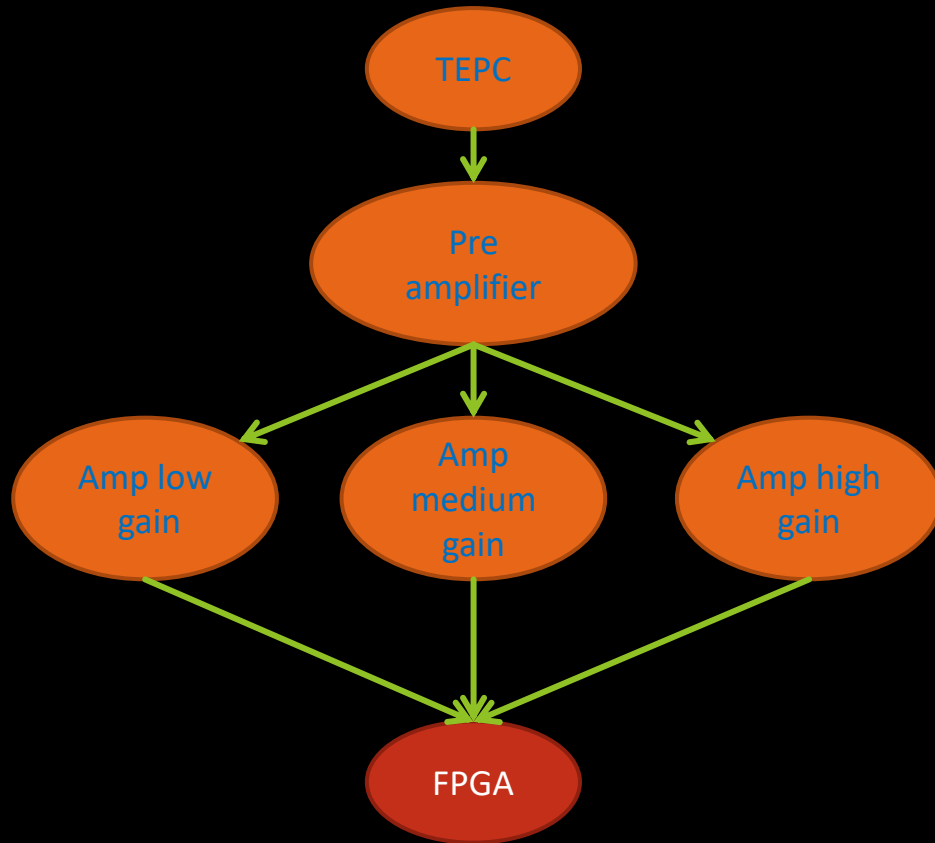
TEPC – readout FPGA

Tissue equivalent proportional counter



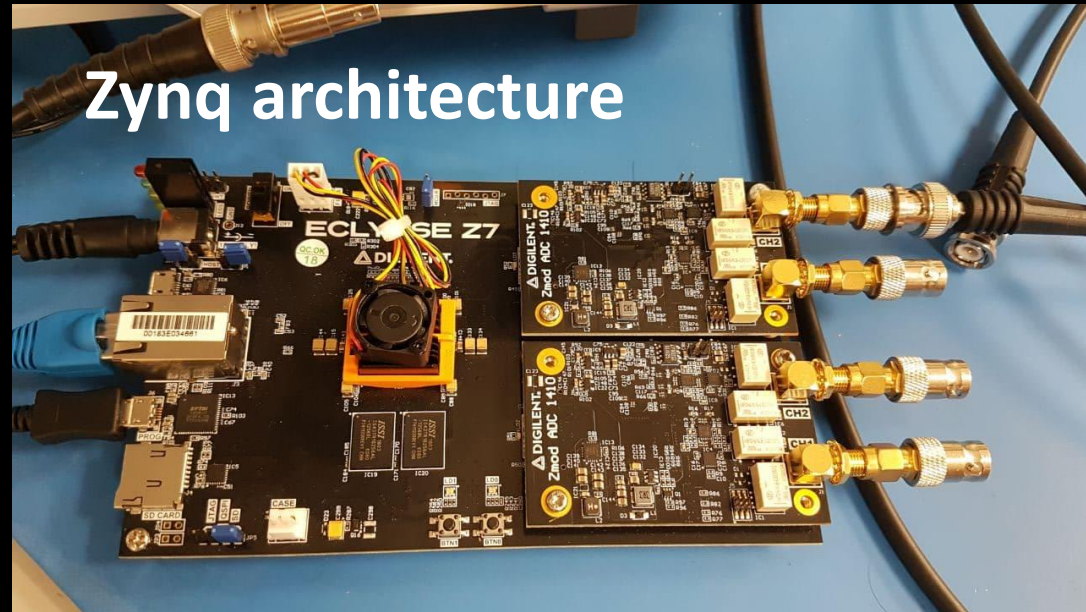
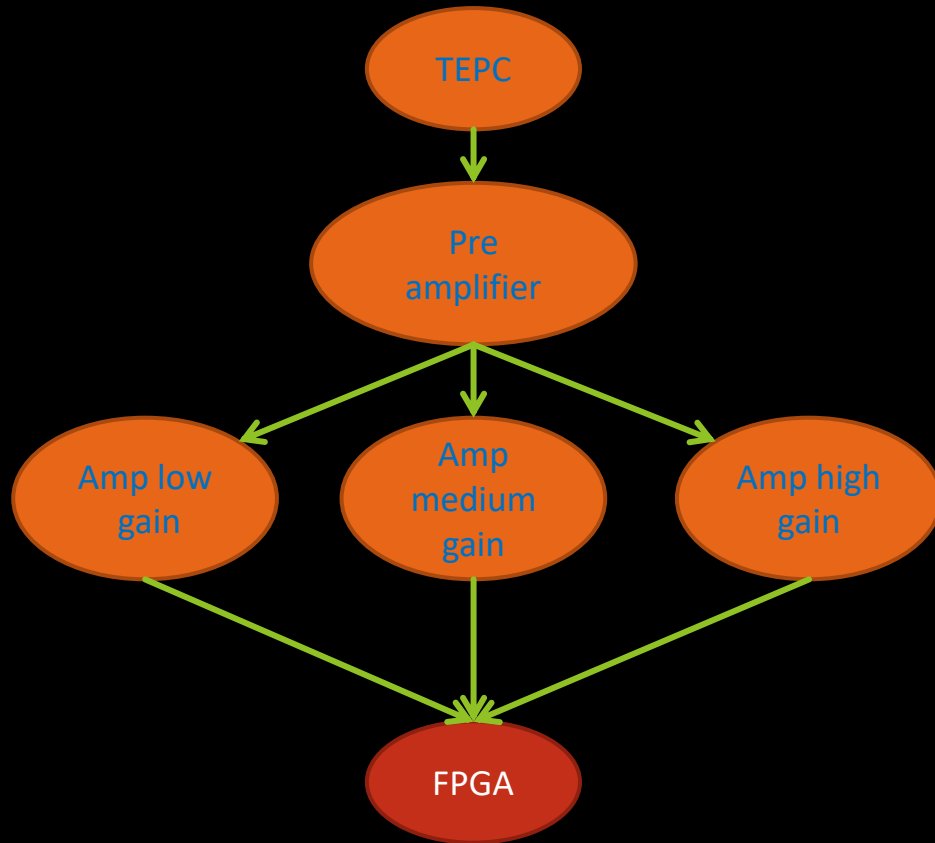
TEPC – readout FPGA

Tissue equivalent proportional counter



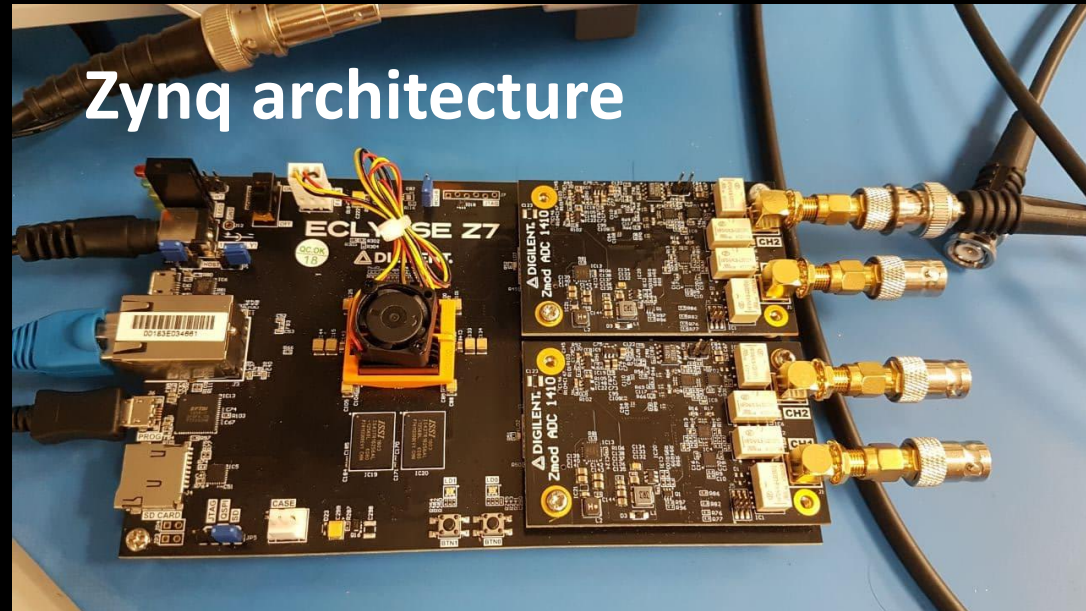
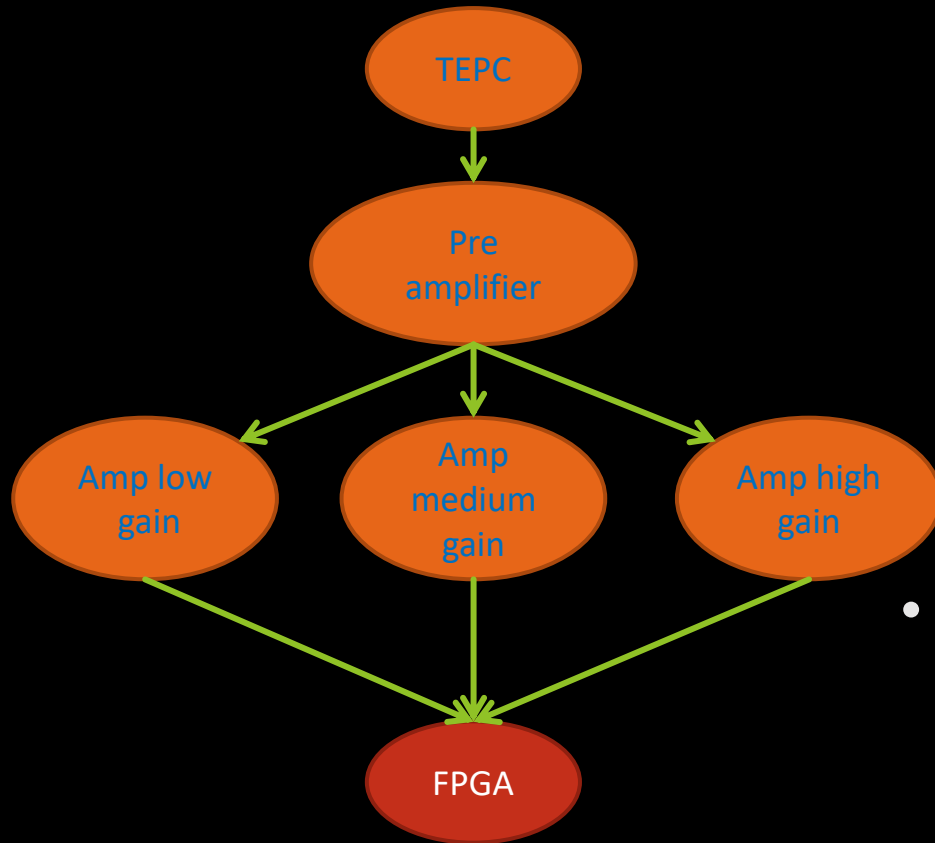
TEPC – readout FPGA

Tissue equivalent proportional counter



TEPC – readout FPGA

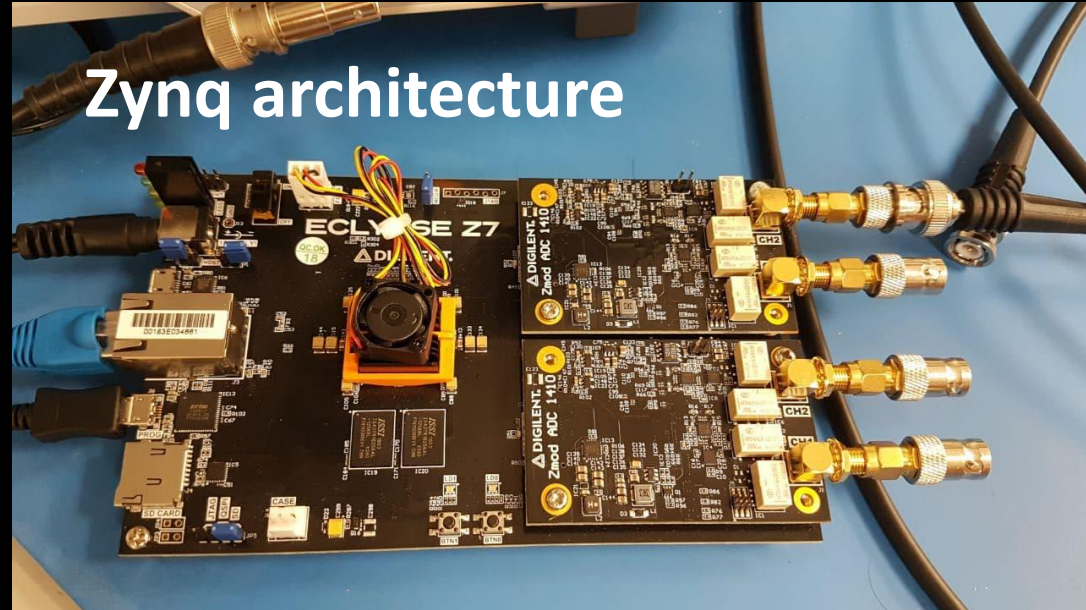
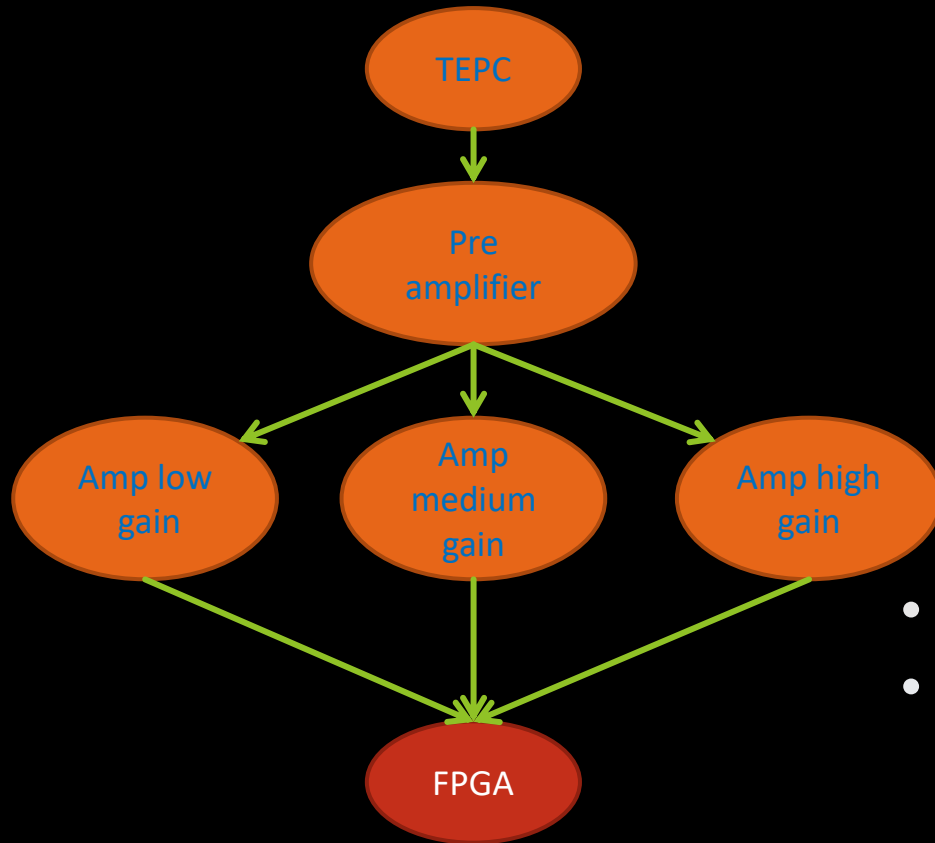
Tissue equivalent proportional counter



- 2 x Zmod ADC 1410; 14 bits resolution, $\pm 25V$

TEPC – readout FPGA

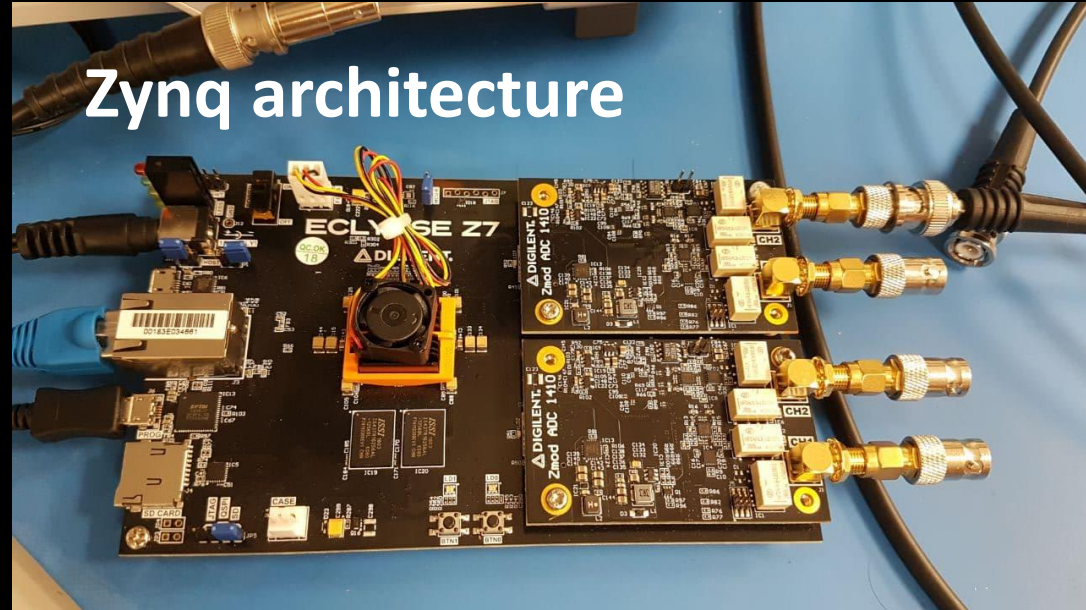
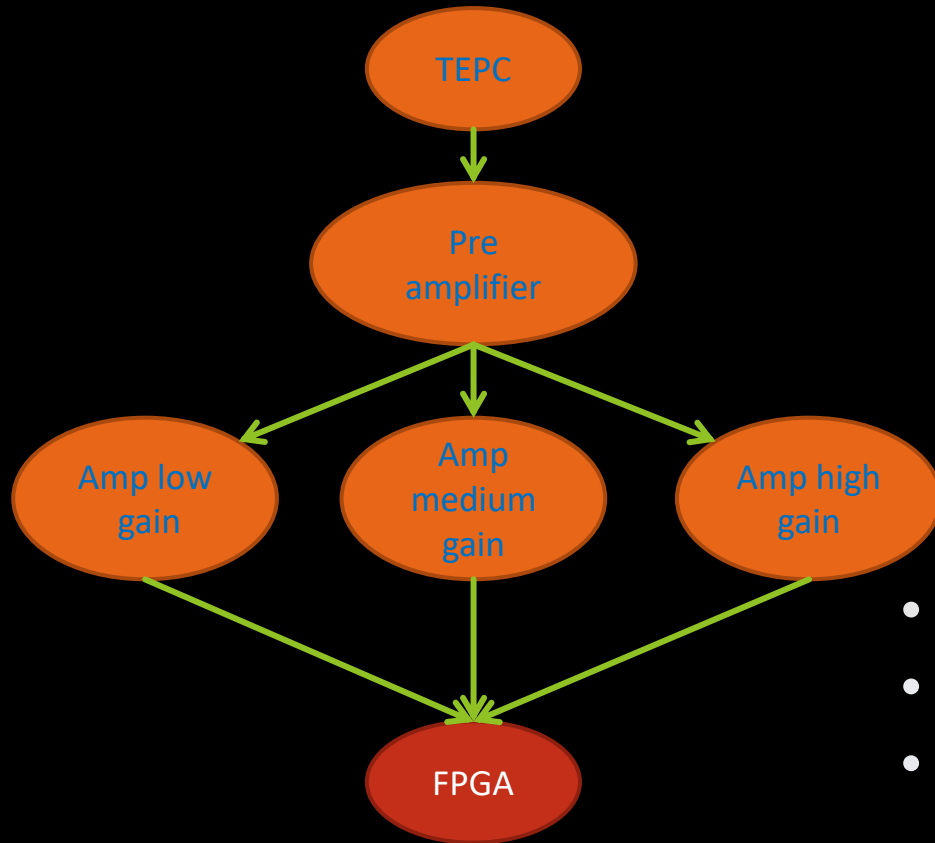
Tissue equivalent proportional counter



- 2 x Zmod ADC 1410; 14 bits resolution, $\pm 25V$
- Fully customizable system

TEPC – readout FPGA

Tissue equivalent proportional counter



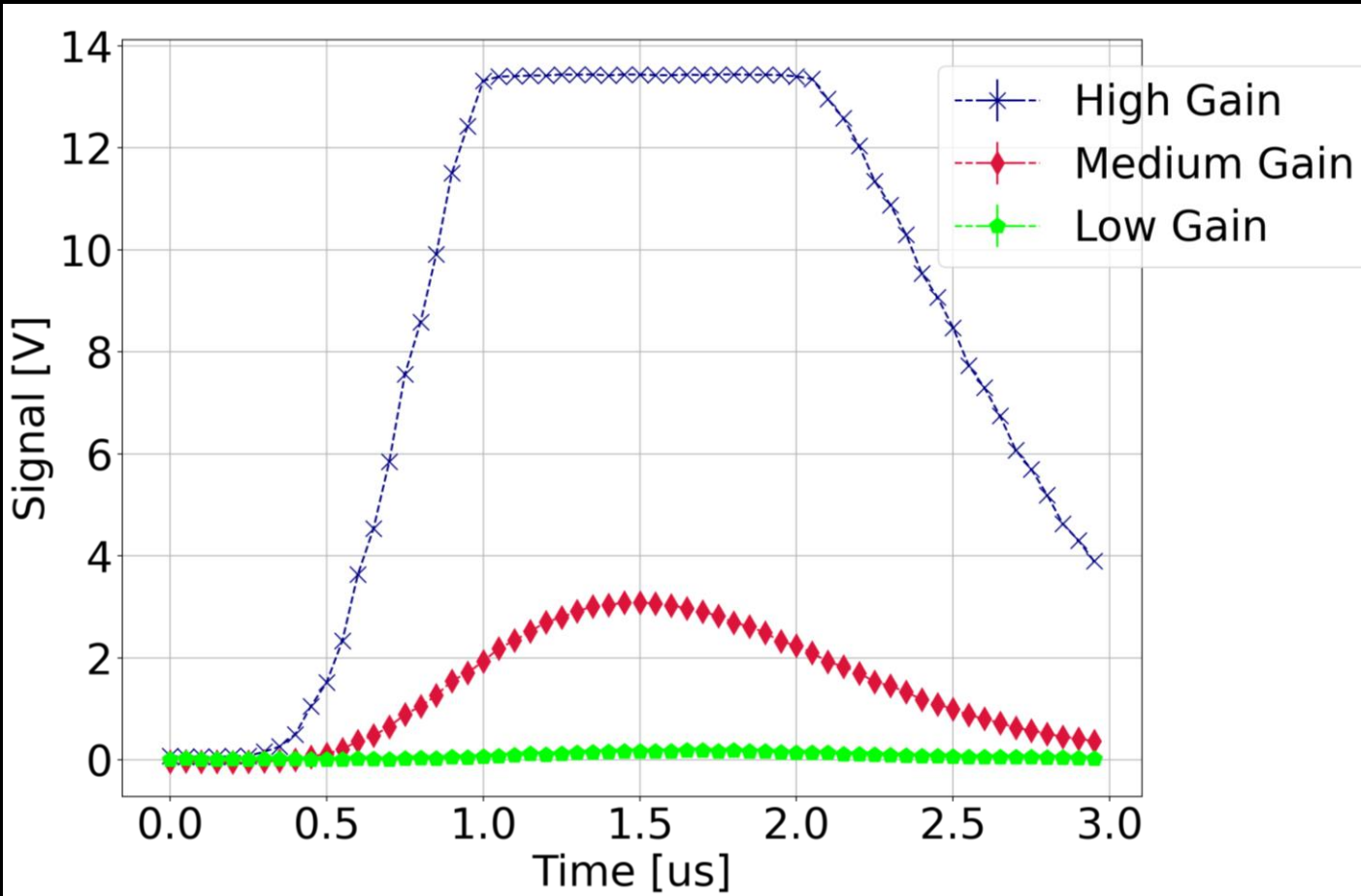
- 2 x Zmod ADC 1410; 14 bits resolution, $\pm 25V$
- Fully customizable system
- Extra channel available

TEPC - readout

Tissue equivalent proportional counter

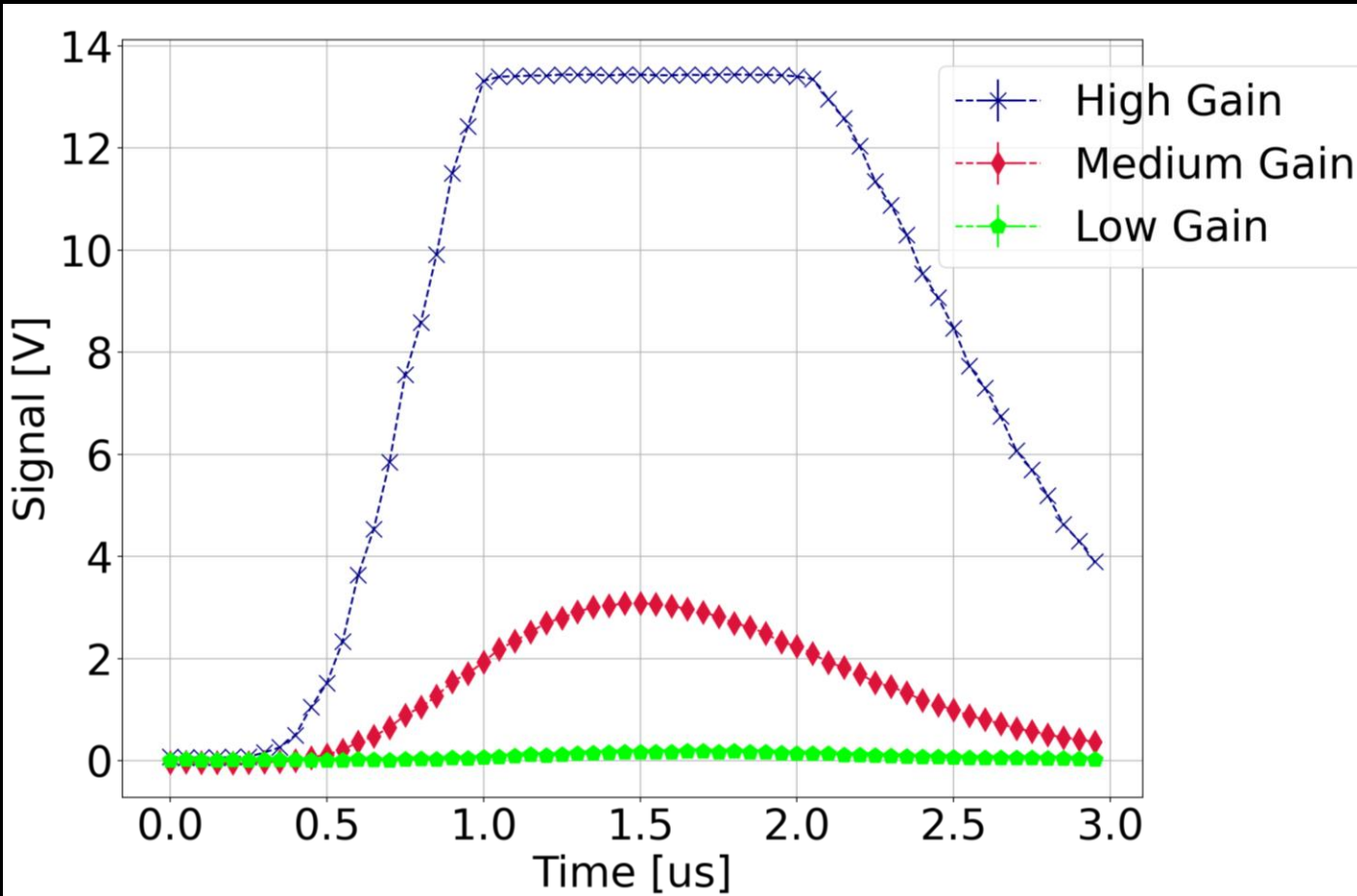
TEPC - readout

Tissue equivalent proportional counter



TEPC - readout

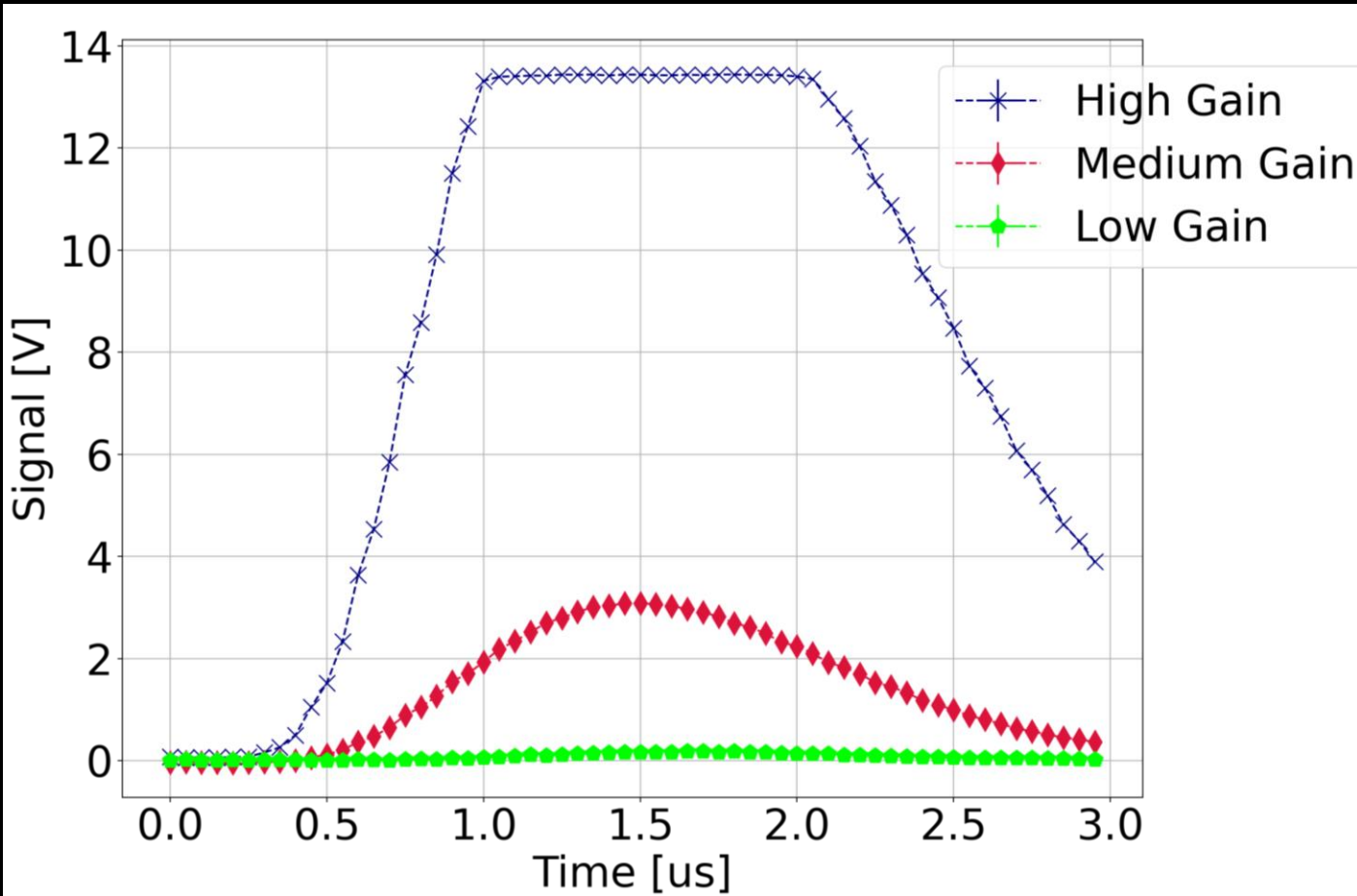
Tissue equivalent proportional counter



- Direct Memory Access (DMA) from the ADCs to an embedded Linux OS.

TEPC - readout

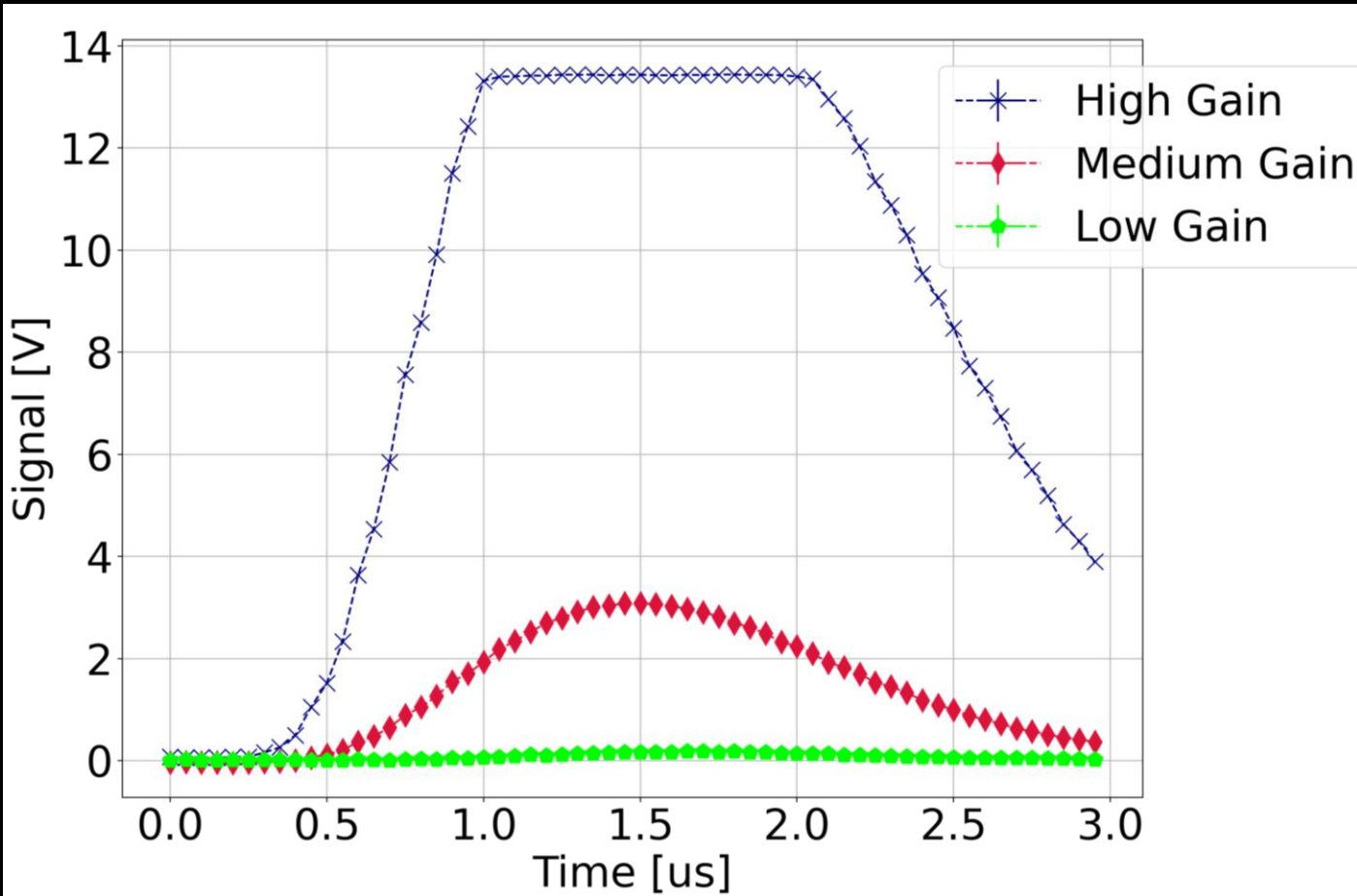
Tissue equivalent proportional counter



- Direct Memory Access (DMA) from the ADCs to an embedded Linux OS.
- Each trigger event is saved and can be sent via TCP-IP

TEPC - readout

Tissue equivalent proportional counter

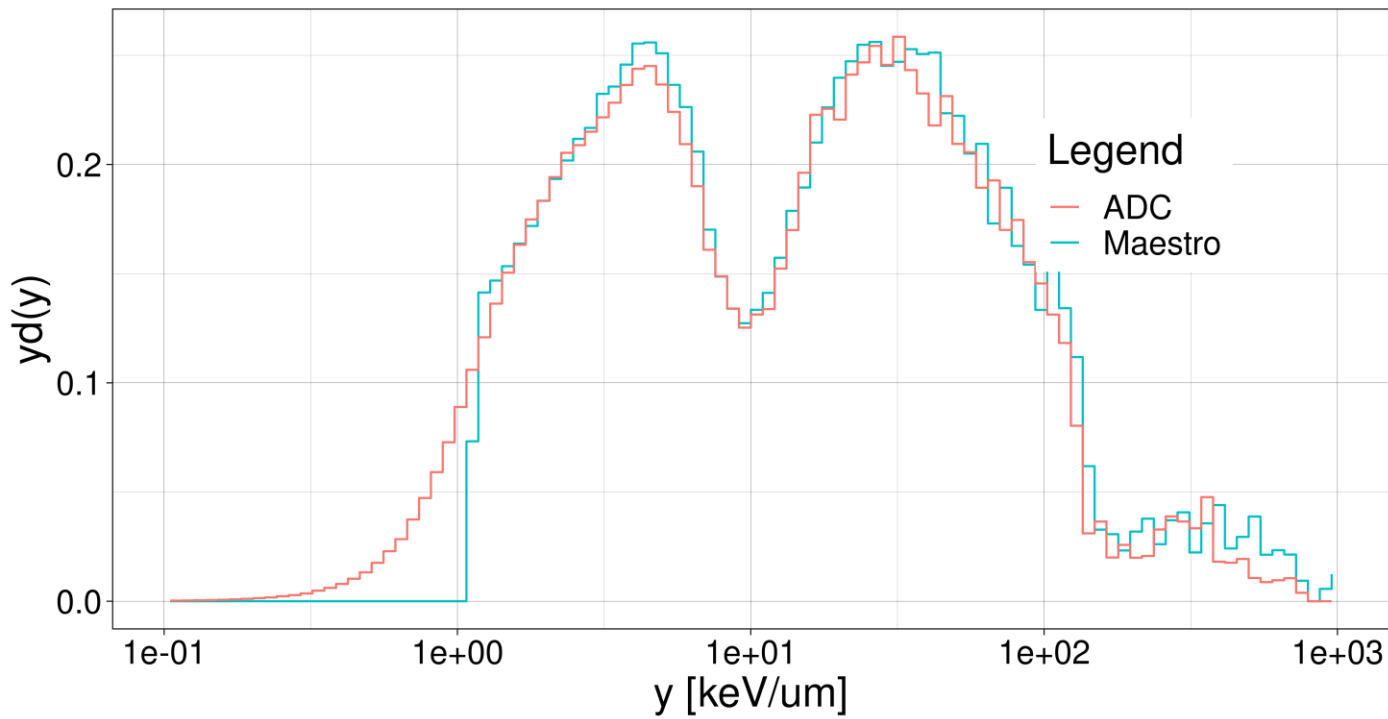


- Direct Memory Access (DMA) from the ADCs to an embedded Linux OS.
- Each trigger event is saved and can be sent via TCP-IP
- External trigger pulse for dead time estimation and possible synchronization with other devices

TEPC - readout

Tissue equivalent proportional counter

yd(y) ADC vs Maestro AmBe source

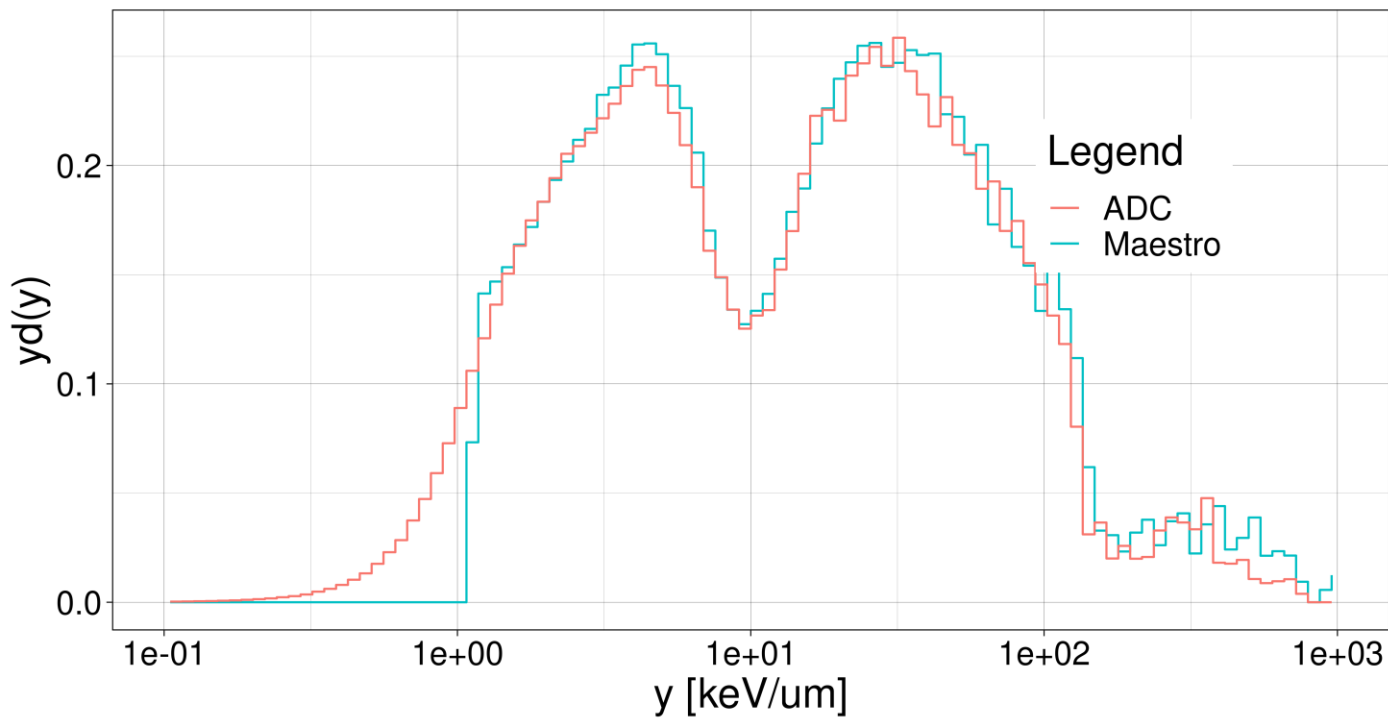


- Direct Memory Access (DMA) from the ADCs to an embedded Linux OS.
- Each trigger event is saved and can be sent via TCP-IP
- External trigger pulse for dead time estimation and possible synchronization with other devices

TEPC - readout

Tissue equivalent proportional counter

yd(y) ADC vs Maestro AmBe source



- Direct Memory Access (DMA) from the ADCs to an embedded Linux OS.
- Each trigger event is saved and can be sent via TCP-IP
- External trigger pulse for dead time estimation and possible synchronization with other devices
- Spectra overlaps. Good.

LGAD Readout - overview

Low Gain Avalanche Detector

LGAD Readout - overview

Low Gain Avalanche Detector

LGADs



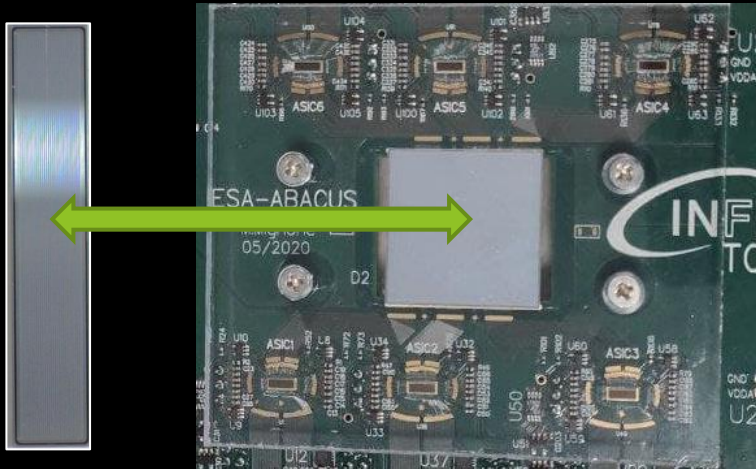
71 channels

LGAD Readout - overview

Low Gain Avalanche Detector

LGADs

ABACUS ASIC



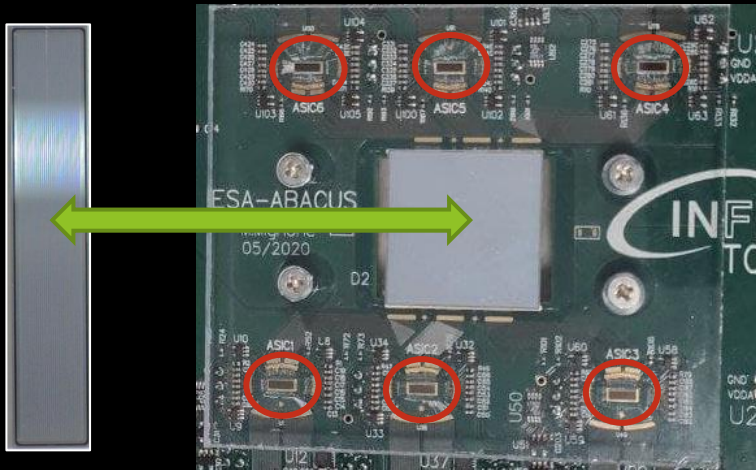
71 channels

LGAD Readout - overview

Low Gain Avalanche Detector

LGADs

ABACUS ASIC



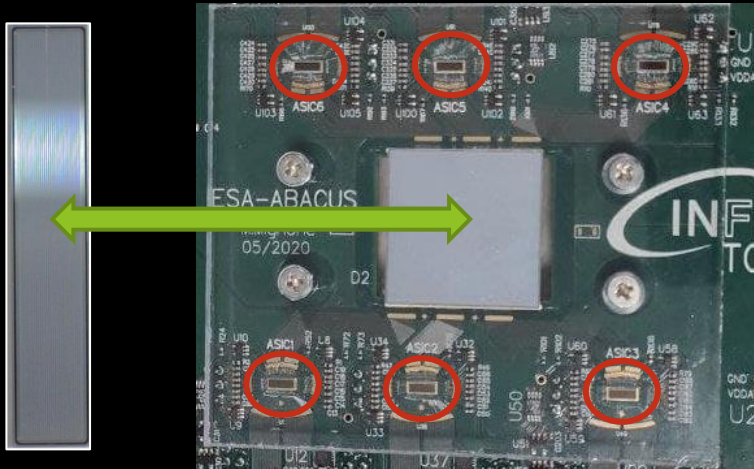
71 channels

LGAD Readout - overview

Low Gain Avalanche Detector

LGADs

ABACUS ASIC



71 channels

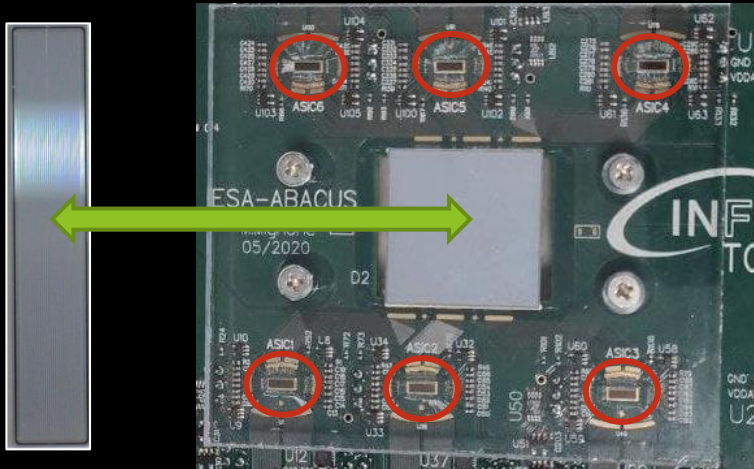
Each chip read a maximum
of 24 LGADs

LGAD Readout - overview

Low Gain Avalanche Detector

LGADs

ABACUS ASIC



71 channels

Each chip read a maximum
of 24 LGADs

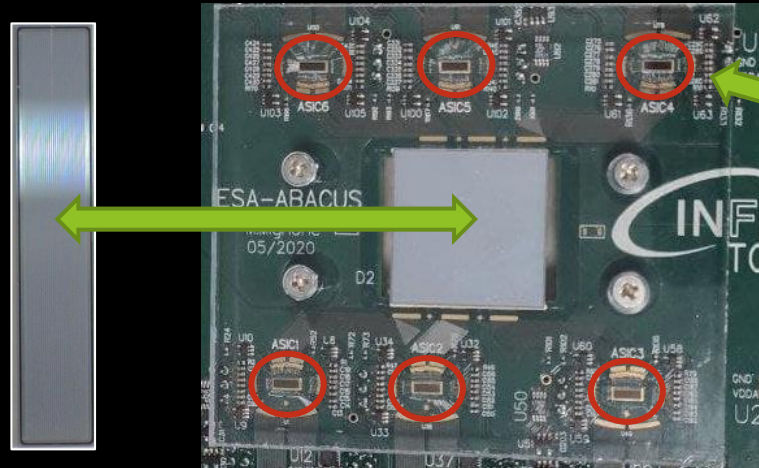
- Adjust thresholds levels
- Signal processing

LGAD Readout - overview

Low Gain Avalanche Detector

LGADs

ABACUS ASIC



71 channels

Each chip read a maximum of 24 LGADs

- Adjust thresholds levels
- Signal processing

Readout based on
ESA_ABACUS and ABACUS
chip developed by INFN-TO

for 

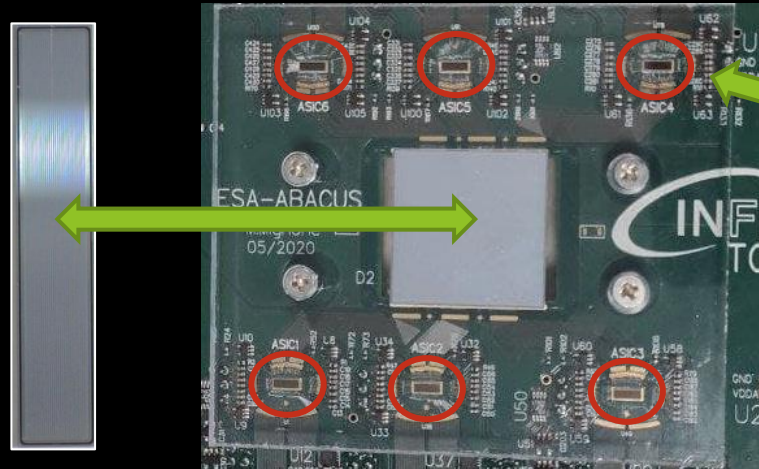


LGAD Readout - overview

Low Gain Avalanche Detector

LGADs

ABACUS ASIC



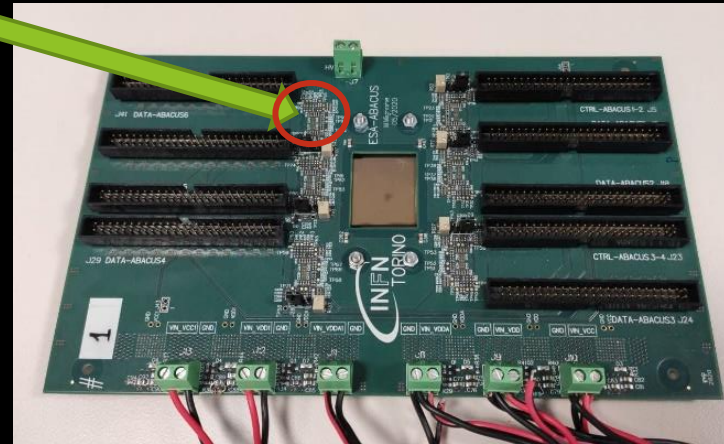
71 channels

Each chip read a maximum of 24 LGADs

- Adjust thresholds levels
- Signal processing

Readout based on
ESA_ABACUS and ABACUS
chip developed by INFN-TO

for 



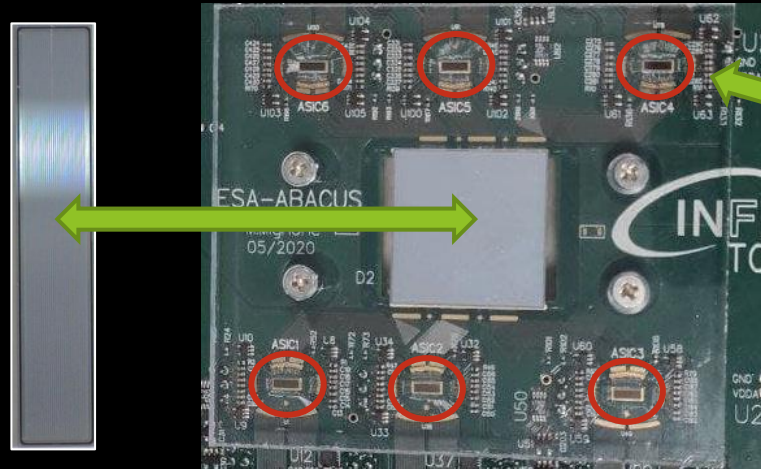
- Physical support
- Power and connections

LGAD Readout - overview

Low Gain Avalanche Detector

LGADs

ABACUS ASIC



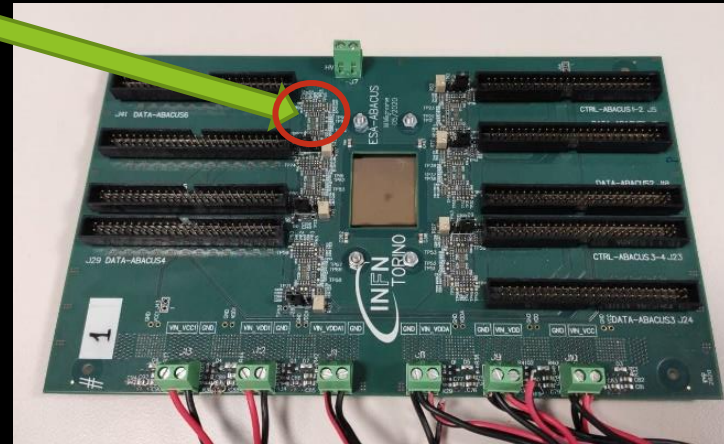
71 channels

Each chip read a maximum of 24 LGADs

- Adjust thresholds levels
- Signal processing

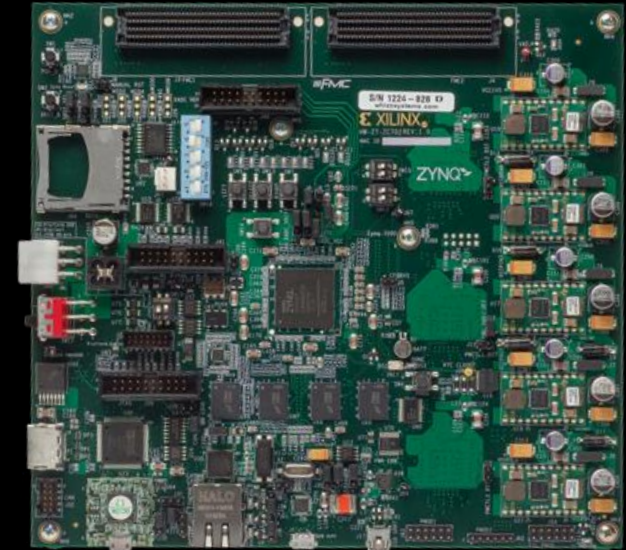
Readout based on
ESA_ABACUS and ABACUS
chip developed by INFN-TO

for 



- Physical support
- Power and connections

Digital signal from ESA_ABACUS
is processed thanks to FPGA
Xilinx model zc702

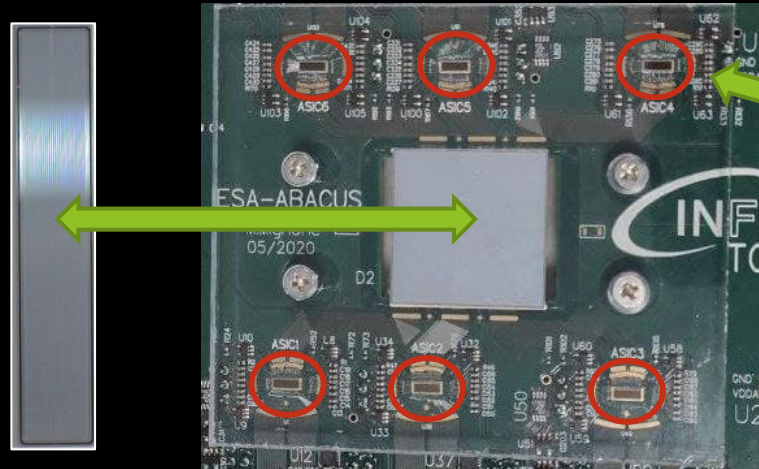


LGAD Readout - overview

Low Gain Avalanche Detector

LGADs

ABACUS ASIC



71 channels

Each chip read a maximum of 24 LGADs

- Adjust thresholds levels
- Signal processing

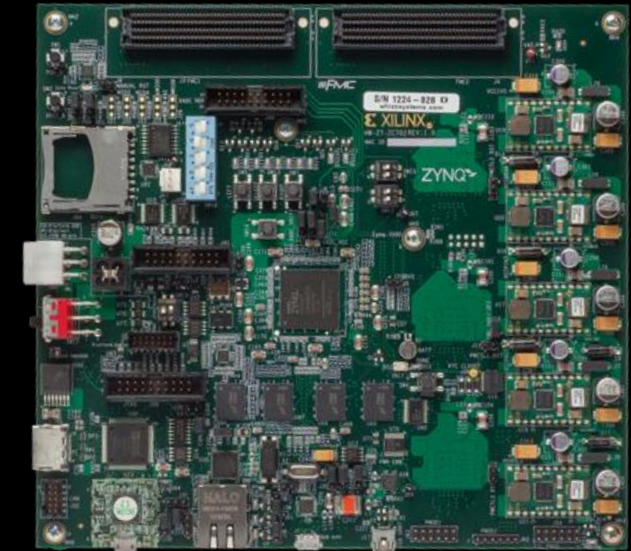
Readout based on
ESA_ABACUS and ABACUS
chip developed by INFN-TO

for 



- Physical support
- Power and connections

Digital signal from ESA_ABACUS
is processed thanks to FPGA
Xilinx model zc702



- Thresholds controls
- Signals from ASICs

LGAD - FPGA

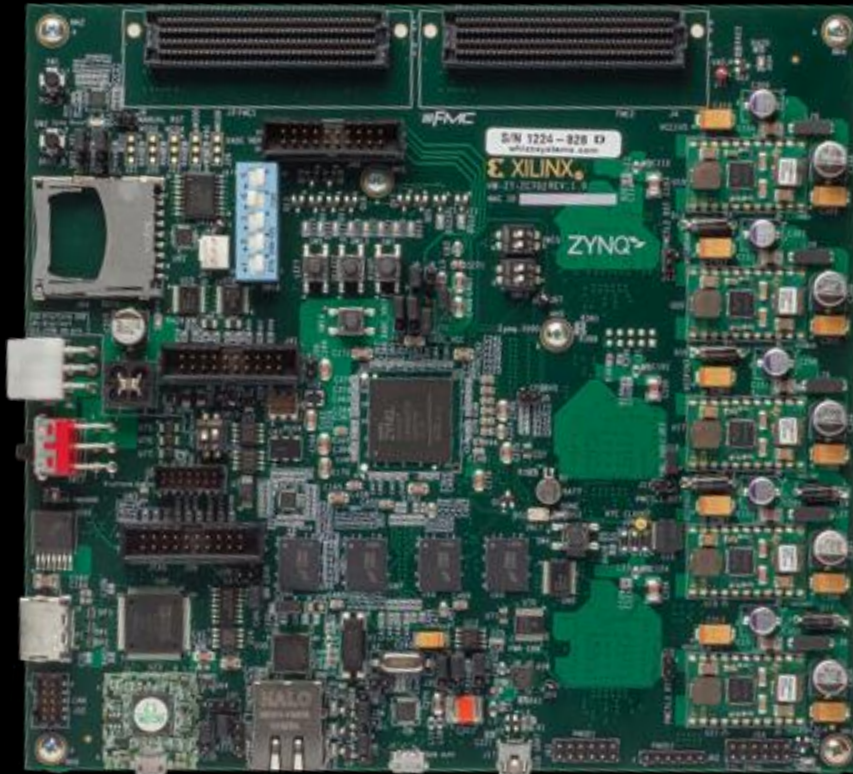
Low Gain Avalanche Detector

LGAD - FPGA

Low Gain Avalanche Detector

Xilinx model zc702

Zynq



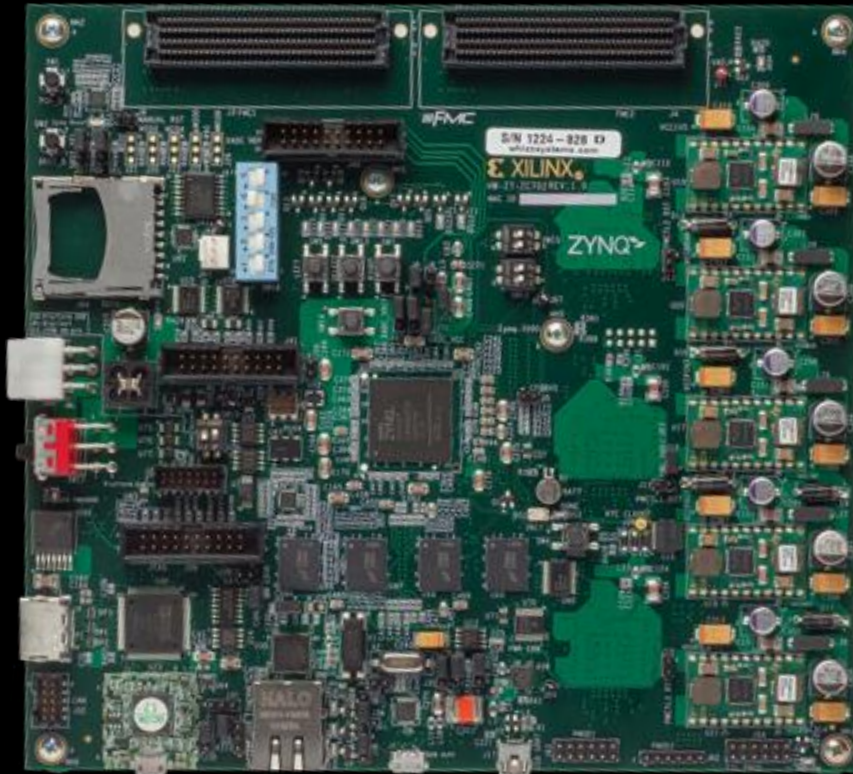
LGAD - FPGA

Low Gain Avalanche Detector

Xilinx model zc702

Zynq

- Counts the digital signal from the ABACUS ASICs

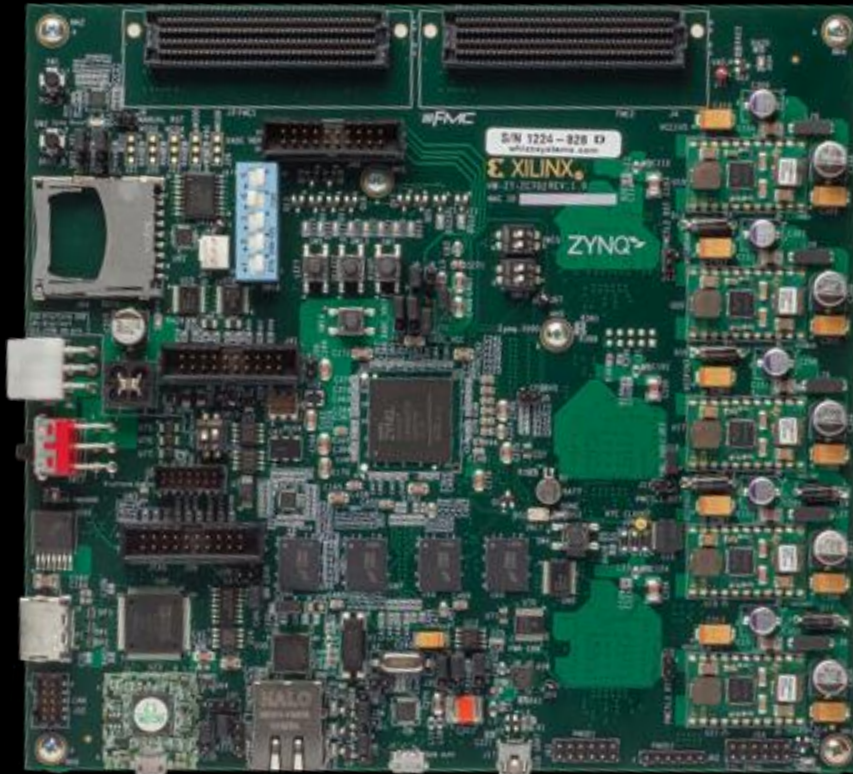


LGAD - FPGA

Low Gain Avalanche Detector

Xilinx model zc702

Zynq



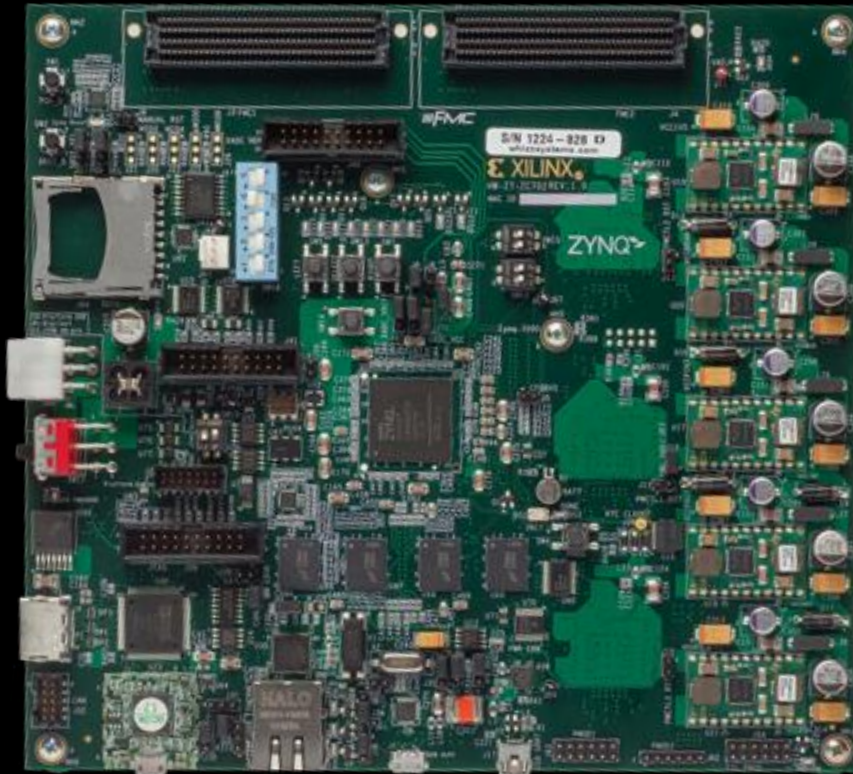
- Counts the digital signal from the ABACUS ASICs
- Direct Memory Access (DMA) used to send the data in the Processing System (PS)

LGAD - FPGA

Low Gain Avalanche Detector

Xilinx model zc702

Zynq



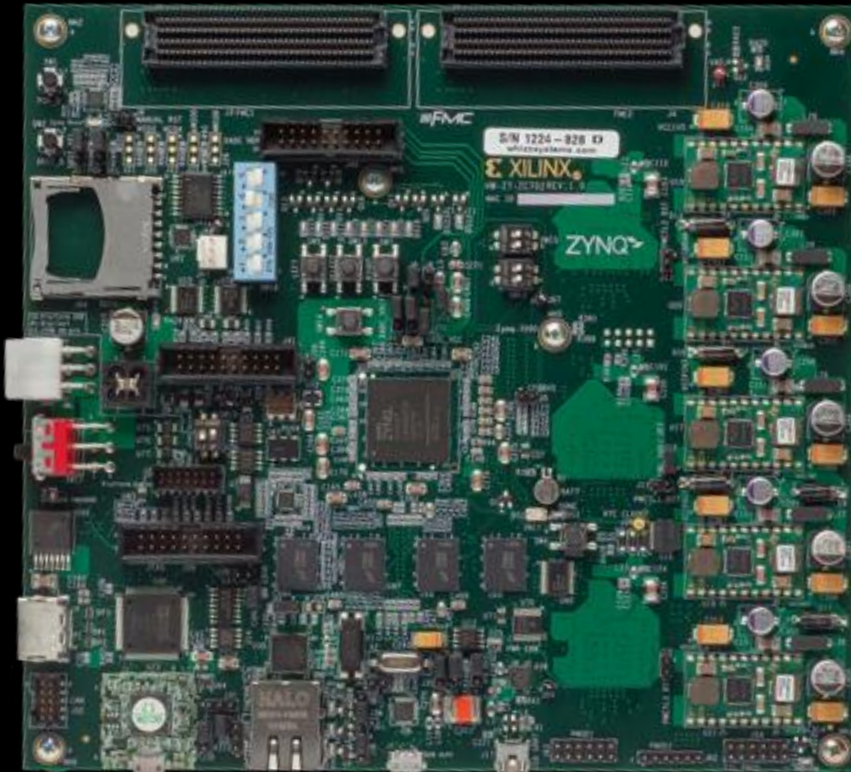
- Counts the digital signal from the ABACUS ASICs
- Direct Memory Access (DMA) used to send the data in the Processing System (PS)
- The PS runs an embedded Linux distribution

LGAD - FPGA

Low Gain Avalanche Detector

Xilinx model zc702

Zynq



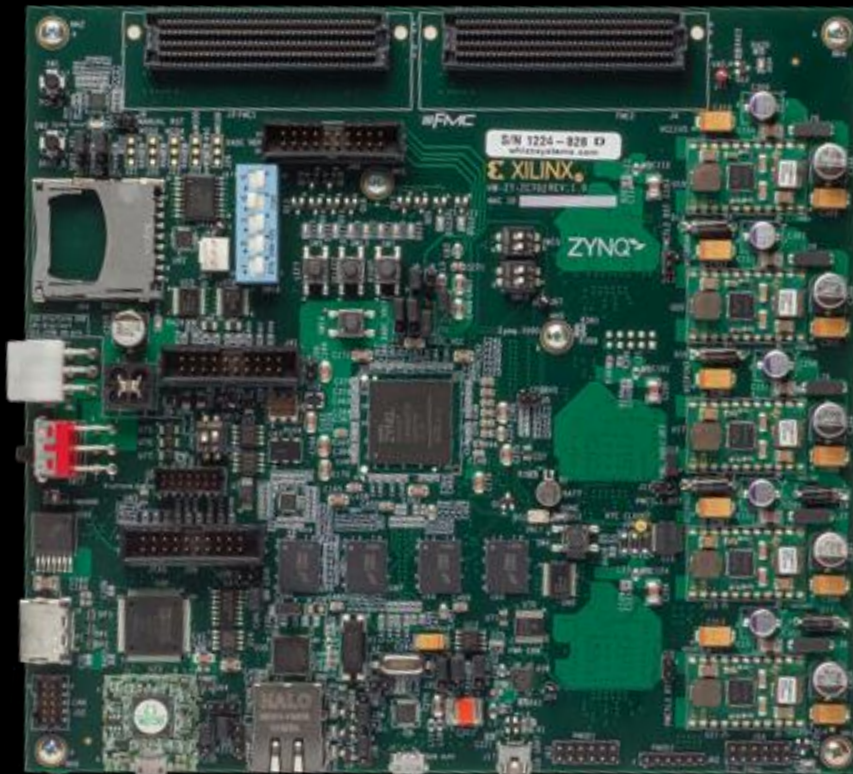
- Counts the digital signal from the ABACUS ASICs
- Direct Memory Access (DMA) used to send the data in the Processing System (PS)
- The PS runs an embedded Linux distribution
- The user can control the thresholds levels easily from the Linux system

LGAD - FPGA

Low Gain Avalanche Detector

Xilinx model zc702

Zynq



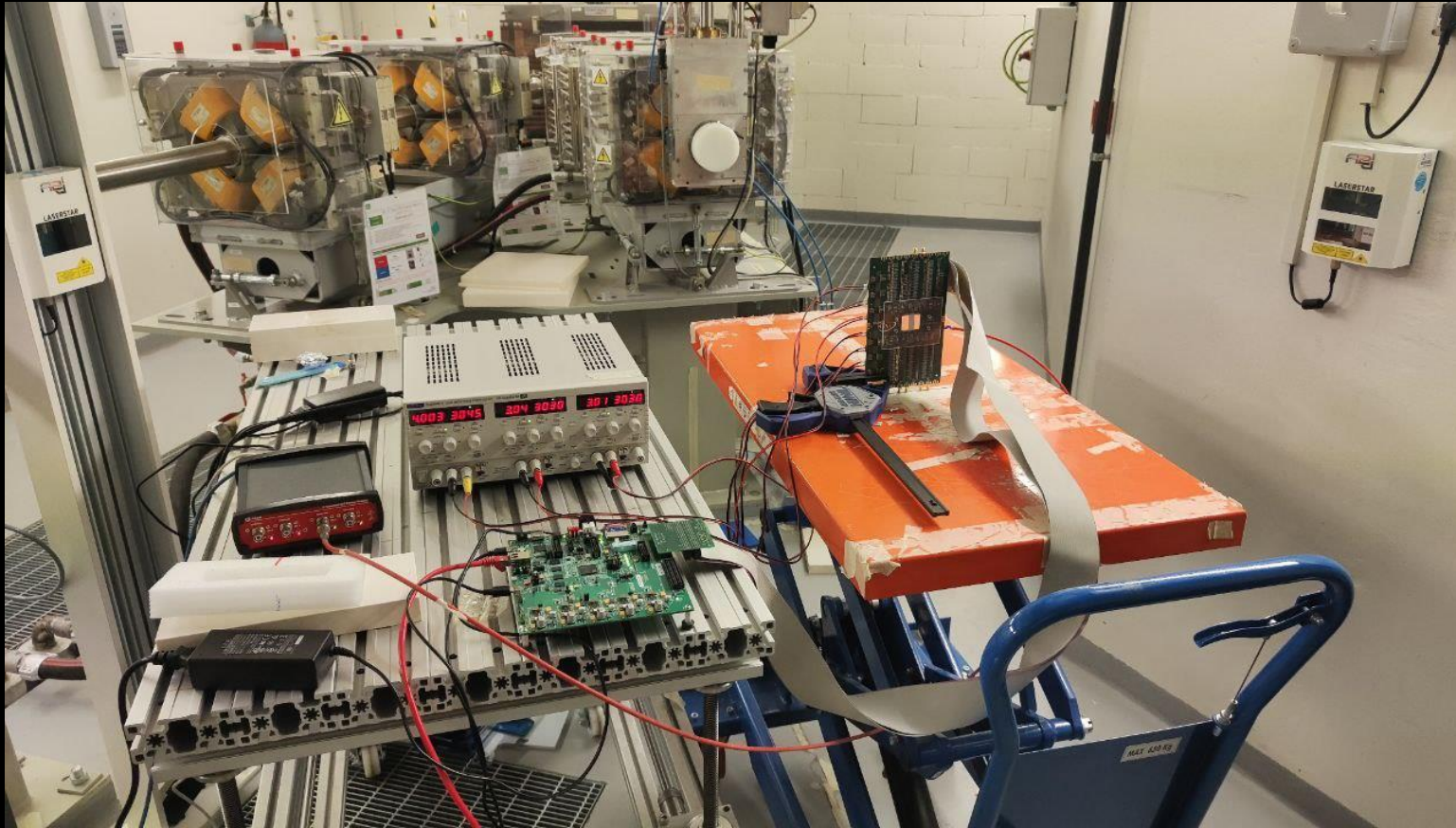
- Counts the digital signal from the ABACUS ASICs
- Direct Memory Access (DMA) used to send the data in the Processing System (PS)
- The PS runs an embedded Linux distribution
- The user can control the thresholds levels easily from the Linux system
- Data is sent via TCP-IP to an external PC

LGAD - Experimental results (Threshold scans)

Low Gain Avalanche Detector

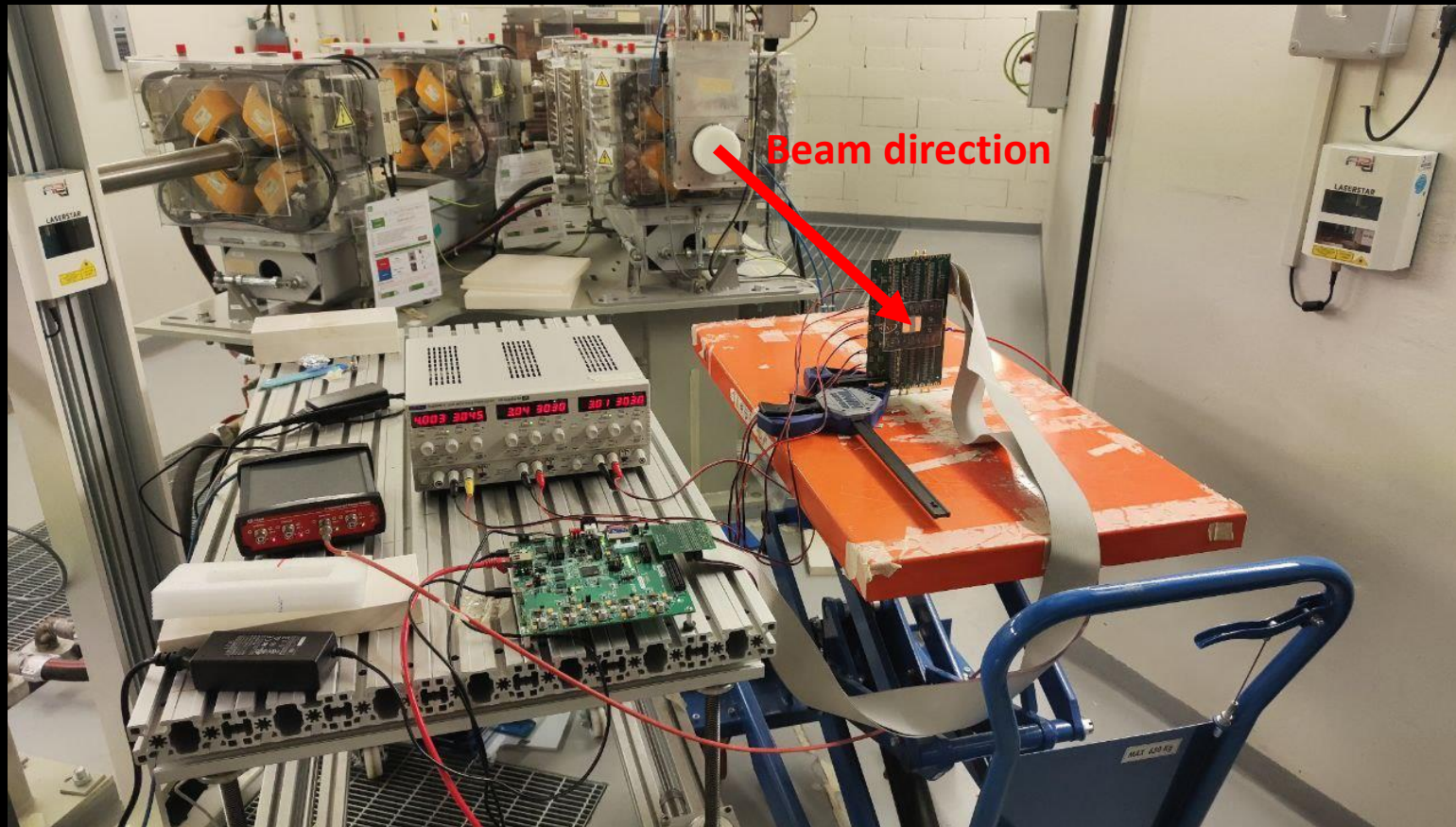
LGAD - Experimental results (Threshold scans)

Low Gain Avalanche Detector



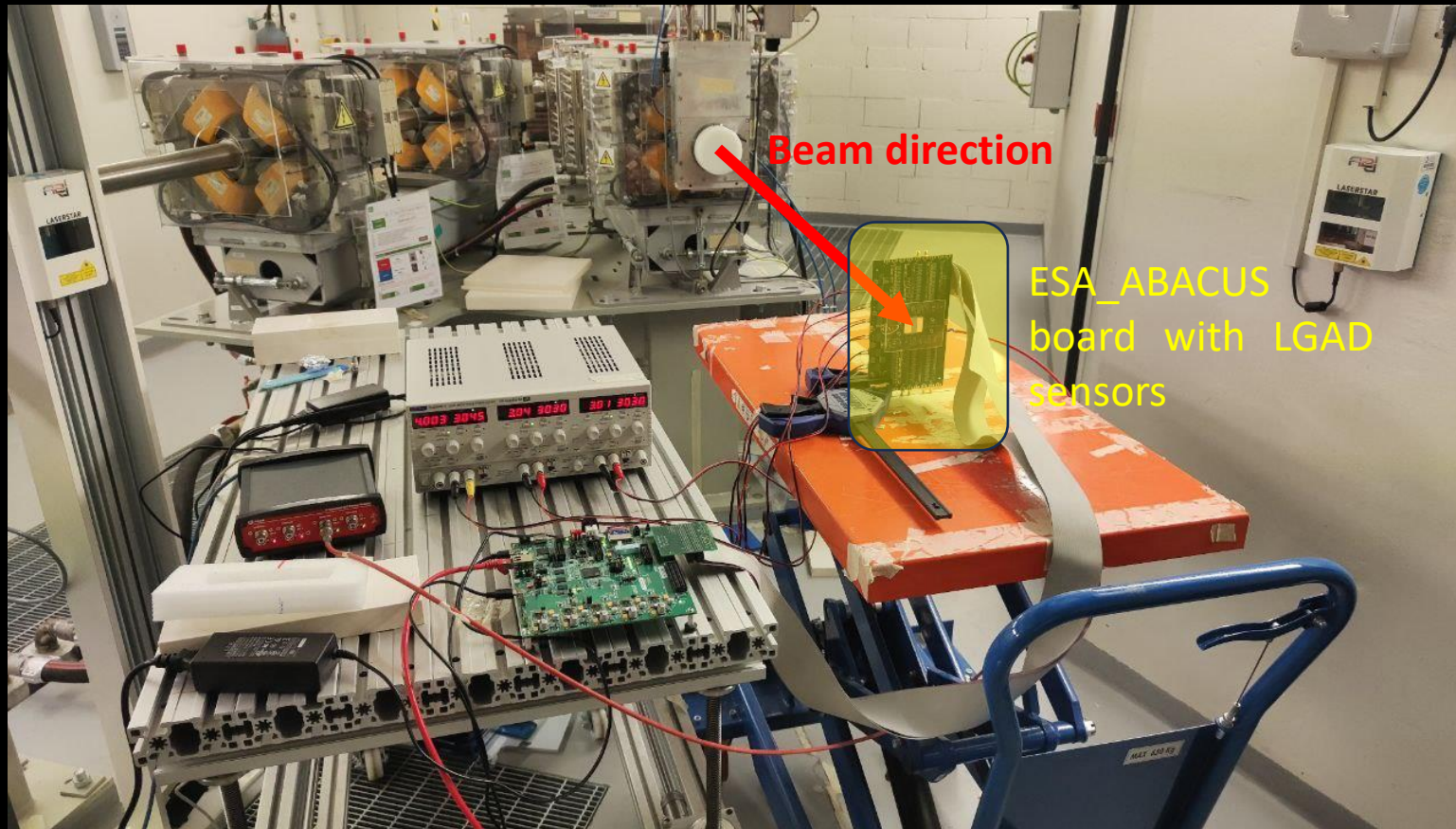
LGAD - Experimental results (Threshold scans)

Low Gain Avalanche Detector



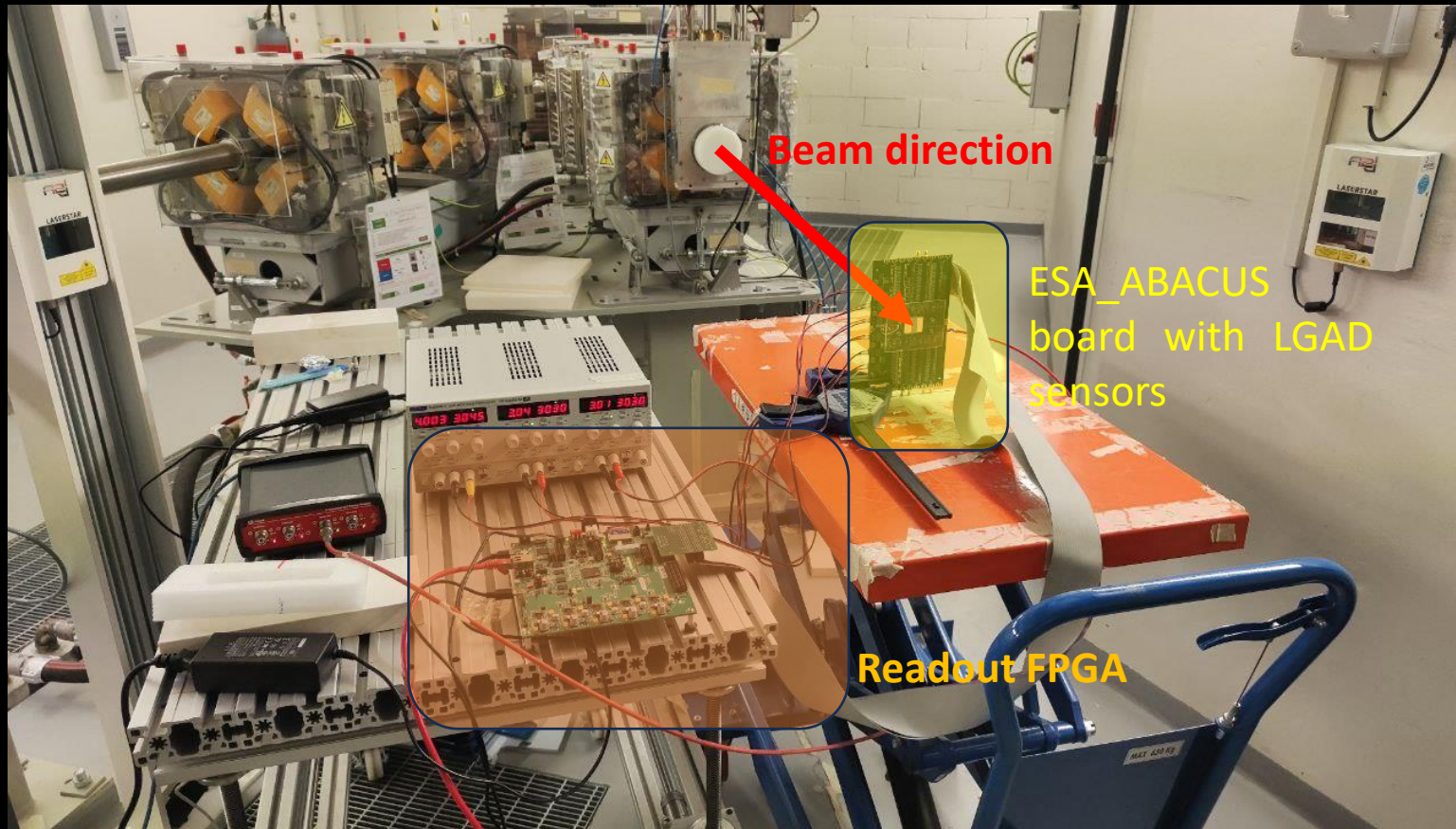
LGAD - Experimental results (Threshold scans)

Low Gain Avalanche Detector



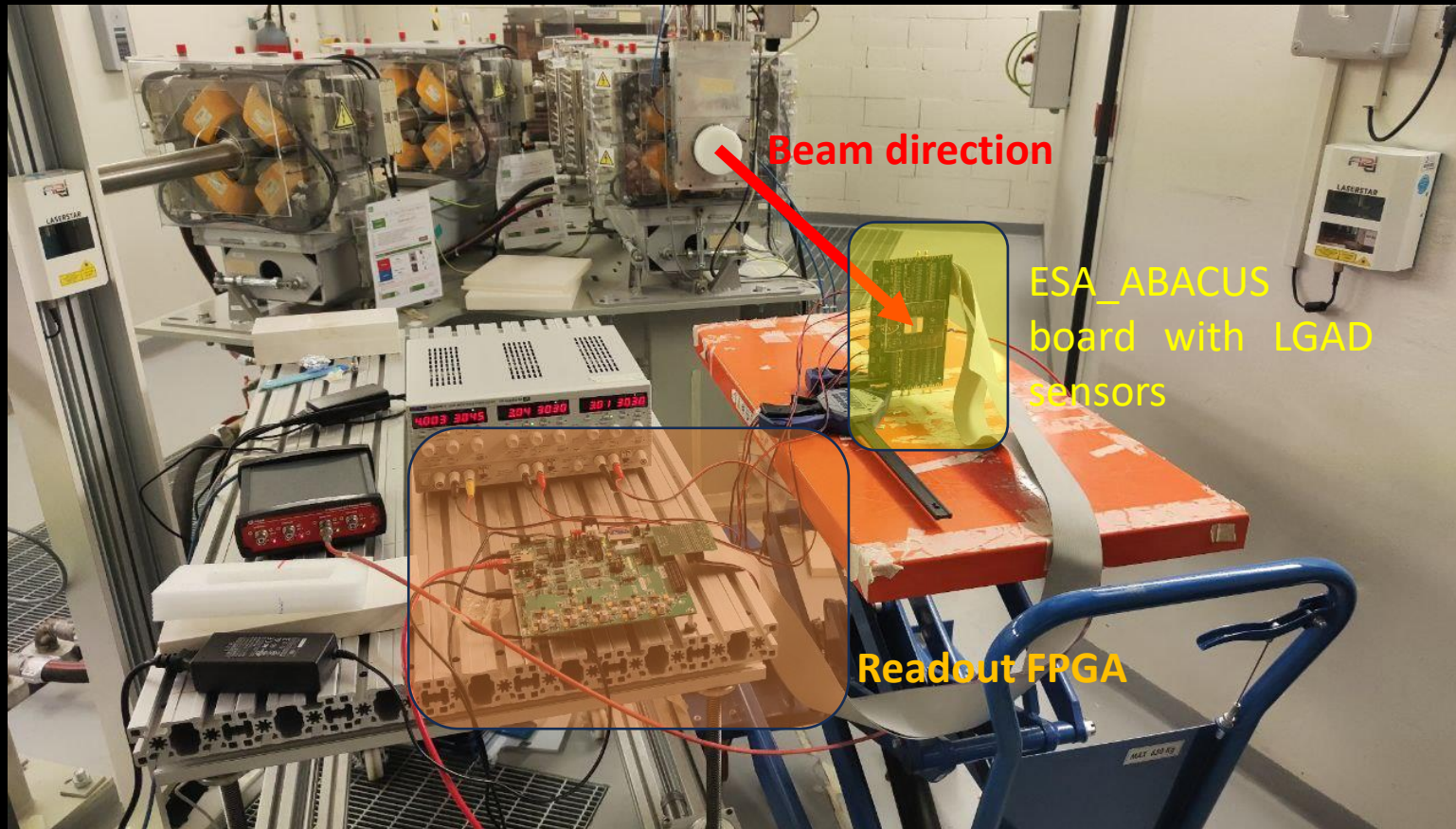
LGAD - Experimental results (Threshold scans)

Low Gain Avalanche Detector



LGAD - Experimental results (Threshold scans)

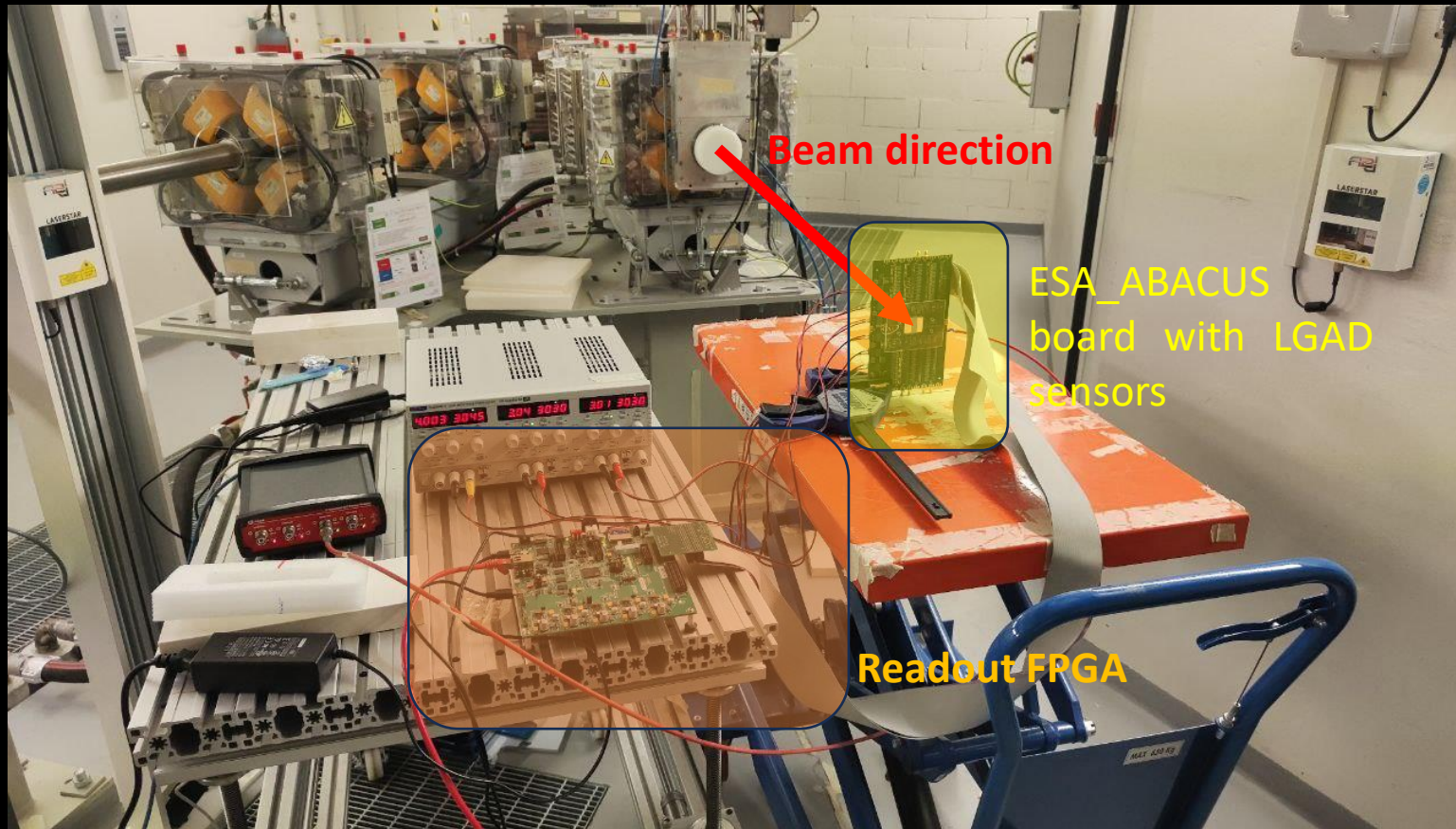
Low Gain Avalanche Detector



Beam test conducted at the Proton Therapy Center in Trento to answer:

LGAD - Experimental results (Threshold scans)

Low Gain Avalanche Detector



Beam test conducted at the Proton Therapy Center in Trento to answer:

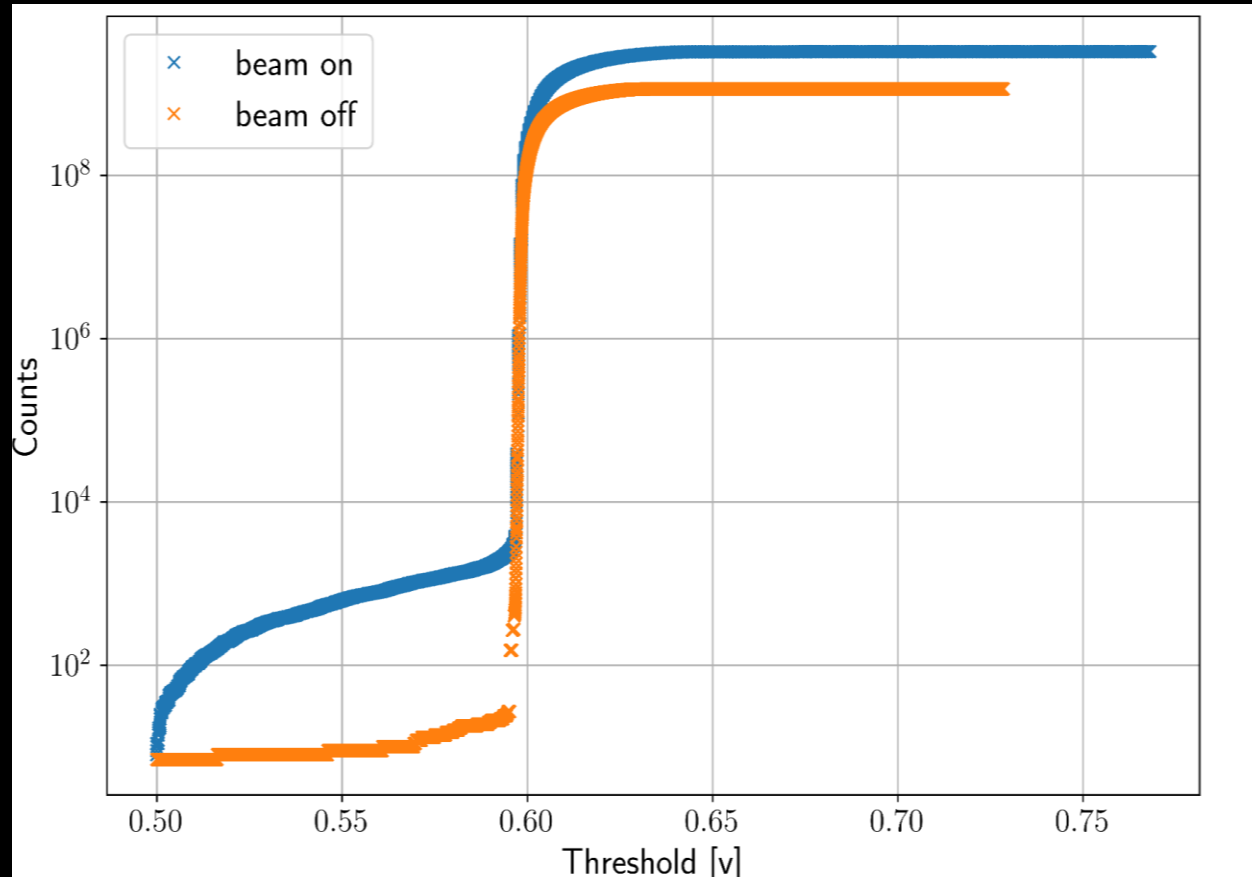
- are the LGADs sensors capable of detecting protons with energy up to 228 MeV?

LGAD - Threshold scan profile

Low Gain Avalanche Detector

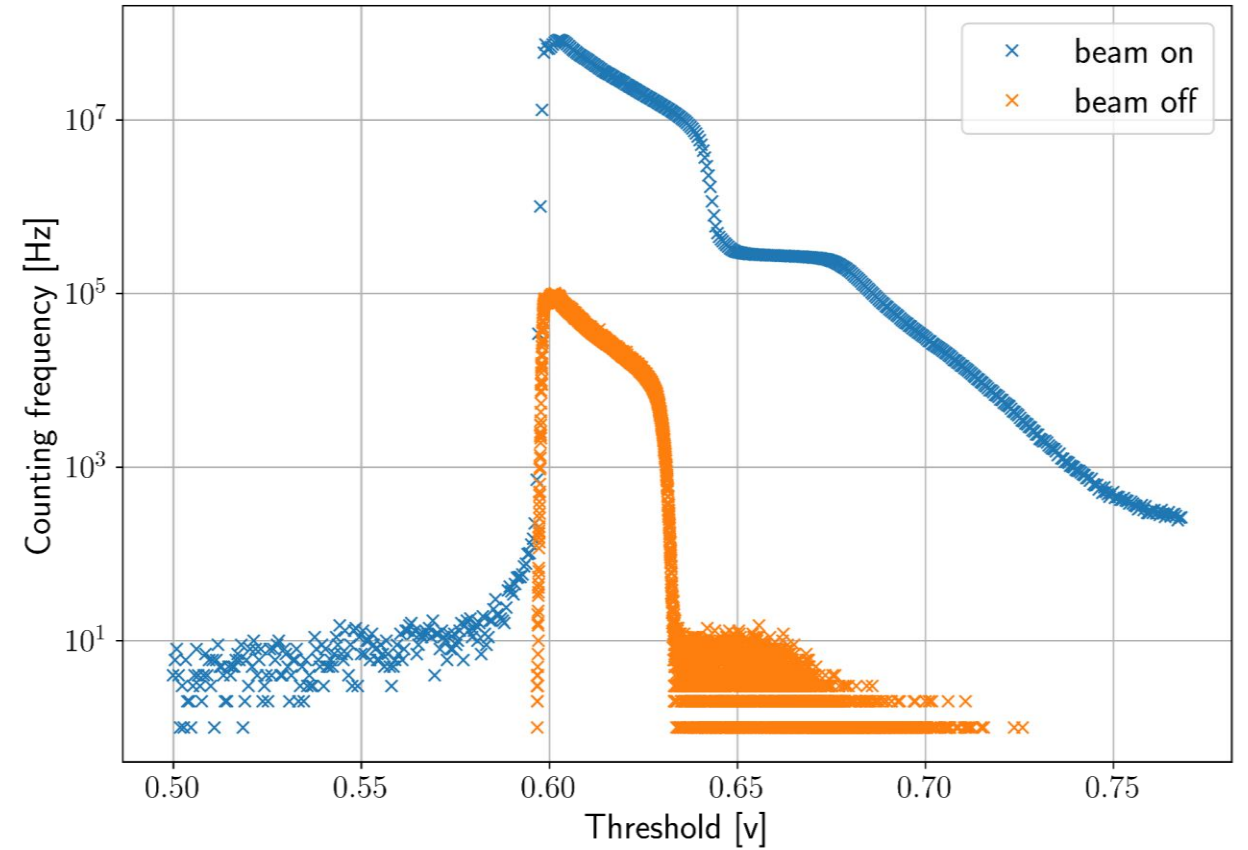
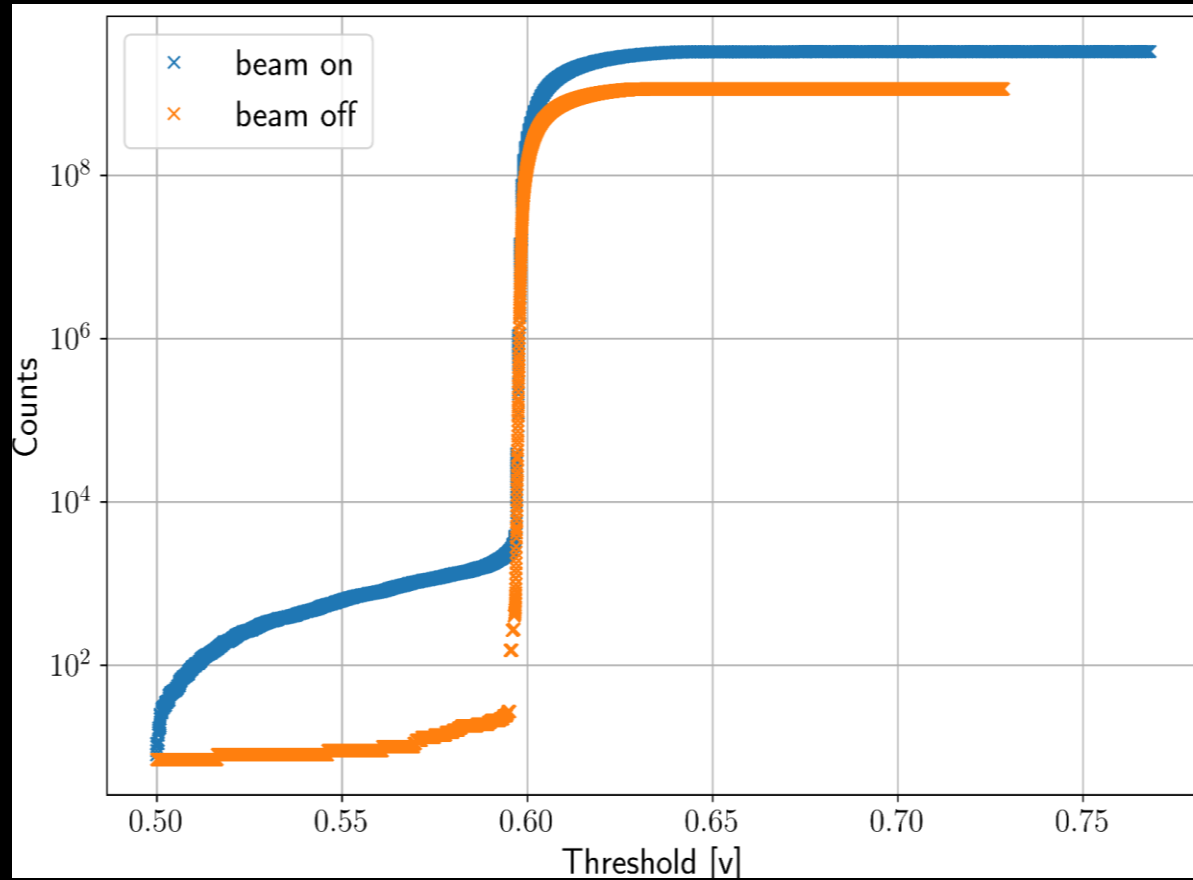
LGAD - Threshold scan profile

Low Gain Avalanche Detector



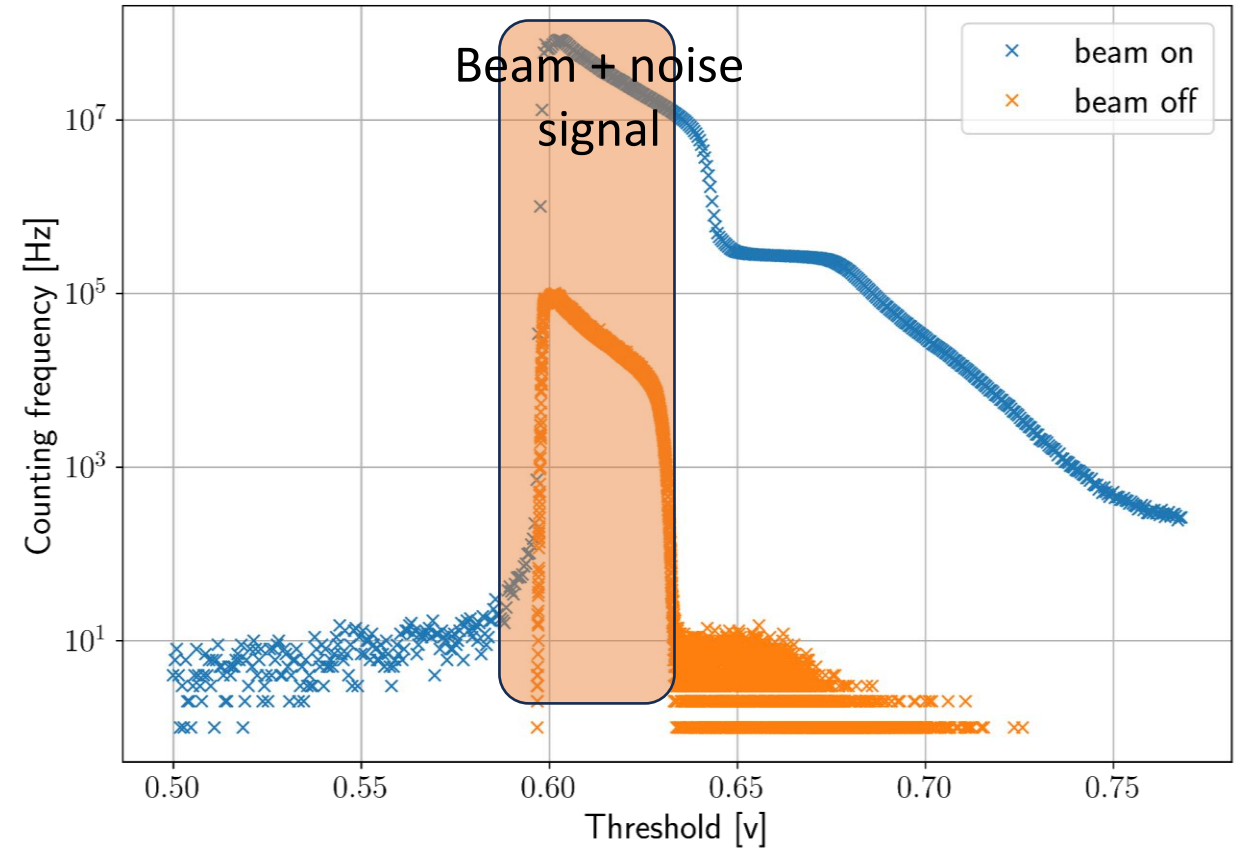
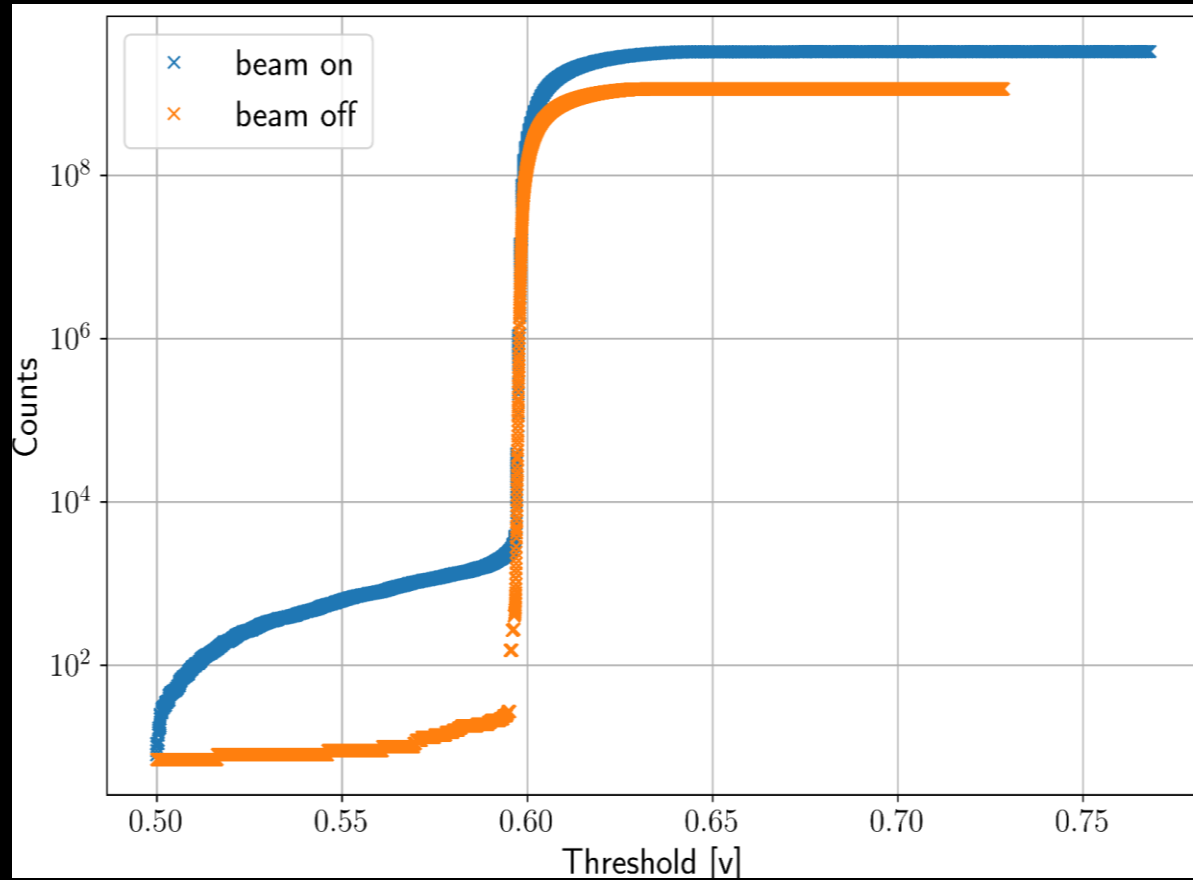
LGAD - Threshold scan profile

Low Gain Avalanche Detector



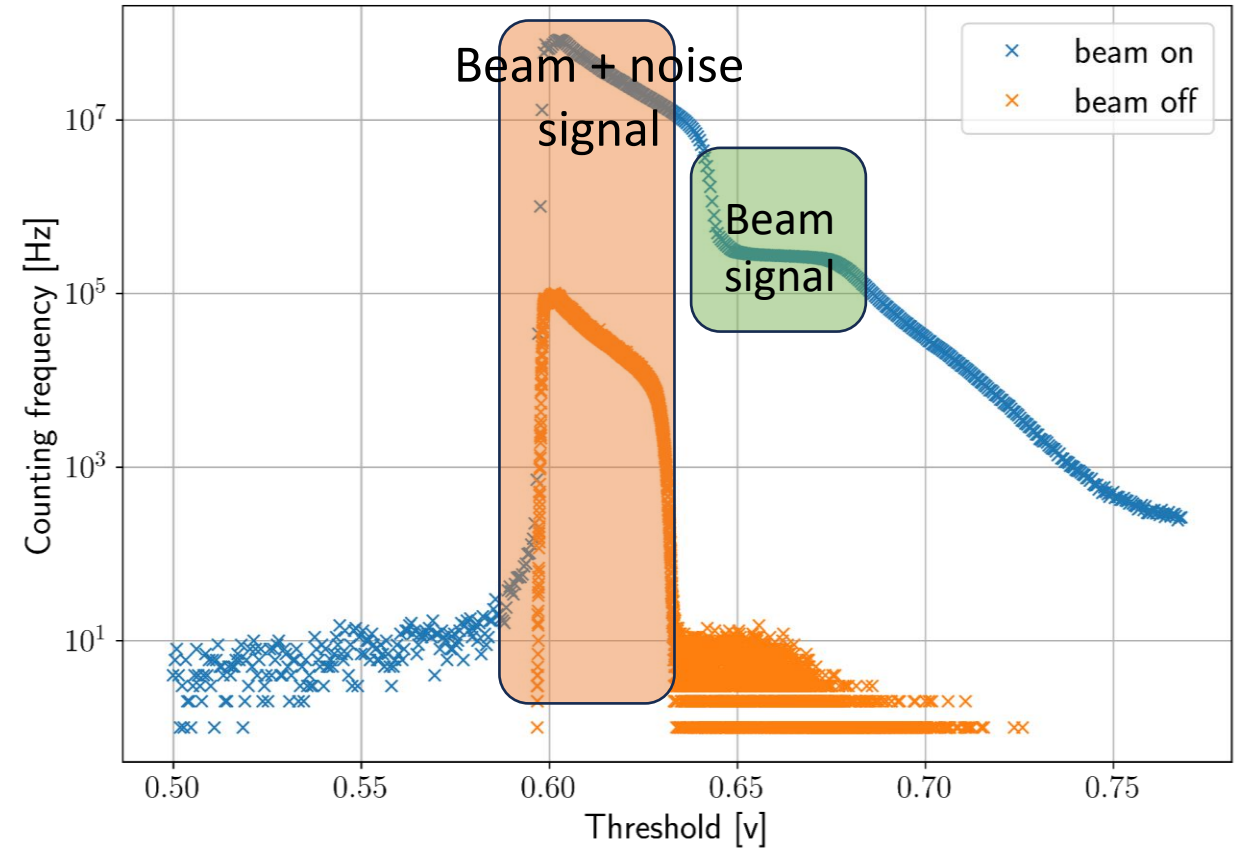
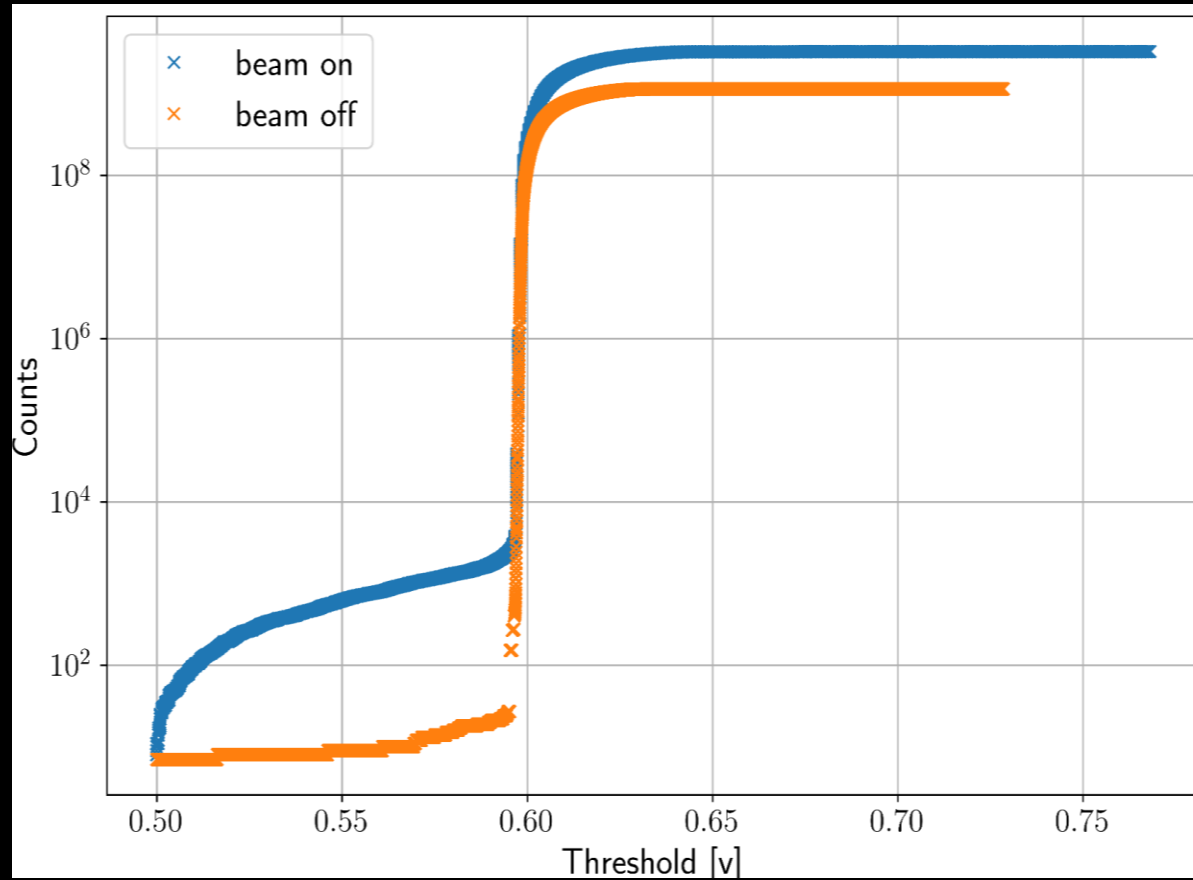
LGAD - Threshold scan profile

Low Gain Avalanche Detector



LGAD - Threshold scan profile

Low Gain Avalanche Detector




LGADs - Landau distributions

Low Gain Avalanche Detector

LGADs - Landau distributions

Low Gain Avalanche Detector

Probability of having a signal
with amplitude $> x_{\text{Threshold}}$


$$f(x \geq x_{\text{Threshold}}) = f_0 \int_{x_{\text{Threshold}}}^{\infty} p(x') d(x')$$

LGADs - Landau distributions

Low Gain Avalanche Detector

Probability of having a signal
with amplitude $> x_{\text{Threshold}}$

$p(x)$ is the probability
distribution of the signal
amplitude

$$f(x \geq x_{\text{Threshold}}) = f_0 \int_{x_{\text{Threshold}}}^{\infty} p(x') d(x')$$

LGADs - Landau distributions

Low Gain Avalanche Detector

Probability of having a signal
with amplitude $> x_{\text{Threshold}}$

$p(x)$ is the probability
distribution of the signal
amplitude

$$f(x \geq x_{\text{Threshold}}) = f_0 \int_{x_{\text{Threshold}}}^{\infty} p(x') d(x')$$

$$p(x) = - \frac{df(x)}{dx}$$

LGADs - Landau distributions

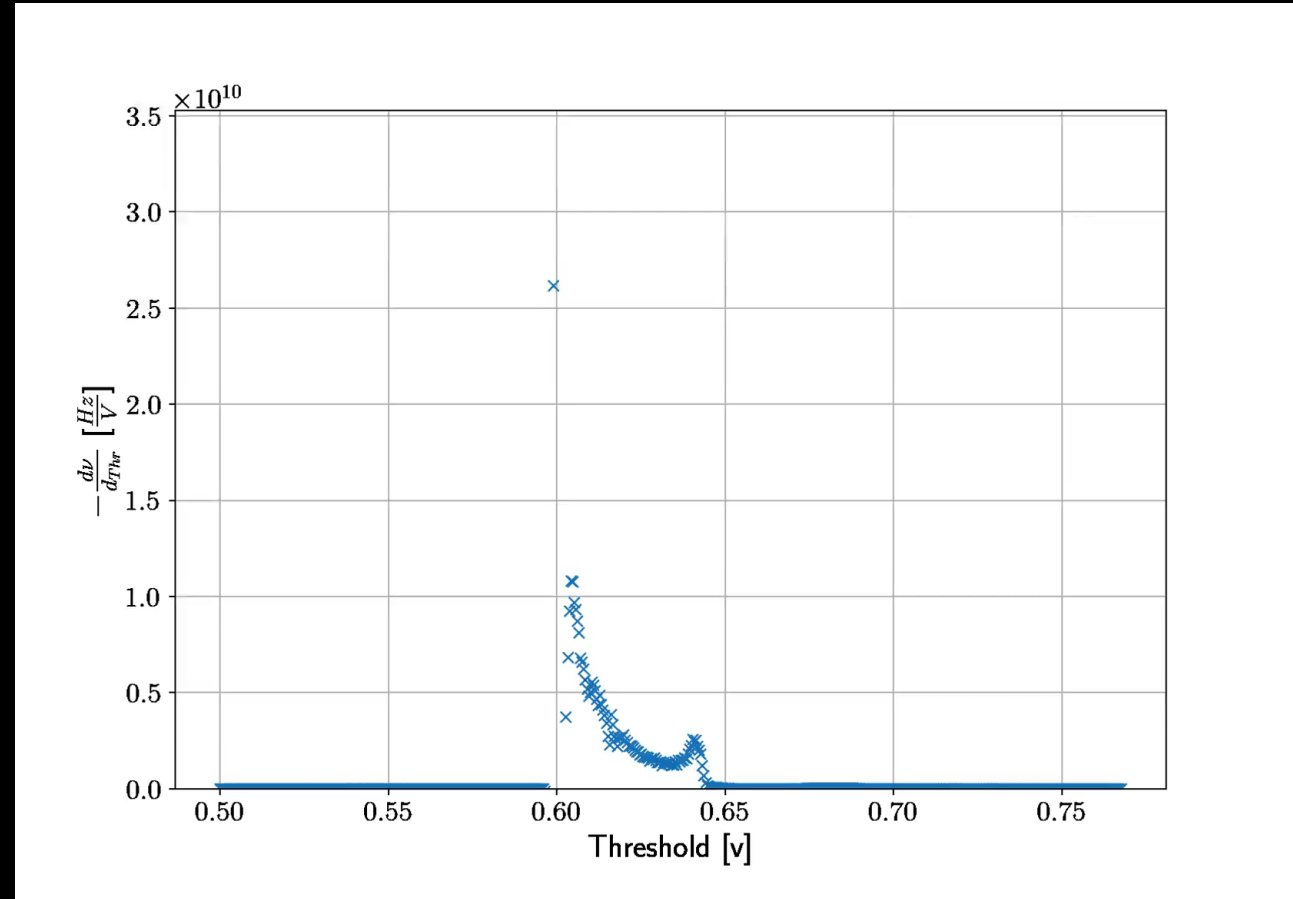
Low Gain Avalanche Detector

Probability of having a signal
with amplitude $> x_{\text{Threshold}}$

$p(x)$ is the probability
distribution of the signal
amplitude

$$f(x \geq x_{\text{Threshold}}) = f_0 \int_{x_{\text{Threshold}}}^{\infty} p(x') d(x')$$

$$p(x) = -\frac{df(x)}{dx}$$



LGADs - Landau distributions

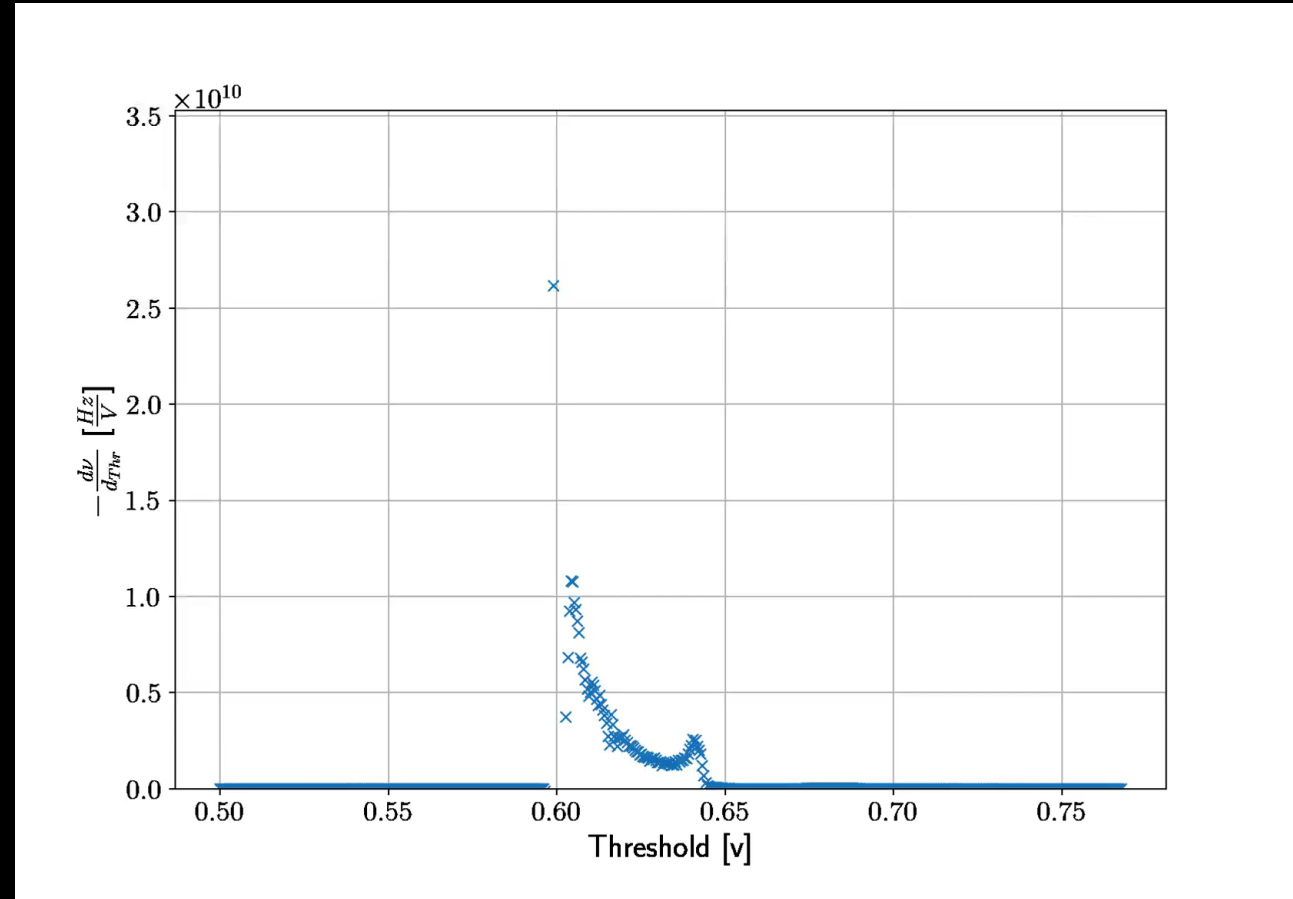
Low Gain Avalanche Detector

Probability of having a signal
with amplitude $> x_{\text{Threshold}}$

$p(x)$ is the probability
distribution of the signal
amplitude

$$f(x \geq x_{\text{Threshold}}) = f_0 \int_{x_{\text{Threshold}}}^{\infty} p(x') d(x')$$

$$p(x) = -\frac{df(x)}{dx}$$

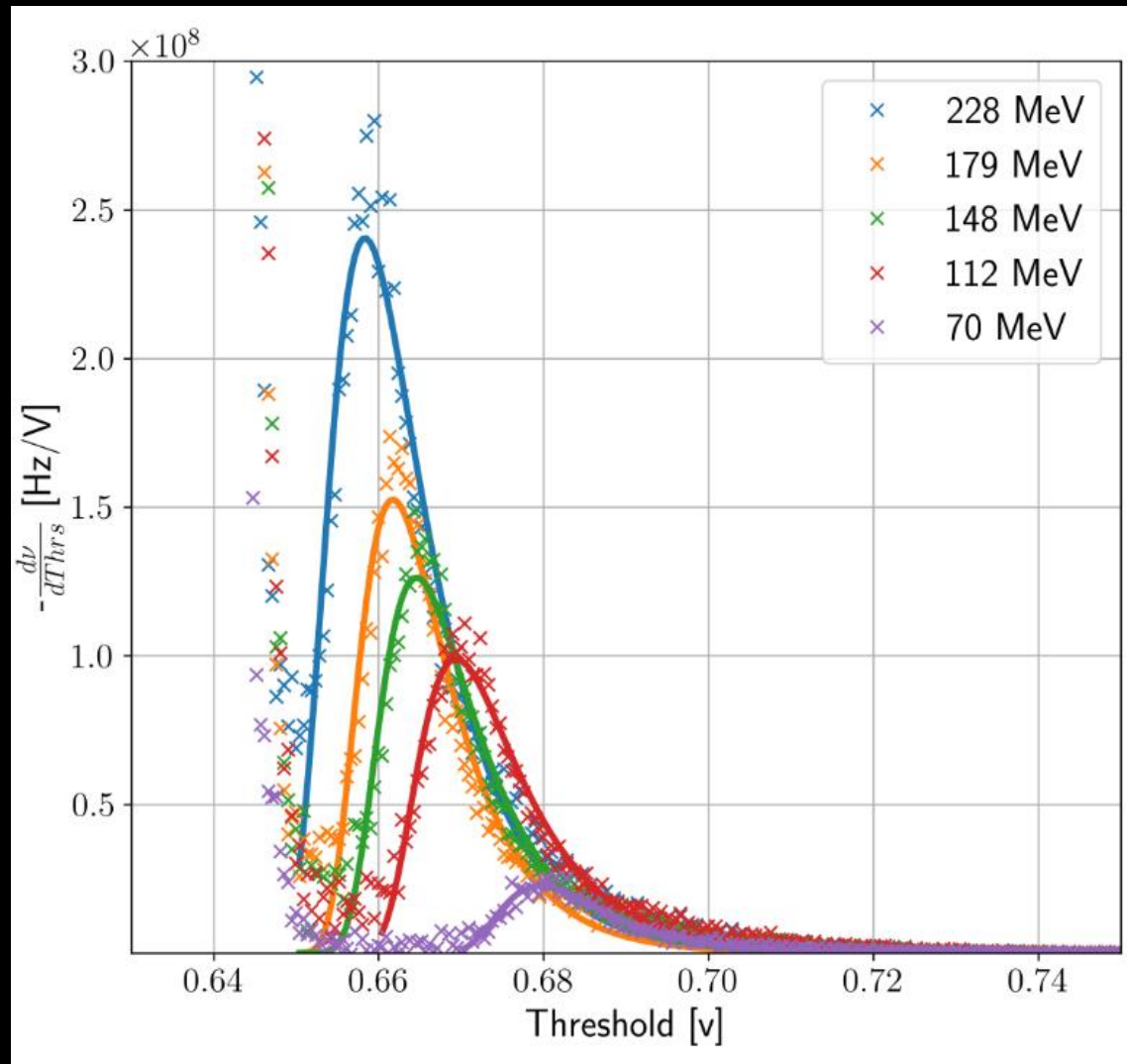


LGAD - Threshold scan results, 228 MeV

Low Gain Avalanche Detector

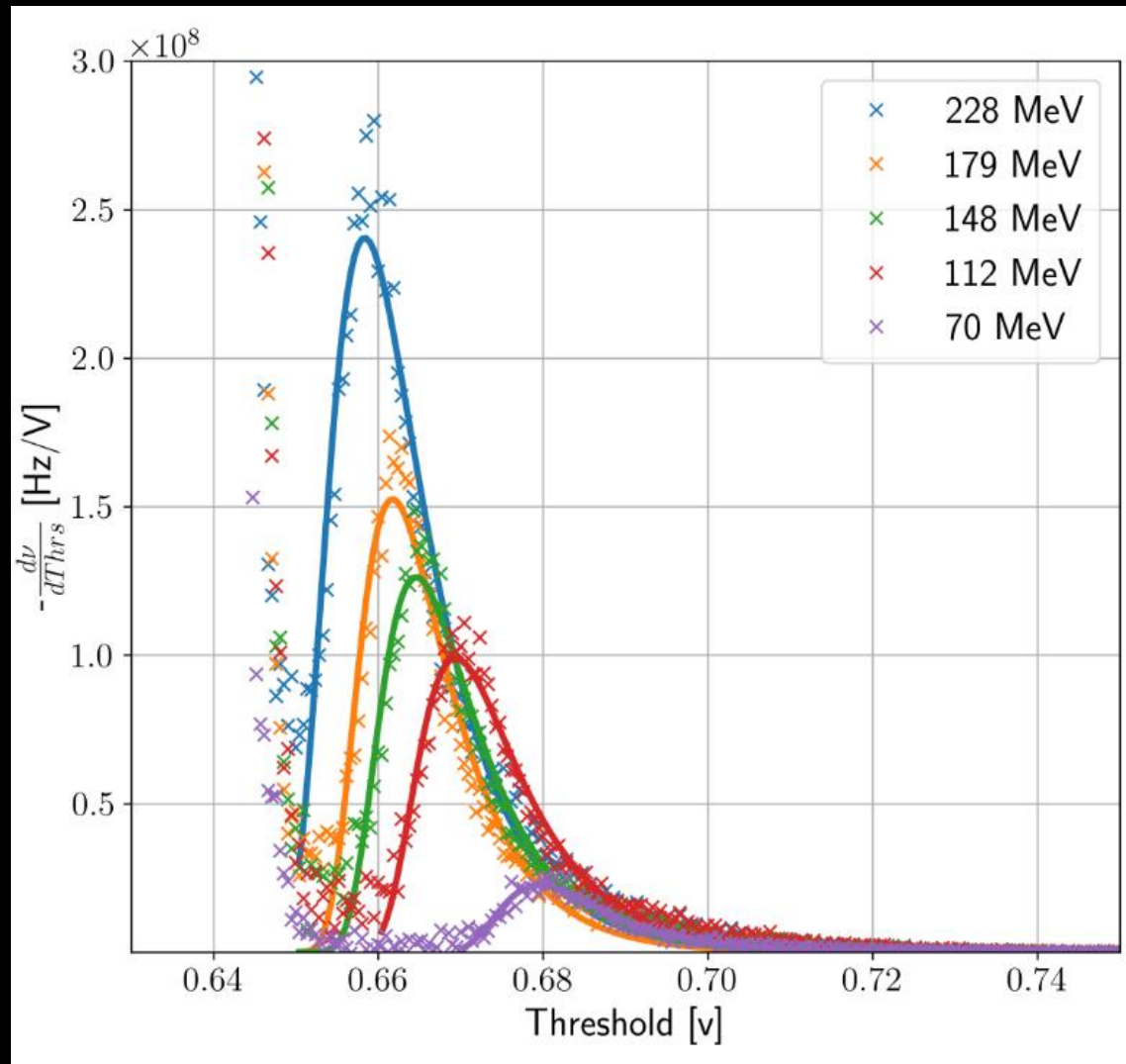
LGAD - Threshold scan results, 228 MeV

Low Gain Avalanche Detector

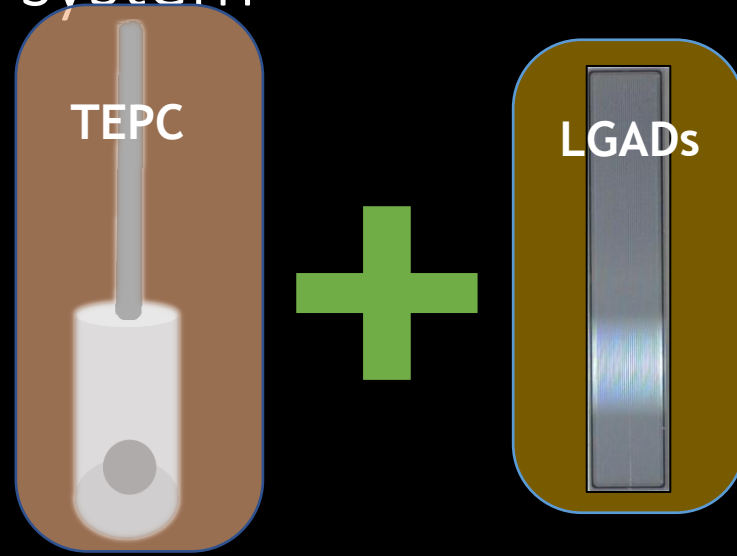


LGAD - Threshold scan results, 228 MeV

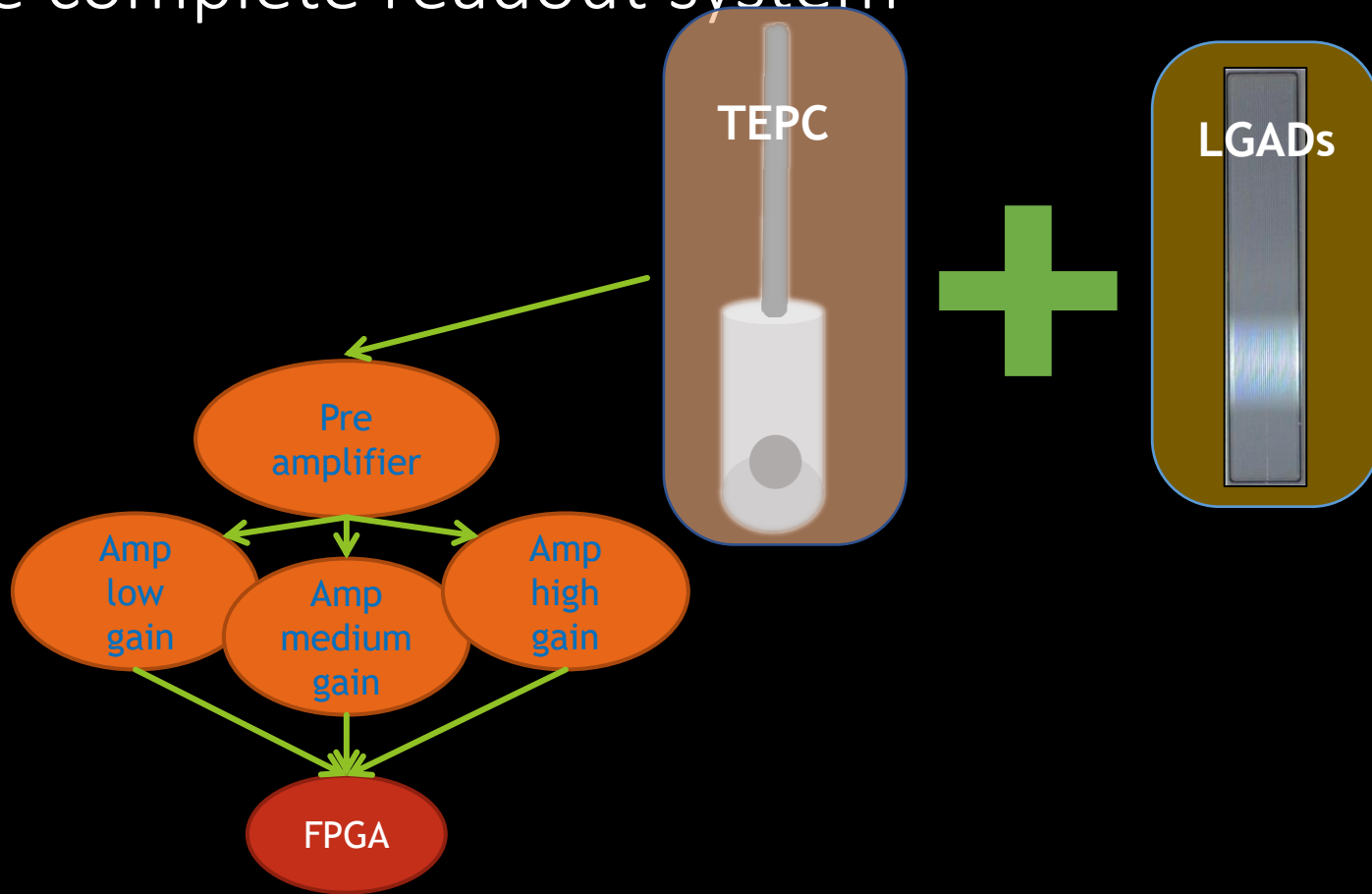
Low Gain Avalanche Detector



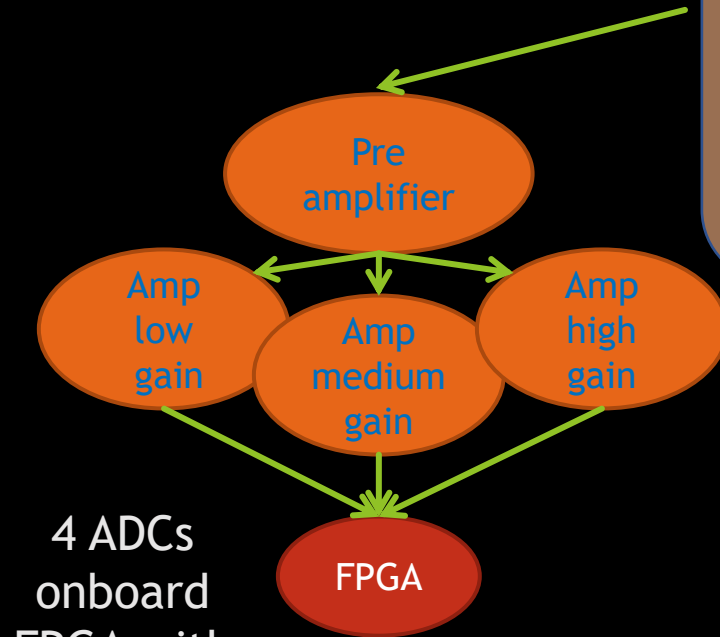
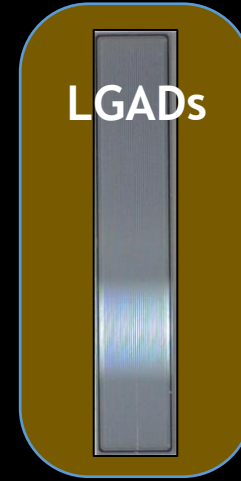
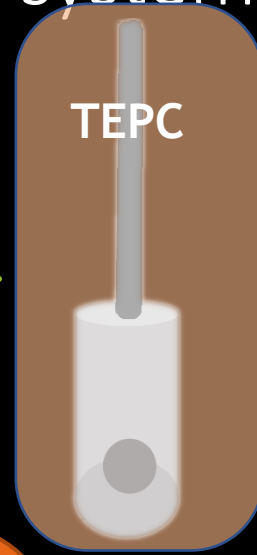
The complete readout system



The complete readout system

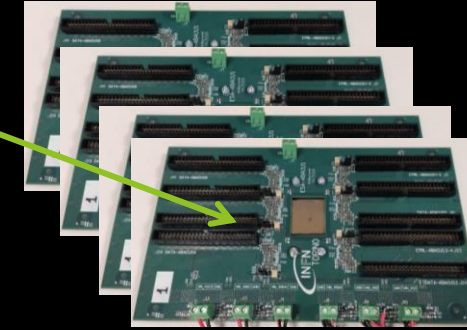
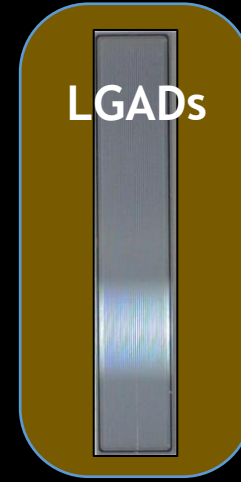
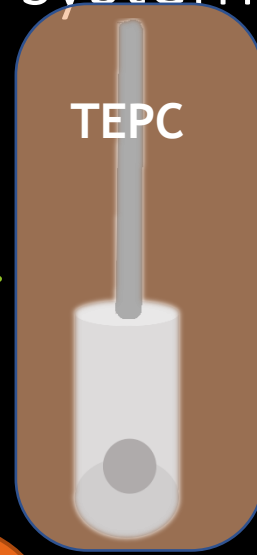


The complete readout system

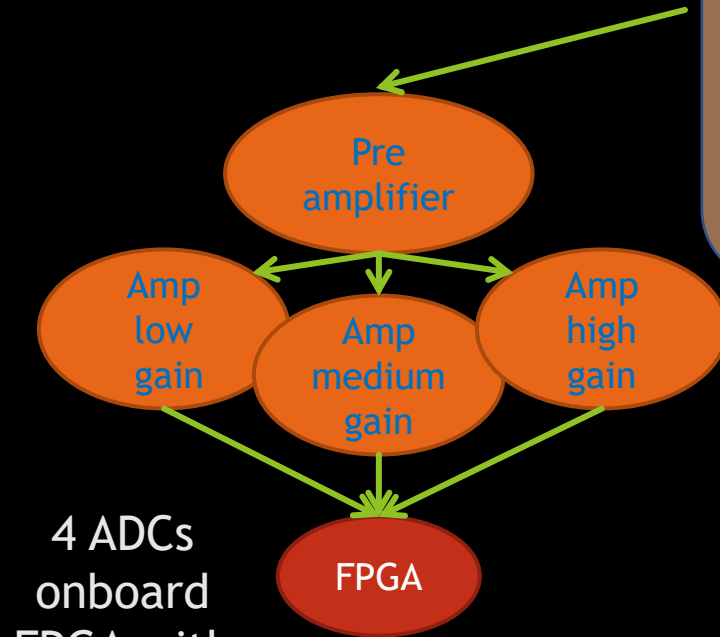


4 ADCs
onboard
FPGA with
custom
firmware

The complete readout system

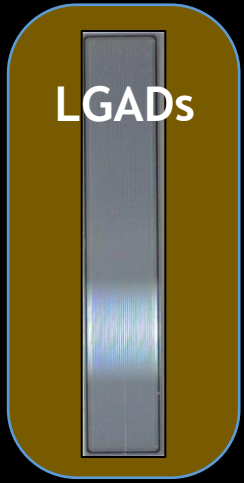
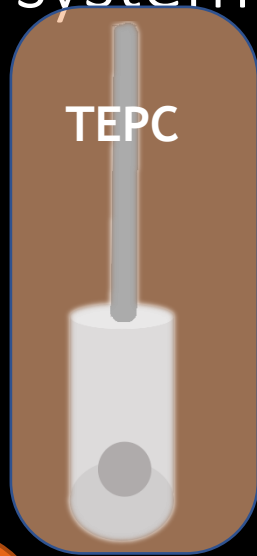


4 X ESA_ABACUS
with 3 ABACUS
chips each

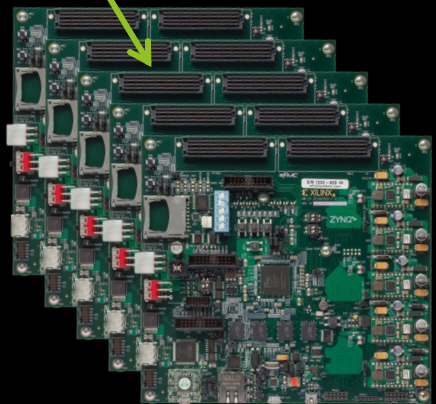


4 ADCs
onboard
FPGA with
custom
firmware

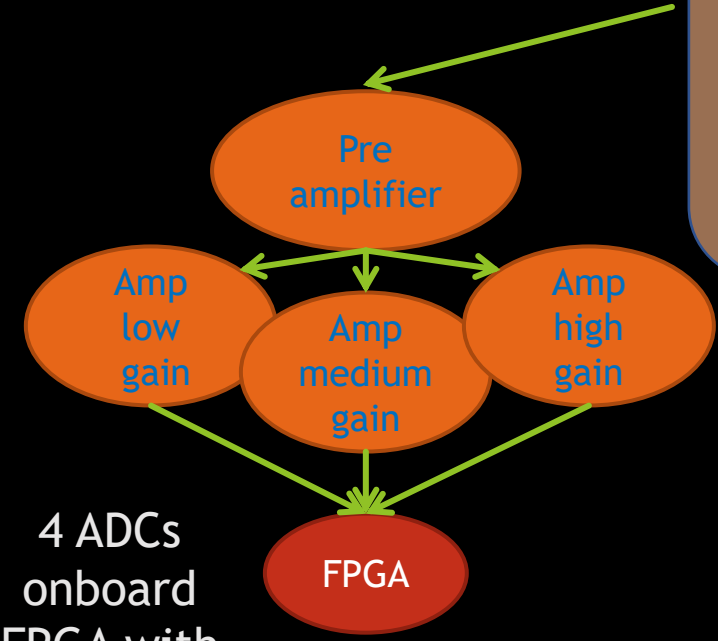
The complete readout system



4 X ESA_ABACUS
with 3 ABACUS
chips each

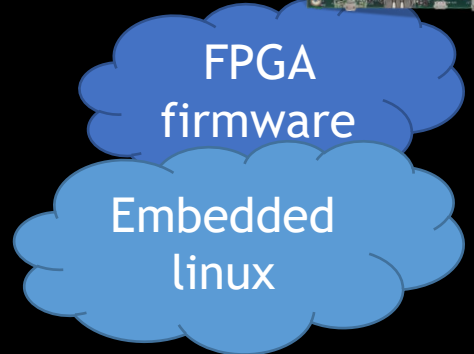
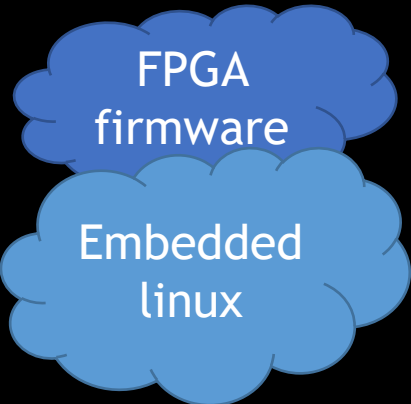
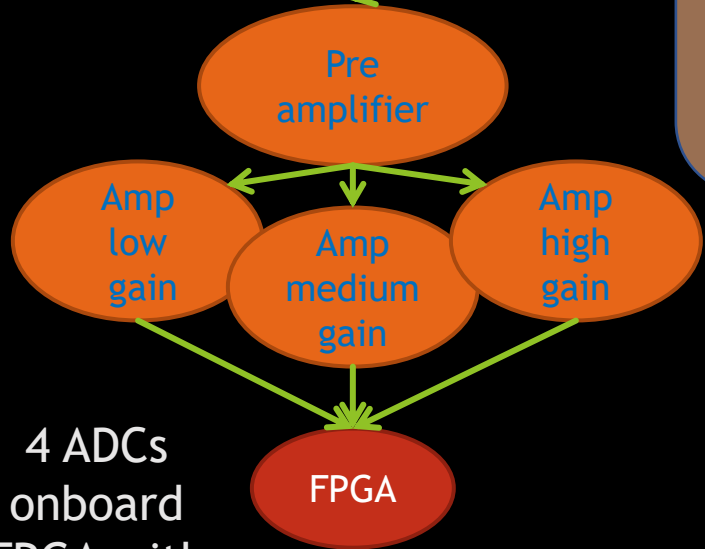
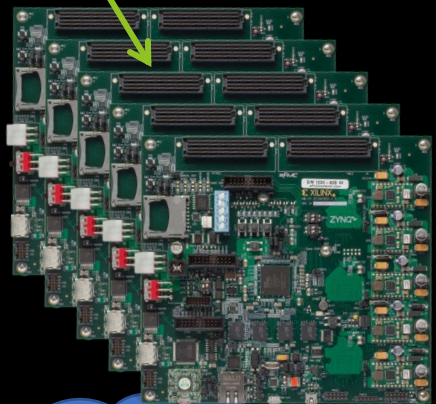
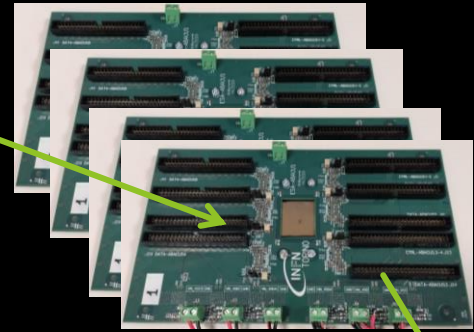
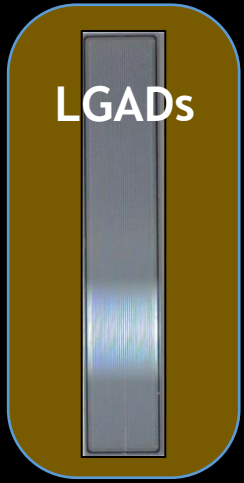
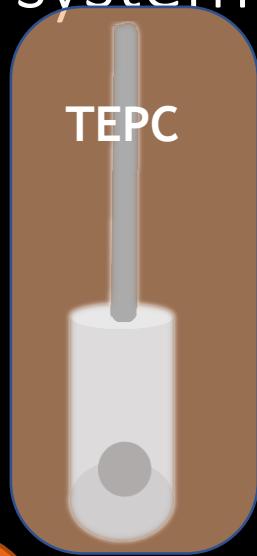


5 X ZC702 FPGA

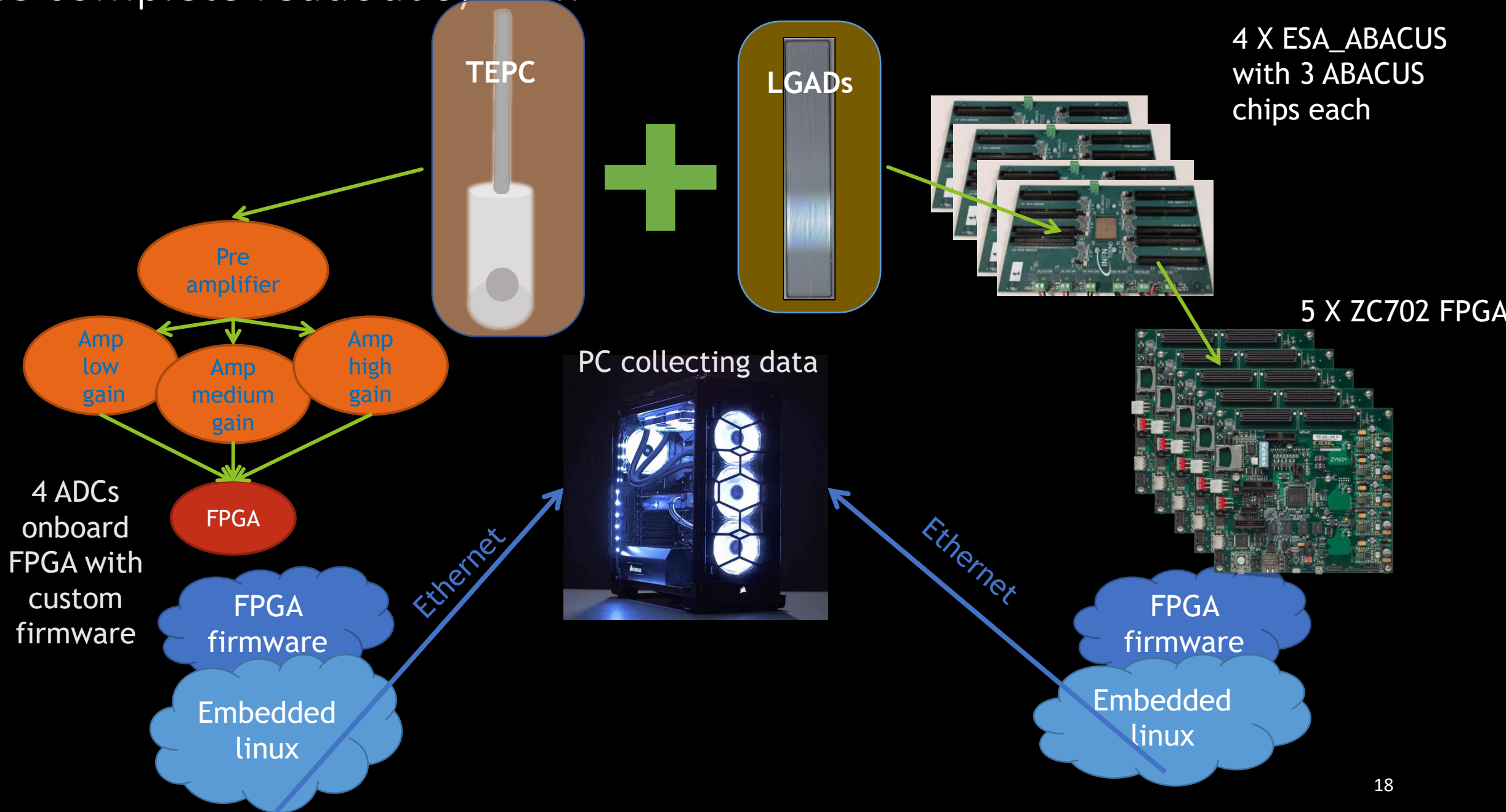


4 ADCs
onboard
FPGA with
custom
firmware

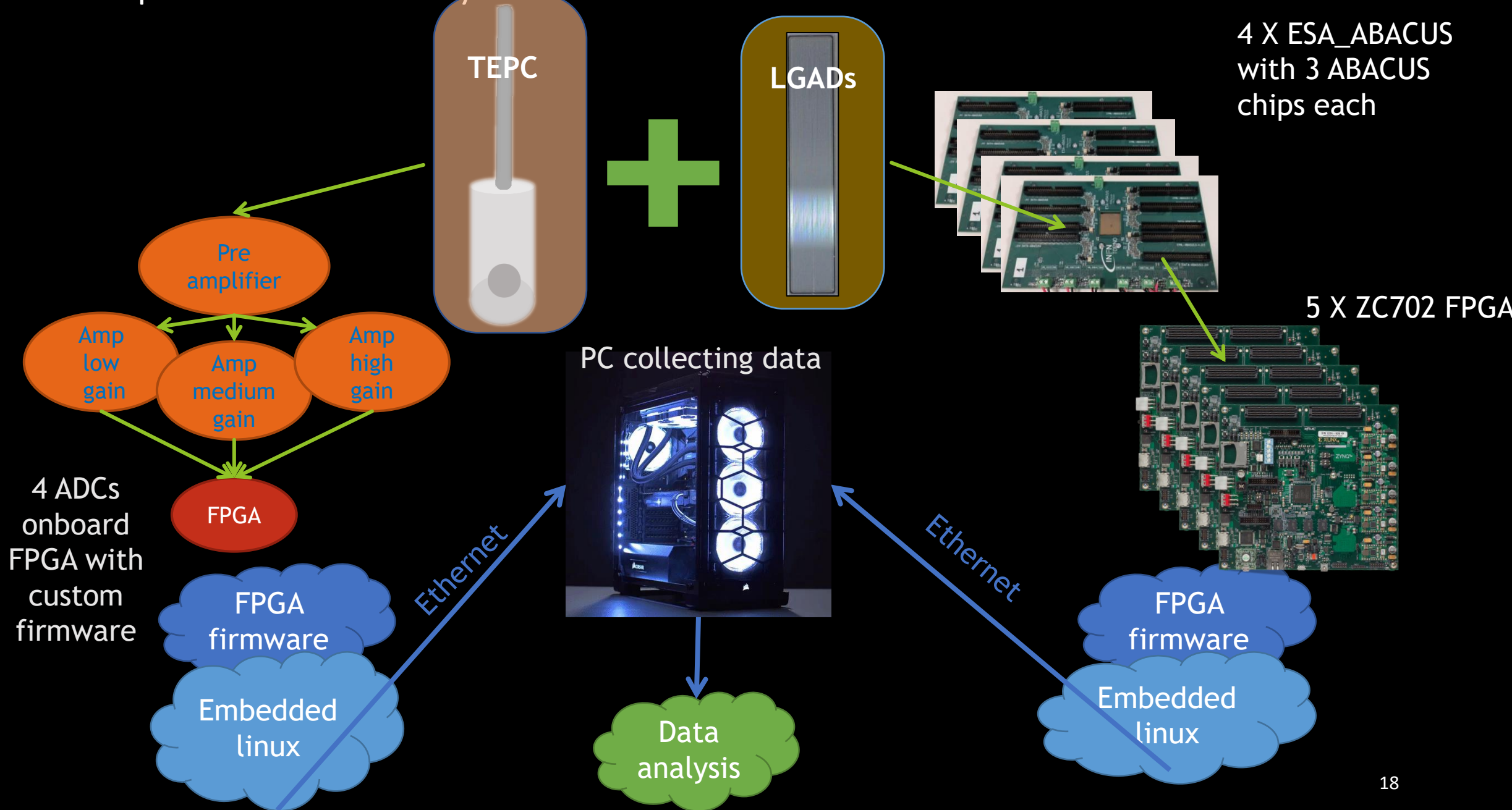
The complete readout system



The complete readout system



The complete readout system



Conclusions

Work in progress

Work in progress

- LGADs sensors thinning

Work in progress

- LGADs sensors thinning
- Synchronization between TEPC and LGAD

Work in progress

- LGADs sensors thinning
- Synchronization between TEPC and LGAD
- Implementation of the triggering condition

Work in progress

- LGADs sensors thinning
- Synchronization between TEPC and LGAD
- Implementation of the triggering condition
- Extend the implementation the 4 layers of LGADs

Work in progress

- LGADs sensors thinning
- Synchronization between TEPC and LGAD
- Implementation of the triggering condition
- Extend the implementation the 4 layers of LGADs

- Data analysis

Conclusions

Conclusions

- HDM is capable of:
 - ✓ Measure particle real track length in TEPC
 - ✓ Improve TEPC spatial resolution
 - ✓ Provide a superior radiation field characterization

Conclusions

- HDM is capable of:
 - ✓ Measure particle real track length in TEPC
 - ✓ Improve TEPC spatial resolution
 - ✓ Provide a superior radiation field characterization

Feasibility study published in *Frontiers in Physics*, 10.3389/fphy.2020.578444

Conclusions

- HDM is capable of:
 - ✓ Measure particle real track length in TEPC
 - ✓ Improve TEPC spatial resolution
 - ✓ Provide a superior radiation field characterization

Feasibility study published in *Frontiers in Physics*, 10.3389/fphy.2020.578444

HDM improved radiation quality description results in a more accurate dose calculation in TPS.

Conclusions

- HDM is capable of:
 - ✓ Measure particle real track length in TEPC
 - ✓ Improve TEPC spatial resolution
 - ✓ Provide a superior radiation field characterization

Feasibility study published in *Frontiers in Physics*, 10.3389/fphy.2020.578444

HDM improved radiation quality description results in a more accurate dose calculation in TPS.

- HDM requires
 - ✓ 284 channels for tracking
 - ✓ 3 ADCs for energy deposition information

Conclusions

- HDM is capable of:
 - ✓ Measure particle real track length in TEPC
 - ✓ Improve TEPC spatial resolution
 - ✓ Provide a superior radiation field characterization

Feasibility study published in *Frontiers in Physics*, 10.3389/fphy.2020.578444

HDM improved radiation quality description results in a more accurate dose calculation in TPS.

- HDM requires
 - ✓ 284 channels for tracking
 - ✓ 3 ADCs for energy deposition information



Complementary information

Conclusions

- HDM is capable of:
 - ✓ Measure particle real track length in TEPC
 - ✓ Improve TEPC spatial resolution
 - ✓ Provide a superior radiation field characterization

Feasibility study published in *Frontiers in Physics*, 10.3389/fphy.2020.578444

HDM improved radiation quality description results in a more accurate dose calculation in TPS.

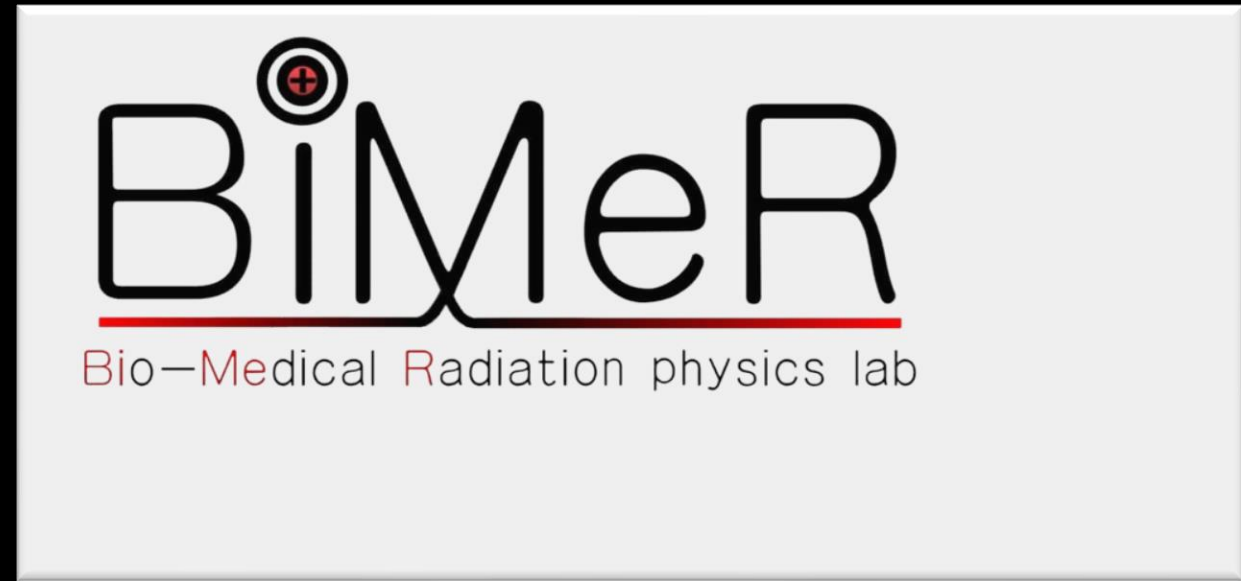
- HDM requires
 - ✓ 284 channels for tracking
 - ✓ 3 ADCs for energy deposition information

Machine learning-based particle track reconstruction published in *Physics in Medicine & Biology* 10.1088/1361-6560/ac8af3



Complementary information

Thank you for your attentions



Conclusions

- HDM is capable of:
 - ✓ Measure particle real track length in TEPC
 - ✓ Improve TEPC spatial resolution
 - ✓ Provide a superior radiation field characterization

Feasibility study published in *Frontiers in Physics*, [10.3389/fphy.2020.578444](https://doi.org/10.3389/fphy.2020.578444)

HDM improved radiation quality description results in a more accurate dose calculation in TPS.

- HDM requires
 - ✓ 284 channels for tracking
 - ✓ 3 ADCs for energy deposition information

Machine learning-based particle track reconstruction published in *Physics in Medicine & Biology* [10.1088/1361-6560/ac8af3](https://doi.org/10.1088/1361-6560/ac8af3)



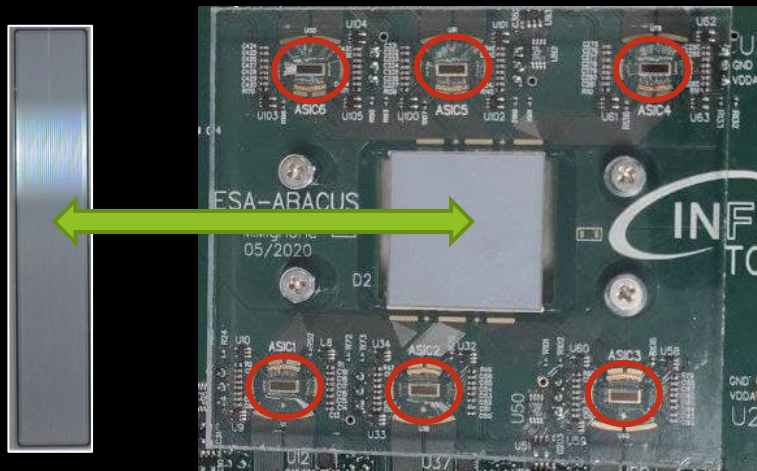
Complementary information

Backup slides

ABACUS ASIC

LGADs

ABACUS chips



Each chip read a maximum of 24 LGADs

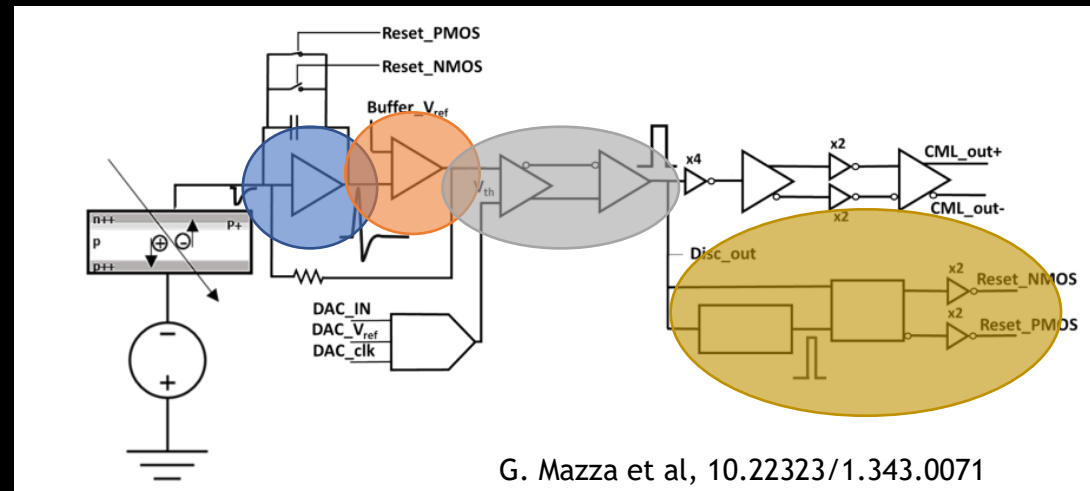
Sets threshold for each channel

- Problem finding a common threshold to multiple channels due to limited range

Preamplifier

Buffer

Output is in Current Mode Logic (CML)

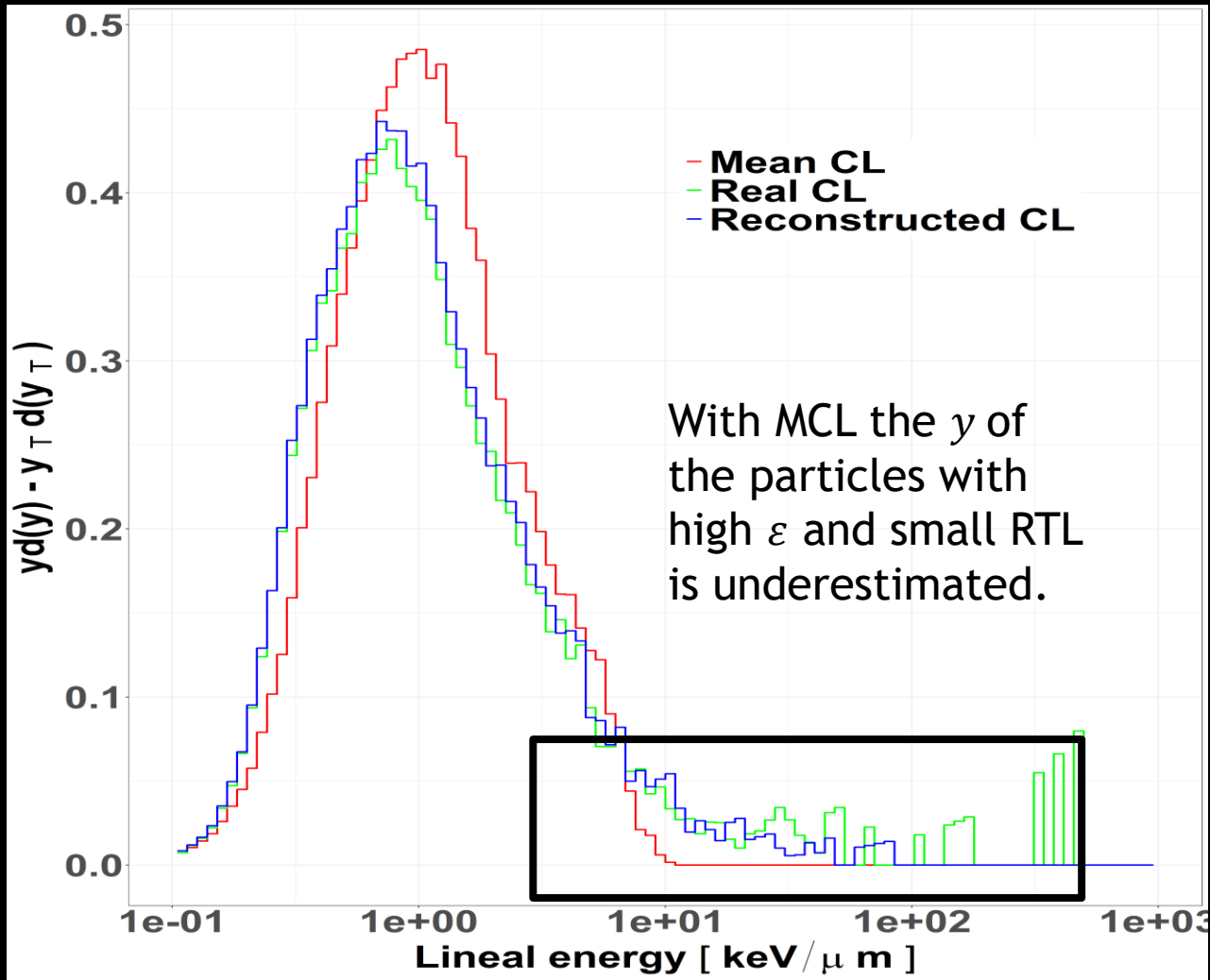


Multistage discriminator

Feedback capacitor signal reset

- + New fixed version of the chip production should start within days

HDM: the spectrum from simulations

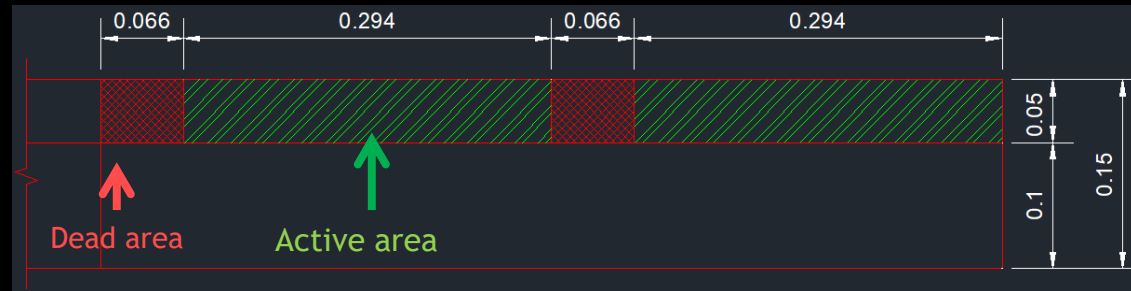


- HDM will improve the radiation quality description and consequentially the treatment planning
- HDM will improve the TEPC spatial resolution

LGADs geometry

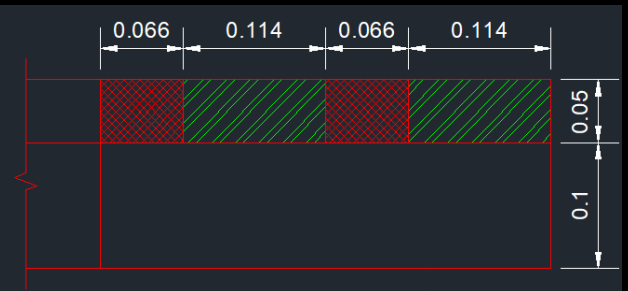


34 strips per sensor



- pitch 360 μm
- better fill factor
- less channels to read

71 strips per sensor



- pitch 180 μm
- better spatial resolution

TEPC Energy deposition equivalence:

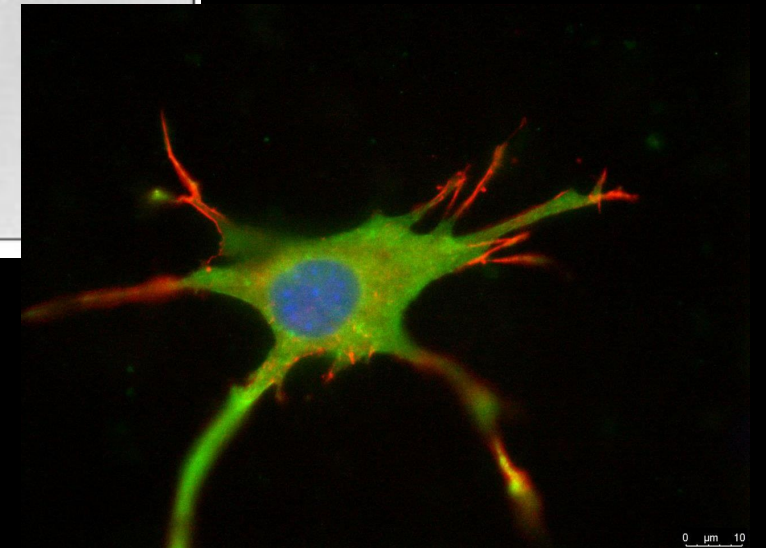
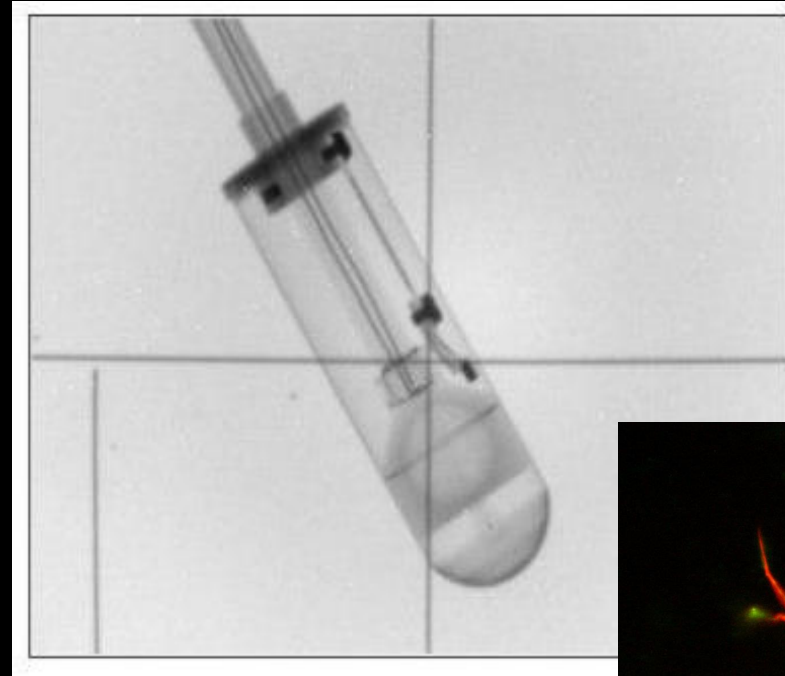
$$\Delta E_{TEPC\ gas} = \Delta E_{Tissue}$$

Mass stopping power

Diameter

Density

$$\Delta E_{TEPC} = \left(\frac{S}{\rho}\right)_{TEPC} (D\rho)_{TEPC}$$
$$\Delta E_{Tissue} = \left(\frac{S}{\rho}\right)_{Tissue} (D\rho)_{Tissue}$$



Landau distribution

$$f(x \geq x_{\text{Threshold}}) = f_0 \int_{x_{\text{Threshold}}}^{\infty} p(x') d(x')$$

$$f_0 \int_{x_{\text{Threshold}}}^{\infty} p(x') d(x') = f_0 \left(\int_{-\infty}^{\infty} - \int_{-\infty}^{x_{\text{Threshold}}} \right) p(x') d(x') = f_0 \left(1 - \int_{-\infty}^{x_{\text{Threshold}}} p(x') dx' \right)$$

$$p(x) = - \frac{df(x)}{dx}$$